

# Phase Characterization of Polar Liquid Crystals Using Dielectric Spectroscopy

JAN P.F. LAGERWALL

Department of Microelectronics and Nanoscience  
CHALMERS UNIVERSITY OF TECHNOLOGY  
GÖTEBORG UNIVERSITY  
Göteborg, Sweden 2000



THESIS FOR THE DEGREE OF LICENTIATE OF ENGINEERING

# Phase Characterization of Polar Liquid Crystals Using Dielectric Spectroscopy

Jan P. F. Lagerwall



Department of Microelectronics and Nanoscience  
Chalmers University of Technology  
Göteborg University  
Göteborg, Sweden, February 2000

Phase Characterization of Polar Liquid Crystals  
Using Dielectric Spectroscopy

© JAN P. F. LAGERWALL, 2000

Department of Microelectronics and Nanoscience  
Chalmers University of Technology  
SE-412 96 Göteborg,  
Sweden  
Telephone: +46 (0) 31 - 772 33 83  
Fax: +46 (0) 31 - 772 34 36  
E-mail: [jpf@fy.chalmers.se](mailto:jpf@fy.chalmers.se)

**Cover**

Skiing on the slopes of a dielectric absorption spectrum.

Printing: Chalmers reproservice  
Göteborg, Sweden 2000

# Phase Characterization of Polar Liquid Crystals Using Dielectric Spectroscopy

JAN P. F. LAGERWALL

Department of Microelectronics and Nanoscience  
Chalmers University of Technology

## ABSTRACT

The discovery of liquid crystals which have a collective polar order – mostly referred to as ferroelectric and antiferroelectric liquid crystals – has made dielectric spectroscopy an indispensable research tool for the investigation of the manifold of different ordered polar states which are permitted in these materials. After a brief introduction to polar liquid crystals (Chapter 1) and an introduction to frequency-domain dielectric spectroscopy (Chapter 2), the different collective and non-collective fluctuations which couple to external electric fields are discussed (Chapter 3).

Polar order in liquid crystals requires absence of mirror symmetry. One interesting way of producing such materials is to start from a matrix which has mirror symmetry and introduce polarity by adding chiral dopant molecules. Investigations on such systems are next described (Chapter 4).

Chirality is a necessary but not a sufficient condition for ferroelectricity to appear. In addition, the symmetry of the liquid crystal has to be further lowered by surface action. This means that the surfaces actually change the crystallographic state of the liquid crystal. In the last years it has become evident that even the characteristic sequence of thermodynamic phases which appear in the liquid crystal might be completely dominated by the influence of the surfaces. Studies of these phenomena are finally discussed (Chapter 5). Some methodological questions and experimental details are summarized in the Appendix.

*Keywords:* dielectric spectroscopy, polar liquid crystals, ferroelectricity, antiferroelectricity, Goldstone mode, soft mode, chiral-dopant mixtures, surface-induced phases

## *List of Publications*

- PAPER 1. ON THE COLLECTIVE OR NON-COLLECTIVE NATURE OF THE LOWER DIELECTRIC MODE OF ANTIFERROELECTRIC LIQUID CRYSTALS  
J. P. F. Lagerwall, T. Fütterer, D. Moro, G. Heppke  
*Presented as poster at FLC '99, Darmstadt, Aug. 29-Sep. 3, 1999. Submitted to "Ferroelectrics"*
- PAPER 2. OPTIC, ELECTROOPTIC AND DIELECTRIC PROPERTIES OF NOVEL ANTIFERROELECTRIC LIQUID CRYSTAL MIXTURES  
A. Dahlgren, P. Jägemalm, J. P. F. Lagerwall, L. Komitov, A. S. Matharu, C. Grover, F. M. Gouda, A. A. Kutub  
*Presented as poster at FLC '99, Darmstadt, Aug. 29-Sep. 3, 1999. Submitted to "Ferroelectrics"*
- PAPER 3. ELECTROOPTIC AND DIELECTRIC SPECTROSCOPY MEASUREMENTS OF BINARY CHIRAL-DOPANT ANTIFERROELECTRIC MIXTURES  
D. D. Parghi, J. P. F. Lagerwall, G. Heppke  
*Presented as poster at ECLC '99, Crete, Apr. 25-30, 1999. Accepted for publication in "Molecular Crystals and Liquid Crystals"*
- PAPER 4. ON THE COEXISTENCE OF SMC\* AND SMC<sub>A</sub>\* PHASES IN BINARY CHIRAL-DOPANT ANTIFERROELECTRIC MIXTURES  
J. P. F. Lagerwall, D. D. Parghi, G. Heppke  
*Presented as poster at FLC '99, Darmstadt, Aug. 29-Sep. 3, 1999. Submitted to "Ferroelectrics"*
- PAPER 5. ELECTROOPTIC AND DIELECTRIC PROPERTIES OF NEW BINARY ANTIFERROELECTRIC LIQUID CRYSTAL MIXTURES  
J. P. F. Lagerwall, G. Andersson, M. Matuszczyk, T. Matuszczyk, R. Dabrowski, W. Drzewinski, P. Perkowski, Z. Raszewski  
*Presented as poster at FLC '99, Darmstadt, Aug. 29-Sep. 3, 1999. Submitted to "Ferroelectrics"*

# 1. INTRODUCTION TO POLAR LIQUID CRYSTALS

---

---

*Variety is the soul of pleasure*  
– Aphra Behn

## OVERVIEW

*In this introduction I will briefly discuss the special properties of liquid crystals in general, and smectics in particular. The focus will soon be set on chiral smectics, especially the SmA\* and SmC\* phases which are the main interest of this thesis, and at the end of the chapter I will discuss the important polar effects which may be found in this class of liquid crystals. The correct definitions of polar phenomena in dielectrics (ferroelectricity, antiferroelectricity and ferrielectricity) will be reviewed.*

### **1.1. Liquid, crystalline and liquid crystalline phases**

Liquid crystals are ordered fluids. They are liquids in the sense that the molecules, which have an anisotropic shape (rod-, disc- or bowl-like), are to a large extent free to move in space (translational motion). But unlike isotropic liquids, which possess no kind of order, liquid crystal phases are characterized by a high degree of *orientational order*, *i.e.* the molecules are (on the average) locally oriented in a well defined way, giving these materials anisotropic macroscopic properties. Their optical and dielectric anisotropies, together with the liquid-like ease of reorienting the molecules, make liquid crystals ideal materials for many electrooptic applications such as in flat panel displays, sensors, optical switches, etc.

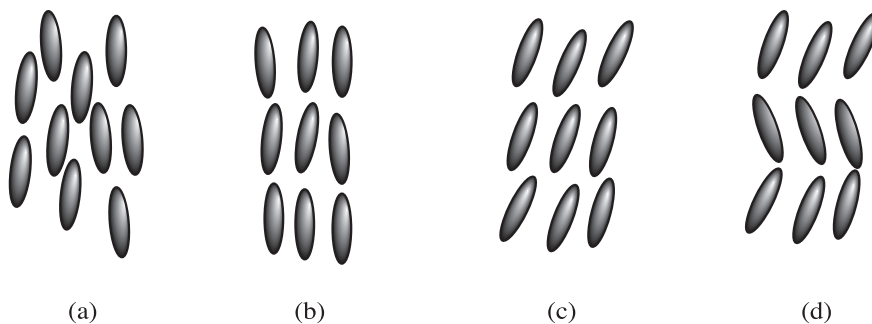


Figure 1. The structures of the most important liquid crystalline phases illustrated for the case of rod-like molecules; (a) nematic, (b) smectic A, (c) smectic C and (d) smectic C<sub>a</sub>.

A liquid crystalline material has, like normal materials, a solid phase (normally crystalline, *i.e.* containing both orientational and 3D positional order) and a liquid (isotropic) phase. However, in between these two phases the material has one or more intermediate liquid crystal phases. The simplest such phase is the *nematic* phase (see figure 1a) where there is no positional order at all, but where the molecules locally orient parallel to a certain direction given by a vector called the *director*, denoted  $\mathbf{n}$ . The nematic phase will not be discussed in this work, but instead we will concentrate on the more ordered *smectic* phases. In these phases the molecules are positionally ordered in layers, *i.e.* there is translational order along one dimension (see figure 1b-d), but within the layers there is no long-range positional order. A number of different smectic phases exist, and some of the most important ones are summarized in table 1 (listed in order of falling temperature). In SmA the director is oriented along the layer normal, while the SmC and SmI phases are distinguished by a non-zero angle (tilt) between the director and the layer normal. The terms *syn-* and *anticlinic* refer to whether or not the tilt changes from layer to layer. In the former case the molecules always tilt in the same direction, while in an anticlinic structure the tilt direction is opposite in neighboring layers.

Table 1: Overview of some important smectic phases.

<i>Phase</i>	<i>Director tilt relative to layer normal</i>	<i>In-layer (short-range) positional order</i>
SmA	No tilt	No order
SmC	Synclinic	No order
SmC <sub>a</sub>	Anticlinic	No order
SmI	Synclinic	Hexagonal order
SmI <sub>a</sub>	Anticlinic	Hexagonal order

## 1.2. Chiral smectic liquid crystals

If the liquid crystal molecules are chiral, *i.e.* they lack mirror symmetry, this may radically change the macroscopic behavior of the phase, and such a phase is therefore differentiated from the achiral one by adding a star after the letter, *e.g.* SmA\*, SmC\*, etc. The molecular arrangement of the chiral phase may be completely similar to the achiral version (as in SmA and SmA\*) or distinctly different (as in SmC and SmC\*), but the physical *properties* of the chiral phases are always different from those of the achiral ones, as will become clear below.

### 1.2.1. The SmC\* phase

The SmC\* phase is a tilted phase, *i.e.* all molecules are inclined an average temperature dependent angle  $\theta$  (called the tilt-angle) relative to the layer normal, just as in the achiral SmC pictured in figure 1. However, the star in the name indicates that the molecules (or at least some of them) are chiral. Thus the phase is chiral, which clearly distinguishes it from SmC. In general, this phase will also tend to form a macroscopic helical structure. As a helix within the layer plane is incompatible with a layered structure<sup>1</sup>, the helix axis must be oriented along the layer normal. The variable that changes

along the helix axis is the *phase-angle* (often denoted  $\varphi$ ), *i.e.* the angle describing the direction towards which the molecules in a specific layer tilt (see figure 2, right part). Instead of the phase-angle (or azimuthal angle as it is also called) one sometimes prefers to speak of the *c-director*, which is simply the projection of the director onto the layer plane, see figure 2 (right part).

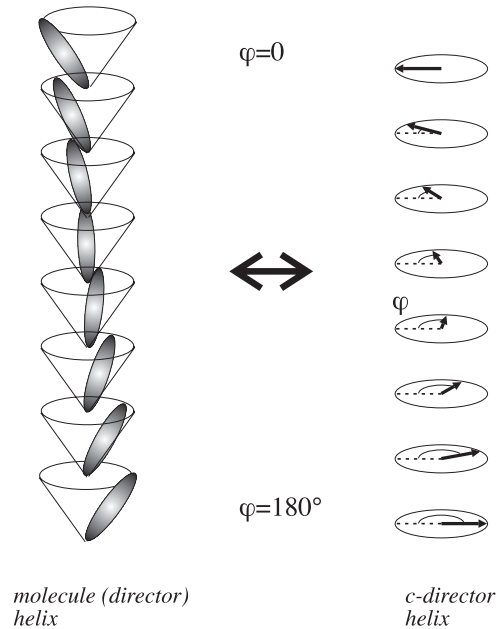


Figure 2. The chiral smectic C\* phase features a helical director configuration, where the helix axis is parallel to the layer normal. The tilt-angle is constant throughout the sample, but the phase-angle changes continuously from layer to layer. Sometimes one prefers to describe the SmC\* structure using the concept of the *c-director*, which is simply the projection of the director onto the layer plane (right part).

The periodicity of the helix, called the *pitch*, often increases somewhat with increasing temperature, but the variation might be much more complex and varies from compound to compound. In some materials there is even a helix inversion, meaning that the pitch first increases to infinity and then decreases, within the SmC\* phase. This occurs when the handedness (or sense) of the helix at the low-temperature end of the SmC\* phase is opposite of the one at the high-temperature end. The only way of continuously going from a right-handed to a left-handed helix is by passing through an infinitely long helix. A helix inversion is easily observed by looking at a quasi-homeotropic<sup>2</sup> sample through a polarizing microscope. In the vicinity of the inversion temperature the texture becomes very unstable and large schlieren constantly appear and disappear. If one studies the optical rotation (see below) on different sides of the helix

- 
1. An in-layer helix would break the layers, and therefore such a helix-structure is incompatible with the layered structure. In certain smectic liquid crystals with very strong twisting power, the layers may actually break up and form ordered defect structures. We can see these so-called TGB (Twist Grain Boundary) phases in a narrow temperature range.
  2. As homeotropic alignment indicates that the director is perpendicular to the sample substrates, the use of this word is not very adequate for smectic phases in which the director tilts relative to the layer normal. In this case I refer to the geometry where the layers are in the plane of the cell, and the layer normal (or the cone axis) thus perpendicular to it, as *quasi-homeotropic*.

inversion one will also see that the sign has changed, reflecting the change of helix handedness.

The helical structure gives the material interesting optical properties. First of all, the medium gets an unusually strong optical activity, *i.e.* it will strongly rotate the polarization plane of linearly polarized light passing through the medium along the helix axis. Secondly, one may see selective reflection in a quasi-homeotropically aligned sample; circularly polarized light with a wavelength equal to the pitch of the helix, and with the same handedness as the helix, cannot propagate through the medium but will be completely reflected (Bragg-reflected). Light with the opposite handedness can pass through unobstructed. This means that if one shines unpolarized white light along the helix axis, most of the light will pass through, but one circularly polarized component of one specific wavelength will be completely reflected. If the pitch length corresponds to visible wavelengths, this is easily seen by the naked eye – the sample becomes brightly colored.

One of the most interesting properties of the SmC\* phase is that its symmetry permits the presence of a *spontaneous polarization*  $P_s$ , within the layer plane and perpendicular to the director [1]. However, because of the steric coupling between the director and  $P_s$ , the helical director configuration will lead to a cancellation of polarization in bulk samples, but in specific geometries the helix may be suppressed and then the SmC\* liquid crystal will exhibit a macroscopic spontaneous polarization which may be switched between two stable states [2]. It thus fulfills the requirements to be called *ferroelectric*, and as such it is extremely interesting for numerous applications. More about this in section 1.3. If referring to the *value* of polarization (*i.e.* in high- or low- $P_s$  materials) I will always use the subscript  $s$ , otherwise I will not use it consistently, especially not when looking at  $P$  as a local polarization.

### 1.2.2. The SmC<sub>a</sub>\* phase

During the latter part of the 1970's and throughout the 1980's, reports on a new chiral tilted smectic phase, with unusual behavior became more and more common [3]. It was not until 1989 ([5] and [6]) that it was made totally clear that the new phase was an *antiferroelectric* liquid crystal, and the new phase was termed SmC<sub>A</sub>\* (also written<sup>3</sup> SmC<sub>a</sub>\*). As is clear from the name, the phase can be regarded as a subphase of SmC\*. It is a chiral tilted smectic phase with no in-plane ordering and it also features the helical arrangement of the molecules described above, and this leads to similar optical effects. The important difference is that the SmC<sub>a</sub>\* phase is *anticlinic* as opposed to the SmC\* phase which is *synclinic*, and it is this structure that gives the phase antiferroelectric properties.

The index  $a$  in SmC<sub>a</sub>\* is often taken to be short for *antiferroelectric*, which was perfectly adequate in the beginning when only chiral SmC<sub>a</sub>\* compounds existed. However, in the last few years several examples of *achiral* SmC<sub>a</sub> liquid crystals have been reported [7] and these *cannot* be antiferroelectric. A better interpretation of the subscript is therefore “ $a$  as in anticlinic” or “ $a$  as in alternating tilt”, since these two properties are common to both the chiral and achiral versions of the phase.

---

3. While the phase name was originally written SmC<sub>A</sub>\*, it has been pointed out that, for the sake of consistency, the use of capital letters should be reserved for phases, while indices should be written in lower case. The recommendation is now therefore (see references [3] and [4]) to use SmC<sub>a</sub>\* in place of SmC<sub>A</sub>\*. Even though this is unfortunately not yet very widely acknowledged I will use this notation throughout this work.

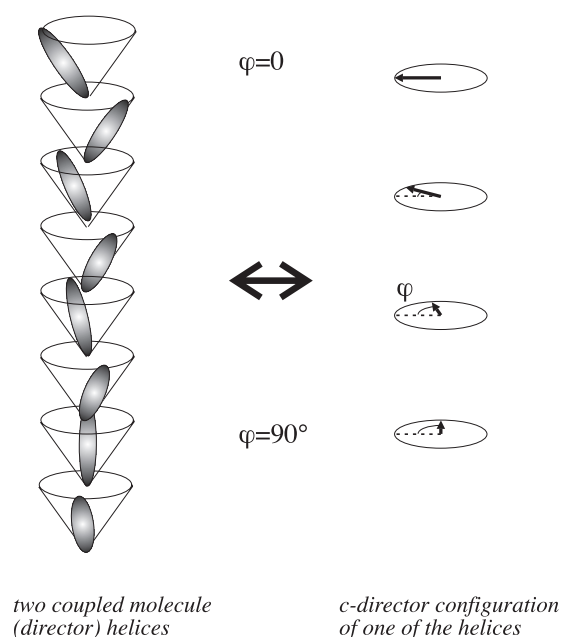


Figure 3. The chiral smectic  $C_a^*$  phase features a combination of an anticlinic structure and a helical director configuration. Such a structure can be obtained by coupling two helices, with a fix phase-angle difference of slightly more than  $180^\circ$  (it cannot be exactly  $180^\circ$  since the phase-angle shift on going between two neighboring layers should be constant).

### 1.2.3. SmC\* subphases: $SmC_\alpha^*$ , $SmC_{1/3}^*$ (= $SmC_\gamma^*$ ) and $SmC_{1/4}^*$

After recognition of anticlinic order it became obvious that SmC\* liquid crystals may have not only synclinic and anticlinic structures, but also intermediates. In one of the first antiferroelectric compounds to be properly characterized, MHPOBC, observations indicated a subphase called  $SmC_\alpha^*$  between the  $SmA^*$  and the  $SmC^*$  phases, and another subphase called  $SmC_\gamma^*$  between the  $SmC^*$  and  $SmC_a^*$  [8]. Later, several other subphases have been reported, but it is doubtful whether all observations really correspond to new thermodynamically stable phases or to other effects such as helix inversions or surface-induced effects. At present, five different chiral tilted smectic phases without in-plane positional order (*i.e.* of the chiral smectic C family, or smectic C\* family for short), including the  $SmC^*$  and  $SmC_a^*$ , have been experimentally confirmed [9].

Several different theoretical models have been presented for the variety of SmC\* structures, but none of them is in agreement with all experimental observations. One of the first models proposed was a one-dimensional Ising model (reviewed in [10]), where the tilt direction took the role of the Ising spin. Considering the very low realism of such a model (there is no room for phase-angles other than  $0^\circ$  and  $180^\circ$ ) it was surprisingly good in predicting most of the observed phases and some more - in fact, it led to the prediction of an infinite number of subphases according to the so-called *Devil's staircase*. A more realistic discrete two-dimensional XY-model (clock model) was later developed by Cepic and Zeks [11], and the predictions of this model agree with the experimental observations based on resonant X-ray scattering made by Mach *et. al.* [9]. However, the subphase structures predicted between  $SmC^*$  and  $SmC_a^*$  by the clock model (depicted in figure 4) give very low magnitude of optical rotatory power, something which is in disagreement with experiments [12].

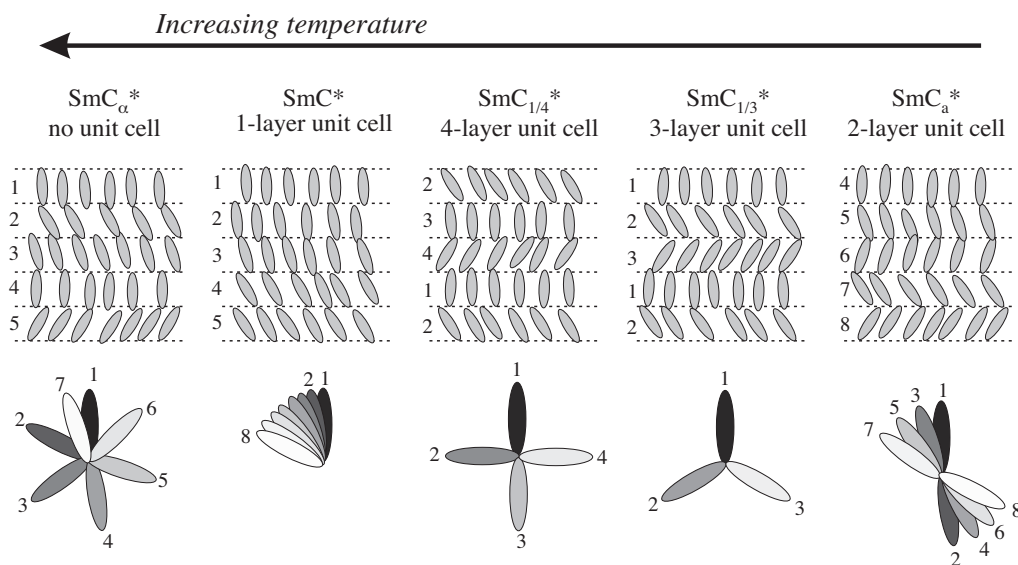


Figure 4. The structures of the five different phases of the smectic  $C^*$  family predicted by the clock model of Cepic and Zeks [11]. Darker molecules are below lighter ones. Each phase except  $\text{SmC}_\alpha^*$  can be considered as having a unit cell consisting of a distinct number of layers. This unit cell is repeated throughout the sample and a macroscopic helix due to the chiral interlayer interactions is then superimposed.

Many names have been given to the  $\text{SmC}^*$  subphases, and the nomenclature which should be used was therefore vividly discussed at the recent workshop on dielectric spectroscopy organized by professor J. K. Vij in Dublin (December 1999). The most reasonable path seems to be to base the names on a certain structural feature, and avoid basing names on the physical *properties* (ferro-, ferri-, antiferroelectricity, etc.) of the phases. For the moment there does not exist much certain knowledge concerning the subphases, but resonant X-ray scattering experiments show that one of the subphases which may appear between  $\text{SmC}^*$  and  $\text{SmC}_a^*$  has a unit cell consisting of three layers, while the other one has a four-layer unit cell. Therefore, a first suggestion was to call these phases  $\text{SmC}_3^*$  and  $\text{SmC}_4^*$ , where the former corresponds to the  $\text{SmC}_\gamma^*$  of MHPOBC and the latter to the one which has often<sup>4</sup> been called simply AF. This has the slight inconvenience of giving the impression that the phases are number three and four in a sequence of phases, which is neither the case nor the intention of the naming method. I will therefore follow the similar terminology suggested in reference [3] where the phase names are based on the magnitude of the wave vector corresponding to the unit cell, *i.e.* the reciprocal of the number of layers in each unit cell. This is in

4. While there is nothing wrong in the name  $\text{SmC}_\gamma^*$ , the term AF for  $\text{SmC}_{1/4}^*$  should definitely be avoided. First of all, such a name does not show that the phase is a member of the smectic  $C^*$  family, and second, it indicates that antiferroelectricity (AF stands for antiferroelectric) would be something unique for this phase. The  $\text{SmC}_a^*$  phase is the phase normally called antiferroelectric and this is the phase of interest when speaking of AFLCs. Very often AF is used to denote antiferroelectricity in general, no matter what phase it appears in (it does not have to be a liquid crystal!), so calling one specific phase AF can only lead to confusion. Actually, also Prof. Fukuda and co-workers have pointed out this problem [14], but unfortunately they did not propose a better alternative.

line with the reasoning of the early Ising models [10], where this value is referred to as the  $q$ -value of the structure. Note that we disregard of the macroscopic helix which may appear as an effect of chiral interactions, when defining the unit cell.

Using this scheme, the subphases between  $\text{SmC}^*$  and  $\text{SmC}_a^*$  are given the names  $\text{SmC}_{1/3}^*$  and  $\text{SmC}_{1/4}^*$ . The corresponding names for  $\text{SmC}^*$  and  $\text{SmC}_a^*$  would be  $\text{SmC}_0^*$  (or  $\text{SmC}_1^*$ ) and  $\text{SmC}_{1/2}^*$ , as the unit cells here correspond to an infinite number of layers (or 1 layer), and two layers, respectively. However, as the old names for these phases are both relevant and well-adopted, there is no reason to abandon them. The subphase which is sometimes found between  $\text{SmA}^*$  and  $\text{SmC}^*$  cannot be given an appropriate name according to this scheme, since it does not have a well-defined unit cell. It is therefore probably a good idea to keep the name  $\text{SmC}_\alpha^*$ .

Summarizing, the names which I will use for the smectic  $\text{C}^*$  family of phases are as follows (listed in order of increasing temperature):

$$\text{SmC}_a^* - \text{SmC}_{1/3}^* - \text{SmC}_{1/4}^* - \text{SmC}^* - \text{SmC}_\alpha^*$$

All phases are helicoidal, but while the helix in the first four phases is a consequence of the chirality, this might not be the case in the  $\text{SmC}_\alpha^*$  phase, according to recent ideas of Cepic and Zeks [11]. In this picture,  $\text{SmC}_\alpha^*$  features an extremely short twist generated by non-chiral interactions, and the chirality only sets the sense of the twisting. The  $\text{SmC}_{1/3}^*$  and  $\text{SmC}_{1/4}^*$  both have extremely long helical pitch lengths, which gives them a quasi-homeotropic texture that under the polarizing microscope looks very similar to that of a  $\text{SmC}^*$  or  $\text{SmC}_a^*$  phase exhibiting a helix inversion. In fact, the transitions from and to these subphases are often connected to a helix inversion.

It might be that a more adequate description of these structures could be achieved with some combination of clock and Ising-like models. One way of achieving such a description would be to allow distortions in the clock model unit cells, *i.e.* having non-constant phase-angle differences between neighboring layers in the  $\text{SmC}_{1/3}^*$  and  $\text{SmC}_{1/4}^*$  phases [12]. The presence of such irregularities seems to be supported by the experimental observations that it, at least in cells, is impossible to achieve a uniform quasi-homeotropic alignment.

### ***1.3. Polar effects in liquid crystals***

The discovery that liquid crystals may be ferroelectric and antiferroelectric has had far-reaching consequences. Not only is it so important from an applicational point of view that all major Japanese producers of flat panel displays are now doing research on chiral smectics, but it has also opened up a new direction in liquid crystal research, and since 1987 there exists a conference series devoted entirely to polar liquid crystals. The conferences are called FLC, for Ferroelectric Liquid Crystals, but deal with all kinds of polar order (heli-, ferri-, antiferroelectric order being subclasses) for which polar liquid crystals is a better collective term.

Unfortunately the large interest in polar liquid crystals has also had the effect that a large number of scientists with a variety of background start using the terms in “their own” way. This has led to a large degree of confusion; especially when one is forced to consider “ferroelectricity in the view of Mr. X or Mr. Y”. A striking example of the chaotic situation may be found in reference [13], where apparently the authors them-

selves could not agree on the nature of the polar effects: “Some of the authors (H. T. and A. F.) suggest the  $S^*_{C_a}$  phase is ferrielectric only just above the  $S^*_C-S^*_{C_a}$  transition. At higher temperatures it has antiferroelectric properties (see [4]). In the following, we will call this phase ferrielectric for simplicity.”, where the [4] refers to an internal reference, and not to reference [4] in this work. Such an attitude can only lead to misunderstandings, and I would therefore like to briefly review the definition of the terms which we will encounter [3].

### 1.3.1. Ferroelectricity, antiferroelectricity and ferrielectricity

All materials can be polarized by an electric field but most materials have no polarization when the field is switched off. The exceptions to this, *i.e.* materials which have a non-zero spontaneous polarization  $P$  in the absence of an electric field, are called either *pyroelectric* or *ferroelectric*. Whereas the polarization of the former can not be changed substantially by applying an electric field, the latter may be switched between *two stable states* by applying an electric field. The states are differentiated by the sign (or direction) of  $P$ , and they are stable in the sense that the sample stays in the one to which it was last switched, even after the field has been switched off.

At higher temperatures the ferroelectric normally has a phase of higher symmetry which more or less reacts like a normal dielectric on applying a field. However, on approaching the transition temperature  $T_c$  from above, the response usually grows to become very large and seems to become infinite at  $T_c$ . In this case we call the high-temperature phase *paraelectric*. Its distinction from a normal dielectric lies in the very large and strongly temperature dependent dielectric susceptibility. Paraelectricity is thus, as we will soon realize, on the threshold to being a collective phenomenon.

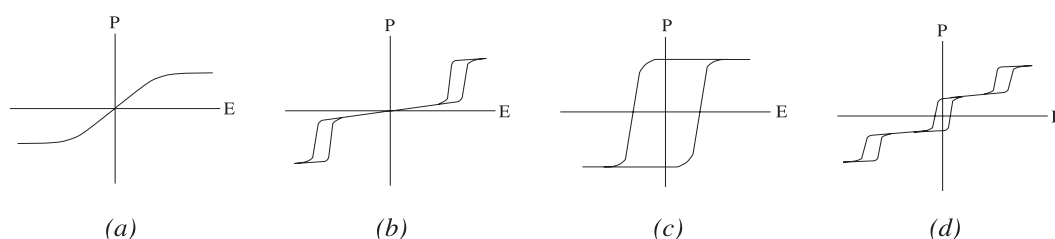


Figure 5. Response of polar dielectrics, *i.e.* materials which contain permanent dipoles, to an external electric field. The dielectric or paraelectric (a) effect is linear in the field, the antiferroelectric (b) is distinguished by a double hysteresis loop: two loops at non-zero field values but only one stable state, and the ferroelectric (c) has two stable (zero field) states and shows a large hysteresis when switching. The ferrielectric effect (d) has characteristics of the two latter and thus shows a triple hysteresis loop: one loop at zero field and two around the threshold fields (positive and negative) for switching to the ferroelectric state.

An *antiferroelectric* material also has no measurable polarization in the absence of a field, but locally antiferroelectrics do have a non-zero spontaneous polarization. However, these materials are made up of two sublattices, in which the directions of the polarizations are opposite, and therefore the total macroscopic polarization cancels to zero. When applying an electric field one will see the standard weak linear (dielectric) response in the beginning, but on passing a threshold value of the field, one sublattice flips over to the direction of the other and we thus obtain the so-called *field-induced ferroelectric state* of the antiferroelectric material.

*Ferrielectricity* represents a different order, and is in a way something in between

ferro- and antiferroelectricity. This term applies for a material with two sublattices, like the case of antiferroelectrics, but where the polarization magnitude of the sublattices is not the same. It equally well applies to a material with three sublattices of equal  $P_s$ -value, which can be switched independently. The response of such a system is drawn in figure 5 (d). Both these systems have an incomplete cancellation of polarization in the ground state, so just like ferroelectrics we have a *bistable zero-field state*, but with much lower values of macroscopic polarization. On switching a ferrielectric, we again flip the different sublattices, and hence we get hysteresis loops at non-zero voltages as well. The typical ferrielectric response is thus very similar to a combination of the ferroelectric and the antiferroelectric.

### 1.3.2. Which liquid crystals can be ferro-, antiferro- or ferrielectric?

As polarization has a direction, the presence of a spontaneous polarization imposes specific symmetry requirements. In liquid crystals, only chiral tilted smectics have a low enough symmetry to permit the presence of a spontaneous polarization, as was pointed out by R. B. Meyer *et. al.* in 1975 [1]. While achiral tilted smectics, such as SmC, have a mirror plane containing the director and the layer normal, the chirality removes this mirror plane, thus allowing a non-zero  $P_s$ -value perpendicular to the director and to the layer normal.

As has already been pointed out, the helical configuration of chiral SmC\* bulk samples leads to a cancellation of the polarization, and a bulk sample is helical antiferroelectric, or *helielectric*, rather than ferroelectric. However, if the compound is introduced in a very thin cell (of the order of the helical pitch), the surface interactions will suppress the helix [2]. In this *surface-stabilized* geometry the helix is intrinsically absent, and such a sample therefore shows ferroelectric properties, *i.e.* in the absence of a field it will exhibit a non-zero macroscopic polarization which may be switched between two stable states. This can easily be verified since any ferroelectric sample will spontaneously form domains of polarization up and polarization down. As these domains in the SSFLC (Surface-Stabilized Ferroelectric Liquid Crystal) by necessity have different orientations of the director, they will look different in the polarizing microscope. If one applies a triangular wave electric field over such a cell one will also see the typical ferroelectric response of figure 5 (c).

The SmC<sub>a</sub>\* phase is also helielectric in the bulk phase but also here the helix may be suppressed by surface interactions. We then obtain a surface-stabilized *antiferroelectric* liquid crystal. By applying an electric field we will see the typical tristate switching pictured in figure 5 (b). Also in a thicker cell one will see a similar response at low frequencies (< 50 Hz) since the helix may be unwound by the electric field at a lower voltage than the threshold for switching to the ferroelectric state. At higher frequencies the relaxation back to the AF state (E=0) is however far too slow, and then the response for the antiferroelectric will change towards the behavior shown by a ferroelectric in figure 5 (c).

What are then the polar characteristics of the subphases between SmC\* and SmC<sub>a</sub>\*? This is an interesting question since they are often referred to as *ferrielectric* phases. In the bulk state the SmC<sub>1/3</sub>\* is helielectric according to the resonant X-ray scattering experiments and to the clock model. However, with a distorted unit cell, indicated by the experimentally observed optical activity of the phase, it might have ferrielectric properties. On the other hand, in the case of SmC<sub>1/4</sub>\*, which has also most often been called ferrielectric, there is nothing reminding of ferrielectricity in its

behavior. The distorted unit cell model would still give it antiferroelectric properties in the bulk [12].

It is in principle possible to imagine that the  $\text{SmC}_{1/3}^*$  phase could be surface-stabilized to a state with a different number of layers having polarization up and layers with polarization down, which would then result in a ferrielectric sample. However, it is now also a well-known fact that the subphases, including the  $\text{SmC}_{1/3}^*$ , can be completely squeezed out by the action of surfaces, and it is thus questionable if a surface-stabilized  $\text{SmC}_{1/3}^*$  structure can at all be obtained. If it can, this should at zero field show bistability and domains of polarization up and polarization down, respectively, but to my knowledge this has not been reported in accounts of “ferrielectric” electrooptic switching. Considering that the cells typically used for electrooptics are rather thin ( $\approx 2 - 10 \mu\text{m}$ ), and that the helical pitch of the  $\text{SmC}_{1/3}^*$  phase is extremely long, the phase, if it still exists in the thin sample, should be surface-stabilized. Within the context of ferrielectricity it is then difficult to explain the absence of bistability. As pointed out in the previous section, however, the ferrielectric response is very similar to a combination of the ferroelectric and the antiferroelectric, so a more probable explanation is that the switching behavior is due to coexistence of  $\text{SmC}^*$  and  $\text{SmC}_a^*$  [15], a phenomenon which is often observed in very thin cells (see chapter 5).

There is no reason to automatically call the subphases “ferrielectric” just because they happen to appear in the temperature interval in between  $\text{SmC}^*$  and  $\text{SmC}_a^*$ . Unfortunately such a terminology has often been used, with the result that “ferrielectric”, when encountered in a paper on liquid crystals, can in principle mean anything.

Also the paraelectric behavior exists in liquid crystals. This is typically found in the  $\text{SmA}^*$  phase, and the paraelectricity is reflected in the electroclinic effect, or soft mode effect, which is a field-induced tilt coupled to the appearance of polarization.

Dielectric spectroscopy is a very interesting technique for studying the different polar liquid crystals, since the occurrence of a spontaneous polarization may contribute greatly to the dielectric permittivity of the sample. The dielectric response of the different subphases in different geometries is the main topic of chapter 3.

## 1.4. Summary

Liquid crystals are fluids with orientational order. Smectic liquid crystals also have a one-dimensional positional order, and therefore appear layered. If the molecules are chiral and tilted, we speak of the smectic  $\text{C}^*$  family of phases. To date five different members of this family have been experimentally verified:  $\text{SmC}_\alpha^*$ ,  $\text{SmC}^*$ ,  $\text{SmC}_{1/4}^*$ ,  $\text{SmC}_{1/3}^*$  ( $= \text{SmC}_\gamma^*$ ) and  $\text{SmC}_a^*$ .

The different members of the smectic  $\text{C}^*$  family all have a low enough symmetry to permit a local spontaneous polarization and are therefore termed *polar liquid crystals*. The polar effects that are observed in these liquid crystals are ferroelectricity (bistable switching) and antiferroelectricity (tristate, but monostable switching). In contrast to polar solids, however, the temperature range of ferroelectricity lies above that of antiferroelectricity, in the case that a liquid crystal exhibits both properties.

The presence of a spontaneous polarization makes the smectic  $\text{C}^*$  family of liquid crystals a good object for study by dielectric spectroscopy, because this is one of the rare techniques which allow to probe both individual molecular motion and collective motion in which a large number of dipoles are interacting coherently.

## 2. DIELECTRIC SPECTROSCOPY

---

*Though this be madness, yet there is method in it*  
– William Shakespeare

### OVERVIEW

*In this chapter I will discuss the experimental technique which is the basis for this study. I will try to give an understanding of how the technique works and what we can do with it. The starting point will be a discussion of how dielectric materials respond to steady-state and alternating electric fields. This will bring us to the complex dielectric permittivity and the two most common equations used to model its behavior at varying frequencies; the Debye and Cole-Cole equations. This knowledge will be needed in the next section when the specific case of liquid crystal dielectric spectroscopy is discussed. The chapter ends with an overview of the different techniques available for presenting and analyzing experimental data.*

### 2.1. Polarization of Dielectrics

Liquid crystals are dielectrics, *i.e.* they have low electrical conductivity, but *polarize* in presence of an electric field  $\mathbf{E}$ . This means that the electric field induces an internal charge reorganization, or distortion, in the material, such that a net electric dipole moment per unit volume appears. We call this the *polarization*  $\mathbf{P}$  and the unit is<sup>1</sup> Cm<sup>-2</sup>. By convention, the polarization is (among physicists) defined as pointing from the negative to the positive charge.

The magnitude and direction of the polarization induced by a unit electric field is a characteristic of the material, and it is given by the tensorial material parameter  $\chi$ , which is called the *dielectric susceptibility*:

$$\mathbf{P} = \chi \epsilon_0 \mathbf{E} \tag{1}$$

The physical constant  $\epsilon_0$  is the permittivity of free space and its value is approximately  $8.85 \cdot 10^{-12}$  C/Vm. In dielectric spectroscopy we deal not only with the dielectric sus-

---

1. As the polarization is equal to dipole moment per unit volume, the unit is really (Cm)m<sup>-3</sup>, which of course reduces to Cm<sup>-2</sup>, or charge per unit area. This indicates that there is an equivalence between polarization and surface charge, and this is indeed the case; the net surface charge per unit area is numerically equivalent to the volume polarization [16].

ceptibility, but more often with a related material parameter called the *relative dielectric permittivity* (or dielectric constant<sup>2</sup>)  $\epsilon_r$ .

$$\epsilon_r = 1 + \chi \quad (2)$$

The reason for introducing  $\epsilon$  is that it gives a simple relation to obtain the electric displacement,  $\mathbf{D}$  (which is equivalent to the free surface charge):

$$\mathbf{D} = \epsilon_0 \mathbf{E} + \mathbf{P} = \epsilon_0(1 + \chi) \mathbf{E} = \epsilon_0 \epsilon_r \mathbf{E} \quad (3)$$

Conversely, if we know the dielectric permittivity of a material, we obtain the field-induced polarization through the following relation:

$$\mathbf{P} = \epsilon_0 \mathbf{E} (\epsilon_r - 1) \quad (4)$$

The dielectric permittivity is a *macroscopic* quantity, and this is what makes it so useful; it relates the known *external* field  $\mathbf{E}$  (which is usually different from the local microscopic field  $\mathbf{E}_{\text{local}}$ , which we *don't* know) to the macroscopic polarization. The macroscopic polarization is of course a result of different microscopic polarization mechanisms (modes), and these we may divide into two main categories:

1. *Charge displacement (distortion) polarization.* An applied electric field will push the negative electrons in the material in one direction and the positive nuclei in the other. In the case of an ionic crystal the same kind of displacement will occur for negative and positive ions, respectively. Even though the displacements are very small, they will produce an induced dipole moment, the value of which is given by  $\mathbf{p}_{\text{dis}} = \alpha \mathbf{E}_{\text{local}}$ , where  $\alpha$  is a microscopic material parameter called the *polarizability*. This relation holds provided the field is not so strong that non-linear effects appear.

Charge displacement is very fast and thus such mechanisms contribute to  $\epsilon_r$  up to very high frequencies (IR-UV radiation).

2. *Orientalional polarization.* If the molecules of our sample have permanent dipole moments, we would expect this to give a contribution to the macroscopic polarization. However, the thermal disorder of the undisturbed state leads to random molecular orientations<sup>3</sup> and the dipoles cancel each other. But if an electric field is applied, there will be an aligning force opposing the thermal disorder, and we will get a bias in the molecular vibrations and rotations corresponding to a partial orientation of the dipoles, which gives a contribution

---

2. Since the dielectric constant is *not* a constant, but a function of frequency, I find the name dielectric permittivity less confusing and will therefore stick to this denotation.

3. The molecular directions in a liquid crystal are of course not random, but due to the sign reversal invariance of the director, there can be no net polarization along the director. A molecule with a dipole moment pointing upwards will have neighbors with dipoles pointing downwards, and vice versa, and so the total polarization cancels out also in the liquid crystal case. In the special case of chiral smectic C\* liquid crystals a net polarization *perpendicular* to the director is allowed by symmetry. More about this further on...

to the macroscopic polarization. Of course this holds only provided that the molecules have sufficient possibilities to reorient, as in fluids.

Certain crystals and liquid crystals (in specific geometries) have symmetries allowing a ferroelectric or antiferroelectric polarization (see section 1.3). If a sufficiently strong electric field is applied over a ferroelectric, the spontaneous polarization will line up with the field and as a result, such materials may have huge dielectric permittivities. In contrast to the just mentioned non-collective molecular reorientation process present for all materials made up of dipolar molecules, this dipole movement is *collective*, *i.e.* a large number of molecules move in phase with one another.

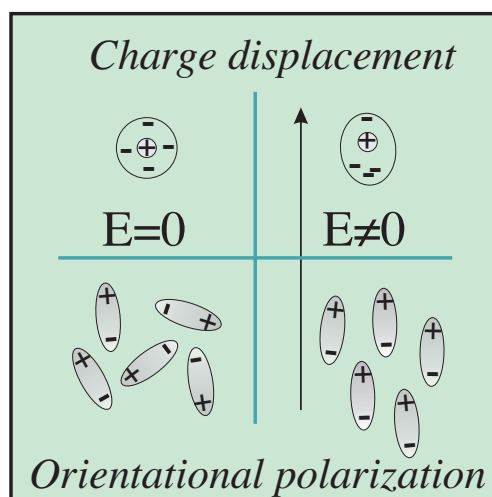


Figure 6. A dielectric material can respond in two ways to an electric field, here illustrated for the case of an isotropic medium. The negative electron clouds and positive atom nuclei, which are normally distributed evenly in a charge-cancelling fashion, may be displaced relative to each other, such that microscopic dipoles are induced (upper part). If the material consists of polar molecules which are normally randomly oriented, the field may cause an alignment of the molecules such that a macroscopic dipole moment appears (lower part). This is of course a very naive picture since the molecules are always vibrating and rotating at very high frequencies. The electric field will, however, bias the vibrations and rotations in a way corresponding to an aligning effect.

Why is the dielectric permittivity of interest in liquid crystal research? Take a look at the mechanisms mentioned above: do all mechanisms always contribute to the measured dielectric permittivity? The answer is no, and this is what makes  $\epsilon$  a very interesting quantity. With an applied DC-field all mechanisms will be present, but for AC-fields the contribution from each mechanism will eventually disappear when the frequency is raised. Each mechanism is counteracted by viscous forces and hence it cannot be driven at infinite speed. If it is driven back and forth at too high a frequency, it simply will not have time to be activated before the driving field changes sign, so at very high frequencies there will be no contribution to the permittivity due to this specific mechanism. On approaching a certain characteristic frequency the driven motion seriously begins to lag behind the force. At this very frequency  $\mathbf{P}$  is  $90^\circ$  out of phase with  $\mathbf{E}$ . The fluctuation amplitude has then decreased to half of its maximum value, and at this point maximum energy is absorbed from the electric field and transformed into heat in the material. This is exactly how a microwave oven works: the oven applies an electromagnetic field with a wavelength of approximately 10 cm, and the orienta-

tional polarization mechanism of the water molecules in the food will be excited, at a rate close to its limiting frequency. Therefore the dipolar reorientations will always be about  $90^\circ$  out of phase with the field, energy is absorbed, and the food is warmed up. At higher frequencies the absorption, and also the response amplitude, would rapidly decrease to zero.

In figure 6 the polarization mechanisms have been illustrated for the case of an isotropic material. In a liquid crystal the picture is much richer. In a nematic, because of directional anisotropy, we have two modes of orientational polarization and we have to distinguish between  $\parallel$  and  $\perp$  (parallel and perpendicular to the director). In the SmA\* phase (it needs to be chiral) we have a second collective mode which is a new dielectric mode, the electroclinic or soft mode. In the SmC\* phase we have a strong mode, giving a high contribution to  $\epsilon''$ , from the important polarization of each layer, which tries to align in the direction of the field by the easy azimuthal motion around the smectic tilt-cone. This mode is often called the Goldstone mode. Finally, in the SmC<sub>a</sub>\* phase we have two well-defined modes, at least one of which seems to be collective. We will have to discuss all these modes and their characteristics in depth in the next chapter.

The limiting frequency is one example of several important quantities in the field of dielectric spectroscopy, without good and completely accepted names. It is often referred to as the critical frequency ( $f_c$ ) or relaxation frequency ( $f_r$ ), but neither of these names give any information about what is actually going on. I therefore prefer to call this frequency the *absorption frequency* of the mode,  $f_a$ . The polarization mechanisms possible in liquid crystals are summarized in table 2.

Table 2: Character of polarization mechanisms possible in liquid crystals. The method of study depends on in which range the absorption frequency,  $f_a$ , is found.

<i>Mechanism</i>	<i>Type</i>	<i>Method of study</i>
Electronic polarization	Induced dipoles	UV/VIS-absorption spectroscopy
Non-collective orientational polarization	Permanent dipoles aligned	Dielectric spectroscopy, IR-absorption spectroscopy
Collective orientational (ferroelectric) polarization	Permanently aligned dipoles reoriented	Dielectric spectroscopy

## 2.2. What do we measure with dielectric spectroscopy ?

The dielectric spectrum becomes interesting in the vicinity of the absorption frequencies of the polarization mechanisms (modes) present in the material under study, and in frequency-domain spectroscopy (which is the essential method applied in this thesis) we therefore measure the dielectric permittivity while scanning the frequency of the measuring field. As the equipment is limited to the approximate frequency range 1 Hz - 1 GHz, this means that charge displacement modes cannot be studied with dielectric spectroscopy since their absorption frequencies lie much higher. The same normally holds for contributions from reorientation of molecular segments. The study of such mechanisms is instead performed in absorption spectroscopy (IR – intramolecular reorientation, UV/VIS – electronic polarization).

### 2.2.1. The complex dielectric permittivity

Now we have reached the stage when it is time to get down to some formalism regarding the dielectric permittivity. A good starting point is the behavior in time of the induced polarization  $P$  after turning on a static electric field  $E$  across the dielectric. We turn on the field at  $t = 0$  and want to know its value an arbitrary time thereafter. After waiting a very long time,  $P$  will have reached its final saturation value  $P_f$  given by:

$$P_f = \chi(0) \epsilon_0 E \quad (5)$$

where  $\chi(0)$  denotes the static (the zero stands for zero frequency) susceptibility. It is reasonable to assume that, before reaching the equilibrium value,  $P$  will change at a rate which is proportional to its deviation from that value. This corresponds to the basic assumption in irreversible thermodynamics, describing how a thermodynamic variable approaches its new equilibrium value, or how a perturbation in a variable relaxes back towards equilibrium, once brought out of it by some force [17]. We therefore write

$$\dot{P} = -\frac{P_f - P}{\tau} \quad (6)$$

where we have introduced the proportionality constant  $1/\tau$  with dimension of inverted time. Rewriting the expression as

$$-\frac{d}{dt}(P_f - P) = \frac{1}{\tau}(P_f - P) \quad (7)$$

we can immediately integrate it to

$$-\ln(P_f - P) = \frac{t}{\tau} + \text{constant} \quad (8)$$

Inserting  $P = 0$  for  $t = 0$ , the constant is found to be  $-\ln P_f$ , hence

$$\ln(P_f - P) - \ln P_f = -\frac{t}{\tau} \quad (9)$$

or

$$\frac{P_f - P}{P_f} = e^{-t/\tau} \quad (10)$$

which is reshaped to

$$P = P_f(1 - e^{-t/\tau}) \quad (11)$$

As this equation shows, the polarization is approaching its saturation value in an exponential way, with a characteristic time constant  $\tau$ , called the *relaxation time*. If, after a

long time, when  $P$  has reached the value  $P_f$ , we would instead turn off the field ( $E = 0$ ) we would, by the same simple analysis, have found that the polarization decays to zero according to

$$P = P_f e^{-t/\tau} \quad (12)$$

thus relaxing back with the same characteristic relaxation time which is a property of the medium, and more specifically of the polarization mechanism under consideration.

If we now instead apply an AC field,  $E = E_0 e^{i\omega t}$ , to a dielectric with a given relaxation time  $\tau$ , we want to investigate the response of the medium as we vary the frequency  $\omega$ . With  $P$  now written as

$$P = \chi(\omega) \epsilon_0 E \quad (13)$$

we assume that equation (6) is still valid at any instant. The response of the medium is now described by the frequency-dependent susceptibility  $\chi(\omega)$ . We can find  $\chi(\omega)$  with the ansatz

$$P = \chi(\omega) \epsilon_0 E_0 e^{i\omega t} \quad (14)$$

*i.e.* assuming that the induced polarization varies with the same frequency as the applied field. A phase difference between  $E$  and  $P$  will be hidden in  $\chi(\omega)$  which in general will be complex. Inserting (14) in (6) gives

$$i\omega P = i\omega \chi(\omega) \epsilon_0 E = \frac{\epsilon_0 E - \chi(0) \epsilon_0 E}{\tau} \quad (15)$$

hence

$$i\omega \chi(\omega) = \epsilon_0 - \chi(0) \quad (16)$$

or

$$\chi(\omega) = \frac{\epsilon_0}{1 + i\omega\tau} \quad (17)$$

Splitting in real and imaginary parts this gives

$$\chi'(\omega) = \frac{\epsilon_0}{1 + \omega^2 \tau^2} \quad (18)$$

$$\chi''(\omega) = \frac{\epsilon_0 \omega \tau}{1 + \omega^2 \tau^2} \quad (19)$$

This result was first published by Peter Debye in 1927 [17a] and a mechanism contributing to the polarization in the material in accordance with equations (17), (18) and

(19) is therefore called a Debye-type mechanism. Graphs of equations (18) and (19) are shown in figure 7. If we sweep the frequency  $\omega$  from zero to infinity it is seen from equation (18) that  $\epsilon'$  has a practically constant value  $\epsilon'(0)$  until  $\omega$  approaches  $1/\tau$ . It then decreases, having an inflexion point at  $\omega\tau = 1$  and becomes zero for  $\omega \gg 1/\tau$ . As for  $\epsilon''$ , it is vanishingly small except in the neighborhood of  $\omega\tau = 1$ , where it has a maximum (easily found on differentiating equation (19) with respect to  $\omega$ ). This is where the absorption occurs.

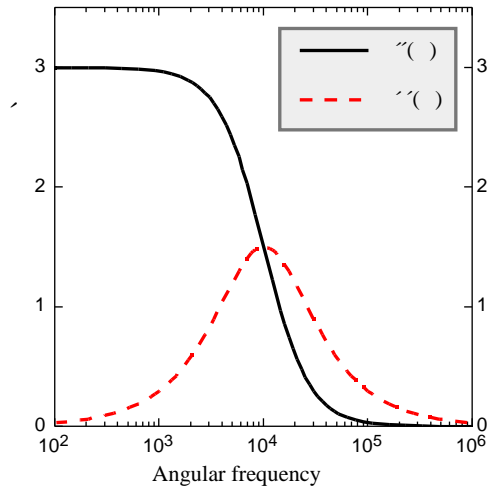


Figure 7. The real (continuous curve) and imaginary (dashed curve) parts of the Debye equation, as a function of angular frequency. The imaginary part has its maximum in the inflexion point of the real part. For this frequency of an applied field the medium is maximally lossy.

So far we have only considered *one* dielectric mode being excited in the medium. In reality there are several modes, often clearly separated in absorption frequency and each giving a contribution to  $\epsilon'$  as long as the applied frequency  $\omega$  is well below  $\omega_c^{-1}$  for the mode in question. In particular, this is true for the electronic excitations which always give a background contribution to  $\epsilon'$  and  $\epsilon''$  in dielectric spectroscopy, because their relaxation times are vanishingly small, so  $\omega\tau \ll 1$  is always valid. Thus their high frequency contributions  $\epsilon'_e$  and  $\epsilon''_e$  (which are consequently frequency independent in our spectroscopy range) have to be added at any applied frequency. Therefore we should, for completeness, extend equations (17), (18) and (19) to

$$\epsilon(\omega) = \epsilon_e + \frac{\epsilon(0)}{1 + i\omega\tau} \quad (20)$$

$$\epsilon''(\omega) = \epsilon''_e + \frac{\epsilon(0)\omega\tau}{1 + \omega^2\tau^2} \quad (21)$$

$$\epsilon'(\omega) = \epsilon'_e + \frac{\epsilon(0)}{1 + \omega^2\tau^2} \quad (22)$$

In terms of permittivity, the Debye equations thus take the form (we use  $\epsilon_r = 1 + \epsilon$  and note that the static susceptibility can be written  $\epsilon(0) = \epsilon_r - 1 = \epsilon_r - \epsilon_\infty$ )

$$\epsilon_r = \epsilon_\infty + \frac{\epsilon_r - \epsilon_\infty}{1 + i\omega\tau} \quad (23)$$

$$\epsilon' = \epsilon_0 + \frac{f_0^{-2}}{1 + \frac{f^2}{f_0^2}} \quad (24)$$

$$\epsilon'' = \frac{\left( \frac{f_0^{-2}}{2} \right) f}{1 + \frac{f^2}{f_0^2}} \quad (25)$$

This is the “official” form of the Debye equations which is most commonly used in the literature. In this form the static susceptibility is replaced with the difference  $\epsilon_0 - \epsilon_\infty$  and it is therefore often written  $\epsilon_0 - \epsilon_\infty$  and referred to as “dielectric strength”. This is a terminology we should try to avoid, since the term is long since used for something completely different. This problem will be discussed more in section 2.2.3, but for now I would just like to point out that there is no reason to abandon the use of the static susceptibility as a measure of the contribution of a mode, just because we are interested in the resulting *permittivity*. To simplify the writing somewhat, especially considering that we may have several contributing modes within the frequency range of dielectric spectroscopy, I will in the following, however, drop the attribute “static” and speak of *susceptibility of a mode*. The corresponding denotation will be just  $\epsilon'$ , or  $\epsilon''_n$ , in the case of several active modes, where  $n$  is an index referring to the particular mode of interest (analogously, we will drop the index  $a$  in the absorption frequency and replace it with an index denoting the mode to which it refers).

In practice we deal not with the angular frequency  $\omega$  and relaxation time  $\tau$ , but with the frequency  $f$  and absorption frequency  $f_a$ , related to  $\tau$  through:

$$\omega = 2\pi f, \quad \tau = \frac{1}{2\pi f_a} \quad (26)$$

The user-friendly form of the Debye equations, which are the ones referring to practical work, will thus be the frequency-domain equations:

$$\epsilon'(f) = \epsilon_0 + \frac{\epsilon_0 - \epsilon_\infty}{1 + \frac{f^2}{f_a^2}} \quad (27)$$

$$\epsilon''(f) = \frac{f}{f_a} \frac{\epsilon_0 - \epsilon_\infty}{1 + \frac{f^2}{f_a^2}} \quad (28)$$

In our experiments we apply a weak AC measuring field over the sample to obtain its conductivity and capacitance, and from these values the real and imaginary permittivity components  $\epsilon'$  and  $\epsilon''$  can be calculated (see appendix section 4). By successively increasing the frequency of the measuring field, one can clearly see how the real part of the dielectric permittivity decreases stepwise, each time the frequency passes an absorption frequency  $f_a$  (see figure 8, upper curve). Just like our theoretical approach predicted, we will at each such frequency also find a maximum value of the imaginary part of the dielectric permittivity (figure 8, lower curve), reflecting absorption of energy around this frequency.

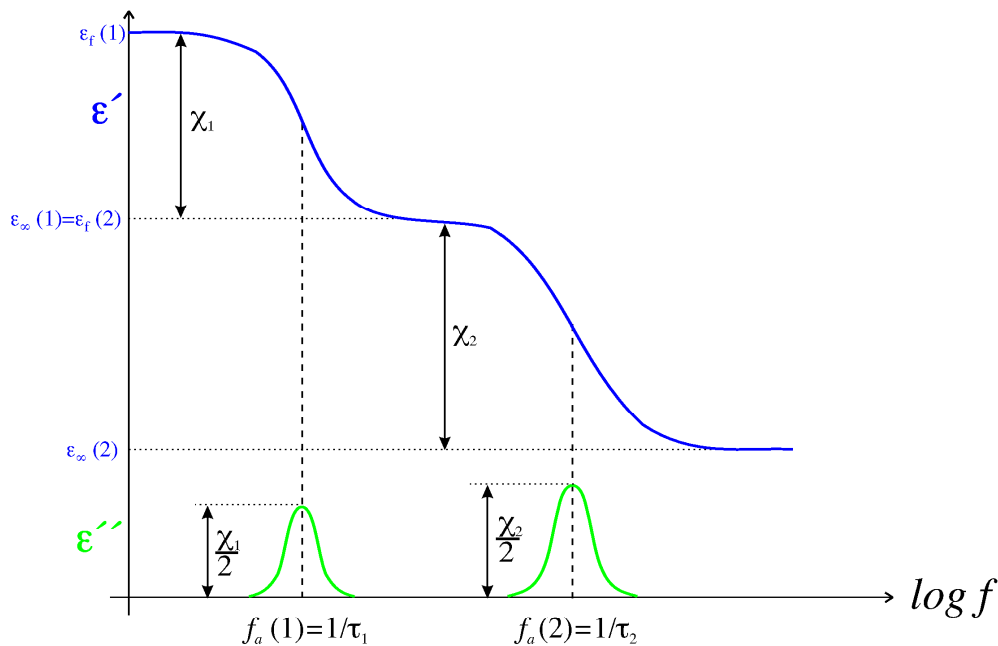


Figure 8. Typical behavior of the real (upper graph) and imaginary (lower graph) parts of the dielectric permittivity as a function of frequency, illustrated for the case of two modes within the measurement frequency window. Note that since the Debye analysis is performed considering only one mode, there will be several different values for the susceptibility (and hence also for  $f_a$  and  $\tau$ ) each corresponding to one mode. As is clear from the figure, the susceptibility in this sense is equal to the maximum contribution to the real part of the dielectric permittivity of one specific mode.

If several modes influence our measurement, we get several  $\chi$  and  $f_a$  values, each corresponding to one contributing mechanism. Each mode will then also get its specific set of  $f_c$  and  $\tau$  which I in the following, when needed, refer to as the *effective*  $f_c$  and  $\tau$  of the mode. The susceptibility is equal to the maximum contribution to the real part of the dielectric permittivity of one specific mode, the effective  $\chi$  value is the permittivity at the minimum frequency of no contribution from the mode, and the effective  $f_c$  is the sum  $\chi_1 + \chi_2$  (see figure 8).

The Debye analysis holds well only for some orientational polarization mechanisms, and not at all for electronic polarization, which is of resonant (harmonic oscillator) type. The latter does not bother us, since the frequencies at which the electronic polarization gets interesting are far above what we are measuring, but the first problem has to be attacked, and that will be the topic of the following subsection.

### 2.2.2. Non-Debye type orientational polarization mechanisms

When applying the Debye result to actual experimental data, one soon discovers that it seldom works very well. For polymer systems, and in many cases also in low molar mass liquid crystals, a mode turns out to be characterized by a *distribution* of relaxation times, and therefore it is impossible to obtain a good fit of equations (27) and (28) to experimental data. In order to cope with this problem, our result of the previous analysis has to be modified. Such a modification was first introduced by K. S. Cole and R. H. Cole<sup>4</sup> in 1941 [18], [19], and their starting expression bears the name the *Cole-*

Cole equation (here given on the frequency-domain form):

$$\varepsilon_r = \varepsilon_\infty + \frac{\chi}{1 + \left(i\frac{f}{f_a}\right)^{1-\alpha}} \quad (29)$$

For  $\alpha=0$  this expression is equivalent to equation (23), considering that  $\omega\tau=1$  corresponds to  $f/f_a=1$ . Separation into real and imaginary components gives us the following very useful expressions:

$$\varepsilon'(f) = \varepsilon_\infty + \chi \cdot \frac{1 + \left(\frac{f}{f_a}\right)^{1-\alpha} \sin\left(\frac{\alpha\pi}{2}\right)}{1 + 2\left(\frac{f}{f_a}\right)^{1-\alpha} \sin\left(\frac{\alpha\pi}{2}\right) + \left(\frac{f}{f_a}\right)^{2(1-\alpha)}} \quad (30)$$

$$\varepsilon''(f) = \chi \cdot \frac{\left(\frac{f}{f_a}\right)^{1-\alpha} \cos\left(\frac{\alpha\pi}{2}\right)}{1 + 2\left(\frac{f}{f_a}\right)^{1-\alpha} \sin\left(\frac{\alpha\pi}{2}\right) + \left(\frac{f}{f_a}\right)^{2(1-\alpha)}} \quad (31)$$

When  $\alpha=0$  the Cole-Cole equations reduce to the previous Debye expressions, but for non-zero values of  $\alpha$  we get a distribution of relaxation times, which in the dispersion plot ( $\varepsilon'$  vs. frequency) gives less distinct steps, and in the absorption plot ( $\varepsilon''$  vs. frequency) results in a broader and flatter curve (see figure 9).

By eliminating the frequency in the Debye (or Cole-Cole) equations one obtains the equation of a circle. This is the basis for a very illustrative way of presenting experimental permittivity data, which will be presented in detail in section 2.3.4

The parameter  $\alpha$  is purely empirical and there is no microscopic theory for it. If we imagine a certain dipole being in a liquid crystal containing only one simple molecular species, we would not be surprised to find a pure Debye behavior, *i.e.*  $\alpha \approx 0$ , or at least,  $\alpha \ll 1$ . Very often, however, we are investigating multicomponent mixtures, in which each particular dipole would not have a unique environment. This would lead to a smear out of the relaxation process and to  $\alpha \neq 0$ . In polymers, this environment is even much more complex and varying, and we would expect a large value of  $\alpha$ . In fact, the  $\alpha$  values found in liquid crystal polymers are generally very large, like  $\alpha \approx 0.9$ .

---

4. The Coles were actually brothers. Kenneth S. Cole, born 1900, Ph. D. from Cornell University 1926, was a renowned biophysicist holding a variety of academic positions, such as at Columbia University, New York and at University of Chicago. He was professor of biophysics at University of California in Berkeley from 1965. His younger brother Robert H. Cole, born 1914, Ph. D. from Harvard 1940, was professor of chemistry at Brown University, Providence, from 1951.

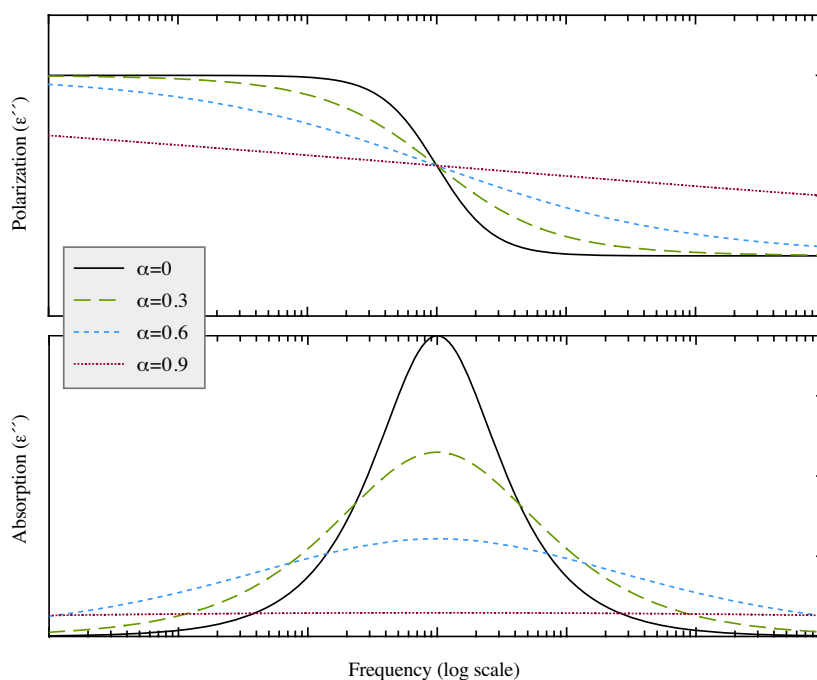


Figure 9. The effect of the parameter  $\alpha$  in the Cole-Cole equation is to broaden and flatten the absorption curve (imaginary part of the dielectric permittivity). This is equivalent to a distribution of relaxation times and often successfully models experimentally observed absorptions.

Sometimes even the Cole-Cole equation will not be sufficient to model experimental data, and therefore also this equation has been extended in a more or less *ad hoc* way. In the *Havriliak-Negami* equation an additional parameter  $\beta$  is added in order to account for asymmetries in the absorption curve. However, this equation is rarely used in the study of liquid crystals, simply because the Cole-Cole equation normally does the job, and also because the fitting easily gets unreliable with the Havriliak-Negami equation: it is not uncommon that you get a very good fit to experimental data with parameter values which are totally unreasonable.

### 2.2.3. Some words on terminology

Instead of utilizing the susceptibility for describing the contribution from a mode, many people introduce the shorthand  $\Delta\epsilon$  for the difference  $\epsilon_f - \epsilon_\infty$ , and often call it the “dielectric strength” or “dielectric contribution”. While the latter name is rather harmless, the former one, which is the more common, is certainly not a good choice. The reason is that dielectric strength already has a well-defined meaning in the field of dielectrics, namely the *maximum field strength a material can withstand before dielectric breakdown occurs*. Perhaps even more misleading is the use of the shorthand  $\Delta\epsilon$  for the difference  $\epsilon_f - \epsilon_\infty$ ; this notation is already well defined as meaning *dielectric anisotropy*,  $\Delta\epsilon = \epsilon_{\parallel} - \epsilon_{\perp}$ .

The nomenclature I use in this thesis, calling the contribution from a mode its susceptibility, is by no means the standard language in the field of liquid crystal dielectric spectroscopy. This solution to the terminology problem was suggested by Prof. J. H. Calderwood at the Dublin workshop on dielectric spectroscopy (December 1999), and it seems to be the simplest solution. There is no need for inventing new ter-

minology, and there is little risk of confusion. One only has to accept that the susceptibility must not always be the total susceptibility for a material, but it can be regarded as belonging to one specific mode. From equation (23) it is clear that we equally well could have defined a static permittivity for each mode, and we have in the Chalmers group previously used such terminology. It turned out, however, that this led to misunderstanding since dielectric spectroscopists may prefer the idea that  $\epsilon$  should be the *total* dielectric permittivity of the sample. Hopefully the division between permittivity and susceptibility makes the situation clearer. To this end, I find the name susceptibility very good, since each polarization mechanism certainly is “susceptible” to a certain degree towards being excited by an external field.

In section 2.2 we introduced the concept of relaxation time for a process contributing to the polarization. This is a macroscopic relaxation time, but can we also speak of a relaxation time for one molecule? Such a concept would certainly be rather difficult to imagine! On the molecular level we may on the other hand easily picture a *frequency* at which a mechanism occurs (e.g. number of flips per second) but can we transfer this to a macroscopic sample? The molecules certainly don't fluctuate as one!

My point is that the ease in the mathematical conversion between the time and frequency domains is not present for the corresponding conceptual conversion. In the case of dielectric spectroscopy one domain (the time domain) treats the matter macroscopically while in the frequency domain we study the dynamics of single molecules or mode fluctuations. Is there then really any meaning in such “transformed” concepts as “relaxation frequency” or “molecular relaxation time”? Unfortunately at least the former is widely used, but in my opinion such concepts should be avoided for sake of minimizing confusion. Therefore I propose that *relaxation time* corresponds to *absorption frequency* to form a conceptually acceptable pair.

Finally I would also like to comment on the names of the real and imaginary components of the permittivity. The latter is often referred to as the absorption, which is of course not quite correct;  $\epsilon''$  is *proportional* to the absorption, or rather absorption per cycle of unit field. The real component,  $\epsilon'$ , has no proper name, but when plotting it as a function of frequency one often speaks of a “dispersion curve”. This does of course not mean that  $\epsilon'$  can be referred to as dispersion (which sometimes occurs) - the curve illustrates the *frequency dispersion of  $\epsilon'$* .

### 2.3. Presentation of experimental data

Dielectric spectroscopy data can be presented in a variety of ways. They all have advantages and drawbacks, and to fully understand publications on dielectric spectroscopy, one should be acquainted with all of them. In the following I will go through the standard presentation forms exemplified with the smectic liquid crystal CG50, supplied by Avtar Matharu. This compound has a rich mesomorphism and a very interesting dielectric response. I will first, however, introduce an alternative way of expressing the absorption.

I should also mention before continuing, the two spurious peaks which always pester any liquid crystal dielectric spectroscopy experiment. At low frequencies there will always be a conduction contribution to the imaginary part of the permittivity,  $\epsilon''$ , which is due to the free ions which to some extent are present in all liquid crystal compounds. In the medium frequency (5 Hz to 13 MHz) dielectric spectroscopy treated in this thesis, one will never see the whole ionic peak, since its absorption frequency is in the mHz range, but one will see the right wing coming into our frequency window. In

the different spectra which will follow, the ionic contribution is therefore recognized as a constant increase in  $\epsilon''$  when approaching the low-frequency end of the diagram.

At higher frequencies we usually face a problem due to the measurement cell. The resistance of the electrodes results in a spurious mode, the so-called “cell relaxation” in the MHz range. The absorption frequency decreases with decreasing cell gap, so in cells of 2-5  $\mu\text{m}$  one will always see this mode in its entirety. In thick cells, only the low-frequency wing of the mode may be seen. Both these unwanted contributions, and how to treat them, will be treated in somewhat more detail in appendix section 2.

### 2.3.1. $\epsilon''$ or $\tan \delta$ ?

An interesting alternative to plotting  $\epsilon''$  in the absorption spectrum is to plot the so-called *loss tangent*, abbreviated  $\tan \delta$ . It is defined through the relation

$$\tan \delta = \frac{\epsilon''}{\epsilon'} \quad (32)$$

In order to realize the usefulness of this transformation it is worthwhile to insert equations (27) and (28) into equation (32) (we perform the calculations in the time-domain, where the equations are slightly less bulky):

$$\tan \delta = \frac{\frac{\epsilon''}{\epsilon'}}{\frac{\epsilon'}{\epsilon'}} = \frac{\frac{\epsilon''}{\epsilon'}}{\frac{\epsilon'}{\epsilon'}} = \frac{\frac{\epsilon''}{\epsilon'}}{\frac{\epsilon'}{\epsilon'}} \quad (33)$$

where I in the second step used that  $\epsilon'' = \epsilon' - \epsilon''$ . We have thus obtained an expression for  $\tan \delta$  which has the same form as equation (28) for  $\epsilon''$ , but where the corresponding susceptibility and relaxation time are rescaled. Transforming equation (33) to the frequency domain ( $\omega = 2\pi f$ ), we end up with the following relation:

$$\tan \delta = \frac{\frac{f}{f_a}}{1 + \frac{f}{f_a}^2} \quad (34)$$

where

$$f_a = f_a \sqrt{\frac{f}{f_a}} = \frac{f_a}{\sqrt{f}} \quad (35)$$

The point is that while  $\epsilon''$  is often rather small<sup>5</sup>,  $f_a$  may be very large in a polar system,

---

5. Remember that the effective  $\epsilon'$  value is the permittivity contribution from all mechanisms active at higher frequencies than the one to which it refers, and the strong contributors are usually found in the low-frequency end of the spectrum

and the absorption frequency is then shifted a considerable amount towards higher values. As will become clear in chapter 3, the  $\text{SmC}^*$  and  $\text{SmC}_{1/3}^*$  phases show polarization mechanisms with very high susceptibility but low absorption frequency. In an  $\epsilon''$  diagram these absorptions may thus to a large part extend past the low-frequency limit of our measurement window, and the part that is still visible is disturbed by the ionic contribution which dominates at low frequencies.

The drawbacks with this solution is that the cell relaxation peak tends to increase in importance (according to equation (35) the susceptibility of each mode is diminished by the square root of their effective  $\epsilon_\infty$  value which is much less for the cell relaxation than for the other modes), and the frequencies around which the absorptions are centered are no longer  $f_a$ . The shifts of equation (35) may also vary quite drastically from phase to phase, which may be a bit misleading (see *e.g.* figure 10 and its caption). Several comparisons between  $\epsilon''$  and  $\tan \delta$  plots will be given in the rest of this chapter.

### 2.3.2. Three-dimensional overviews and two-dimensional slices

A standard liquid crystal dielectric spectroscopy experiment incorporates at least three variables: the measuring frequency, the sample temperature and the dielectric permittivity. We may of course also vary the measuring field strength, the cell thickness or apply a DC-bias of varying magnitude, but let us for the moment consider these parameters as fixed. Since the dependent variable, the dielectric permittivity, is complex, we actually have four variables to consider when we want to present our data. All four can of course not be presented simultaneously in one graph, and it is therefore common practice to present the imaginary and real parts of the permittivity in separate graphs. So-called 3D-plots (strictly speaking they are of course perspective plots) are here very useful as they give a very good overview of how the permittivity of the studied compound varies with temperature and frequency. Some examples from CG50 under the influence of a 35 V DC-bias electric field are given in figure 10. The beauty of the 3D presentation and the good overview of the phase behavior is here quite evident (the interpretation of the response in terms of liquid crystal phases is the topic of the next section). In order to save space, the dispersion spectrum ( $\epsilon'$  vs.  $f$ , figure 10a) is often left out and one has to settle with the absorption spectrum (figure 10b, c or d). This is usually quite adequate.

When plotting the experimental data, the frequency axis is always logarithmic, since the absorption peaks are symmetric around  $f_a$  on this scale. It is often a wise choice to plot also the permittivity logarithmically, the reason being that its magnitude may vary substantially through different phases. If one for instance plots the response in a  $\text{SmC}^*$  phase in the same diagram as that in a  $\text{SmC}_a^*$  phase the latter phase will look completely “dead” on a linear scale adapted for the  $\text{SmC}^*$  phase response (see figure 10d).

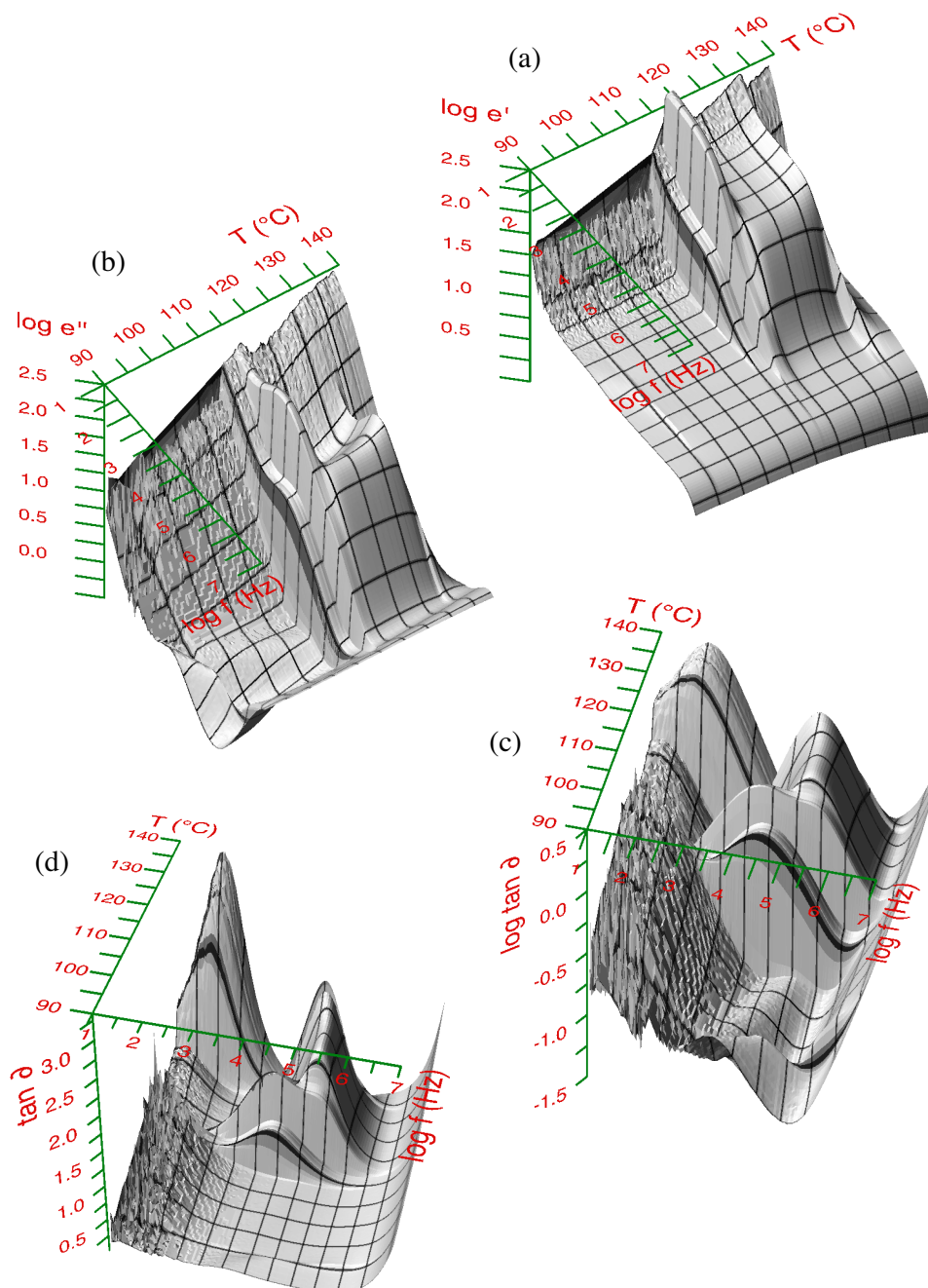


Figure 10. Four different 3D-plots for the material CG50 (see paper 2) in a planar  $50\ \mu\text{m}$  cell. This compound features  $\text{SmI}_A^*$ ,  $\text{SmC}_a^*$ ,  $\text{SmC}_{1/3}^*$  (or  $\text{SmC}_{1/4}^*$  - or both),  $\text{SmC}^*$  and  $\text{SmA}^*$  phases (listed in order of increasing temperature, *cf.* caption to figure 11). The data presented here is obtained with a DC-bias of 35 V applied over the cell, which has an immense effect on the response in the subphase region. Graph (a) shows the real permittivity component ( $\epsilon'$ ), graph (b) the imaginary component ( $\epsilon''$ ) and graph (c) the loss tangent ( $\tan \delta$ ) as a function of temperature and frequency. For comparison the latter is also plotted linearly in (d). Note how the absence of high-susceptibility mechanisms at higher frequencies in the  $\text{SmA}^*$  phase, leads to a very large  $\tan \delta$ -shift of  $f_a$  for the low-frequency ion peak. This is because the effective  $\epsilon_\infty$  value for the ionic contribution is equal to the “real”  $\epsilon_\infty$  (due to processes outside our frequency window) in the  $\text{SmA}^*$  phase, while it in  $\text{SmC}^*$  is increased by the ferroelectric susceptibility. The 3D-plotting program does not permit the use of  $\epsilon$  in the axis labels. Hence, the label  $\log e'$  or  $\log e''$  in 3D-plots in this thesis should read  $\log \epsilon'$  and  $\log \epsilon''$ , respectively.

A common feature of media giving a good overview is the lack of detailed information, and 3D-plots are no exception. It is virtually impossible to judge the magnitude of the permittivity components, and the response of one phase may be covered by that of another. Therefore, the 3D-plots are often complemented with 2D-“slices” showing the response as a function of frequency for one particular temperature. Several such slices may be presented in the same diagram to give a more quantitative picture of the response in various phases.

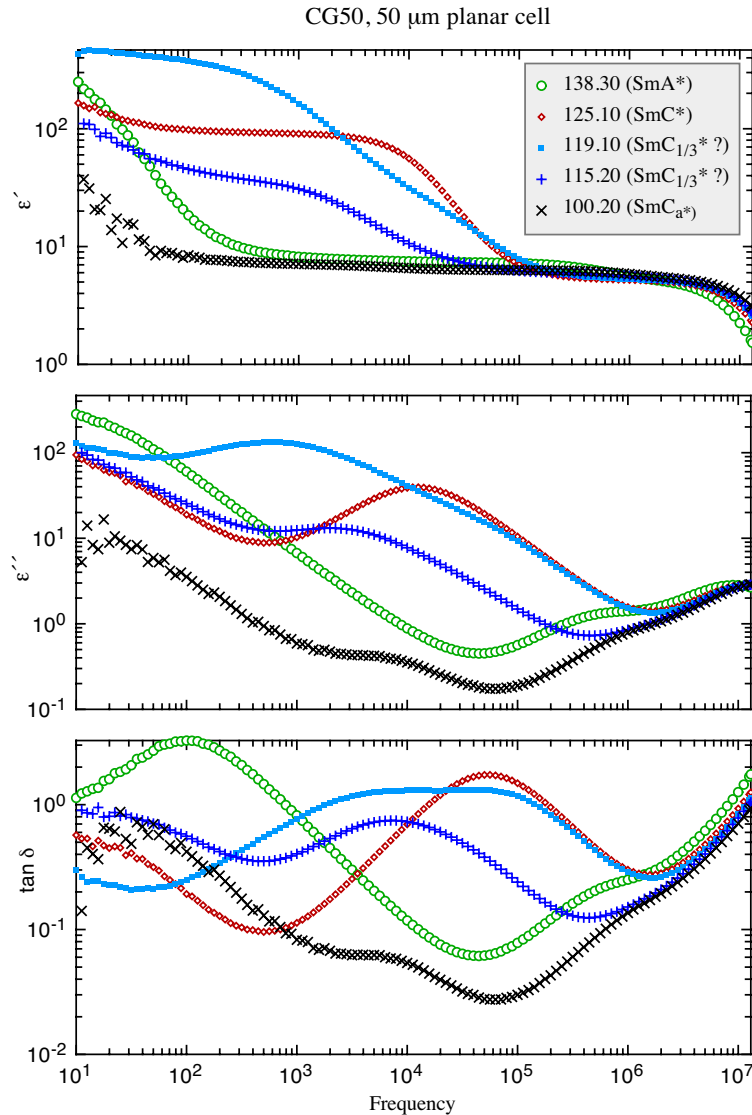


Figure 11. 2D-slices corresponding to figure 10a-c. One representative curve is taken from each temperature region of interest (the corresponding phases are listed in the legend). On their own, these curves are rather difficult to interpret.

The 2D-slice is a good complement to the 3D-overview, but it is not a replacement ! The 3D-plot should always be provided, as it gives not only the best possible overview, but it is also the “truest” presentation of the experimental results. All data points are shown, unmanipulated, in one graph, giving the reader a good picture of the quality of the experiment. Equally important is the ease of observing trends in a 3D-plot - something which is very difficult in 2D-diagrams, regardless how many slices are added (with more than 3-4 slices the diagram starts to get cluttered up).

### 2.3.3. Plotting the “static” dielectric permittivity

A simple, quite common, and often most illustrative way of giving a picture of the dielectric response throughout a large temperature range is to plot  $\epsilon'$  for one specific frequency as a function of temperature. An example corresponding to figure 10 is given below (figure 12). A presentation in this form is usually quite easy to read and it may give a very good overview of the phase behavior, but it suffers from the risk of being overinterpreted, since much information is taken away. First of all, mechanisms with absorption frequencies higher than the chosen plot frequency will “disappear” from the spectrum. To avoid losing vital information one therefore has to choose a low frequency, and hence one often speaks of such a graph as the graph of the “static” permittivity (hence, this is also one of the rare cases in the field of dielectric spectroscopy where it makes perfect sense to speak about the dielectric *constant*). The problem is that at too low frequencies the conductive contribution from ionic contamination may become too dominant. Furthermore, this kind of diagram gives no information on the number of modes active at each temperature, since it only displays the *total* contribution at a specific frequency. In summary, this kind of presentation may be a nice complement to other presentation forms, but is not sufficient on its own.

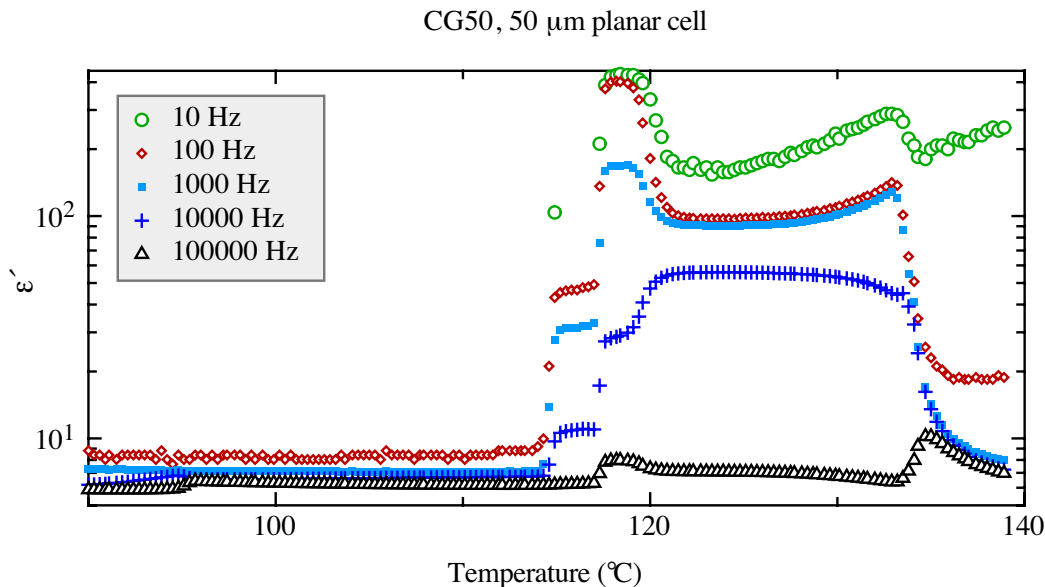


Figure 12. The value of the real permittivity component ( $\epsilon'$ ) for CG50 (taken from the set of data shown in figure 10) at five selected frequencies, as a function of temperature. Each curve will only contain contributions from processes with absorption frequency higher than the frequency at which the curve is taken (processes with lower absorption frequency may show up partially, if the frequency of the curve is not too high). Therefore high-frequency curves are always lower in magnitude than low-frequency curves.

### 2.3.4. The Cole-Cole plot

If we eliminate the frequency in the set of equations (27) and (28) we arrive at the following expression<sup>6</sup>:

6. If you do not recognize this expression from other texts on this topic, you can try inserting  $\chi = \epsilon_f - \epsilon_\infty$  in equation (36).

$$-\epsilon'' + \frac{\epsilon''^2}{2} + (\epsilon')^2 = \frac{\chi^2}{2} \quad (36)$$

This is the equation of a circle centered around the point  $\epsilon' = \epsilon_\infty + \chi/2$ ,  $\epsilon'' = 0$ , and a Debye-type process should therefore produce a semi-circle (we can have no negative  $\epsilon''$  values) if  $\epsilon''$  is plotted as a function of  $\epsilon'$ . Such a plot is called a *Cole-Cole plot* after the scientists (see footnote on page 20) who introduced it [18] in 1941. Much quantitative information may be gathered from this representation of data as illustrated in figure 13. The Cole-Cole plot has no frequency axis, but since the real part of the permittivity is a monotonously decreasing function of the frequency, we know that the higher  $\epsilon'$ , the lower the frequency. Since the maximum absorption occurs at the absorption frequency  $f_a$ , we also know that the “top” of the semi-circle corresponds to this frequency. However, we do not know anything about the frequencies of other data points. The radius of the semi-circle is  $\chi/2$ , and the points where the graph cuts the  $\epsilon'$  axis are  $\epsilon_\infty$  and  $\epsilon_f$ . The Cole-Cole plot may thus be a quick way of obtaining both the absorption frequency and the susceptibility of a mode.

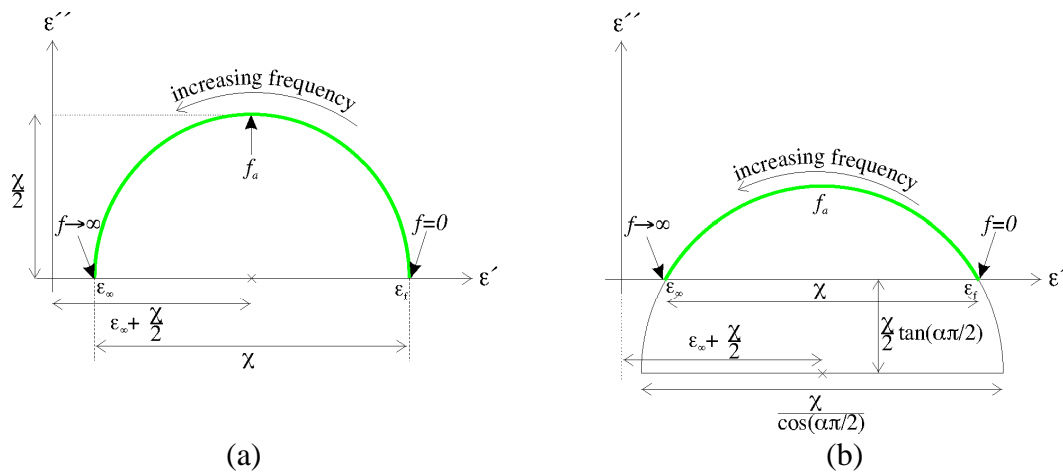


Figure 13. The Cole-Cole plot for the case of one Debye-type process (a), and for one distributed (Cole-Cole) process (b).

As I mentioned earlier, real polarization mechanisms are often characterized by a distribution of relaxation times, and in order to model this behavior, Cole and Cole proposed equation (29). If one performs the frequency elimination in the corresponding real and imaginary equations (30) and (31), one again obtains the equation of a circle, but with some important differences in relation to the Debye case [20].

$$-\epsilon'' + \frac{\epsilon''^2}{2} + \epsilon' + \frac{\epsilon'}{2} \tan \frac{\alpha\pi}{2} = \frac{\chi^2}{2 \cos \frac{\alpha\pi}{2}} \quad (37)$$

The radius of the circle has now grown by a factor  $1/\cos(\alpha/2)$ , and the center has moved to  $\tan(\alpha/2)$  below the  $\epsilon'$  axis. In other words, permittivity data from a distributed mode will produce an arch with an opening angle less than  $180^\circ$ , as illustrated in figure 13b. If we can locate the center of the circle, or measure the radius of it, we will thus get a value of the distribution parameter  $\alpha$ .

When plotting real experimental data one often encounters the problem of several partially overlapping modes being active simultaneously. In figure 14 Cole-Cole plots are given for our example CG50 data for the same five temperatures as in figure 11. Only the data obtained at 125.1°C (SmC\*) shows a fairly clean Debye semi-circle, the others have a more or less complex look.

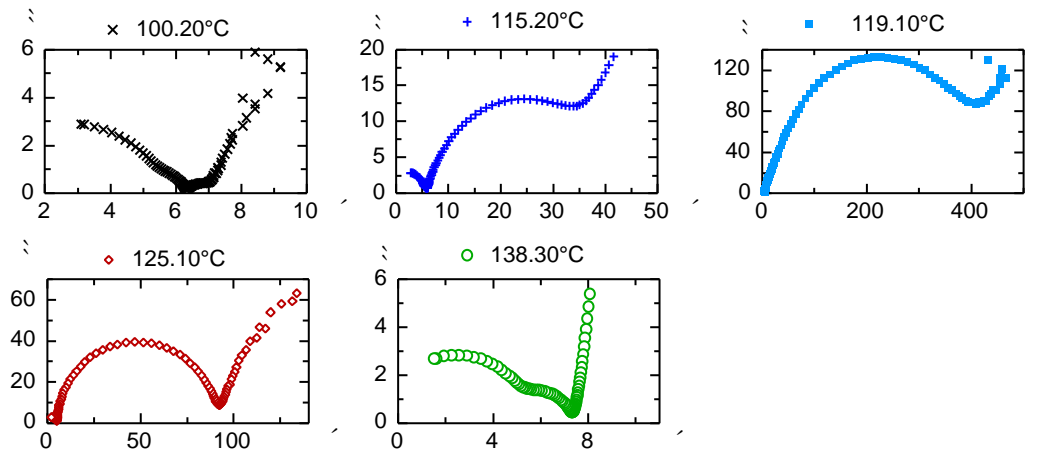


Figure 14. Cole-Cole plots for the CG50 data of figure 10, taken at the same temperatures as in figure 11. Only the SmC\* (125.1°C) response is easy to interpret, the other plots are more or less complex due to overlapping modes and deviation from pure Debye behavior.

To gain a better understanding of experimental Cole-Cole plots I have in figure 15 given synthetic plots, together with the dispersion/absorption spectra, for six sets of simulated data, in which I have varied the number of modes, and the distribution of relaxation times. The upper left-hand example corresponds to the ideal case of one Debye-type mechanism, while in the two other examples of this row there are two Debye-type modes with well separated and very close absorption frequencies, respectively. While it is easy to read off the data of interest ( $f_a$  and  $\chi''$  for the active modes) in the first two examples, it gets much more difficult in the last case. It may still be possible to estimate the respective absorption frequencies, but the susceptibilities of the modes can no longer directly be obtained from the diagram.

When the modes are distributed, as in the second row, things may get more complicated. Again the examples from left to right correspond to one mode, two separated modes and two overlapping modes, respectively. In the two first examples it is still easy to obtain the central absorption frequencies and susceptibilities of the modes, and after some work with a pair of compasses, one can also get a good estimate of the distribution parameters. In the last case, however, it is almost impossible to get any clear information from the Cole-Cole plot at all. In such a case one has to resort to fitting the Cole-Cole equations (30) and (31) to the experimental data, and the discussion of this procedure will be the closing section of this chapter.

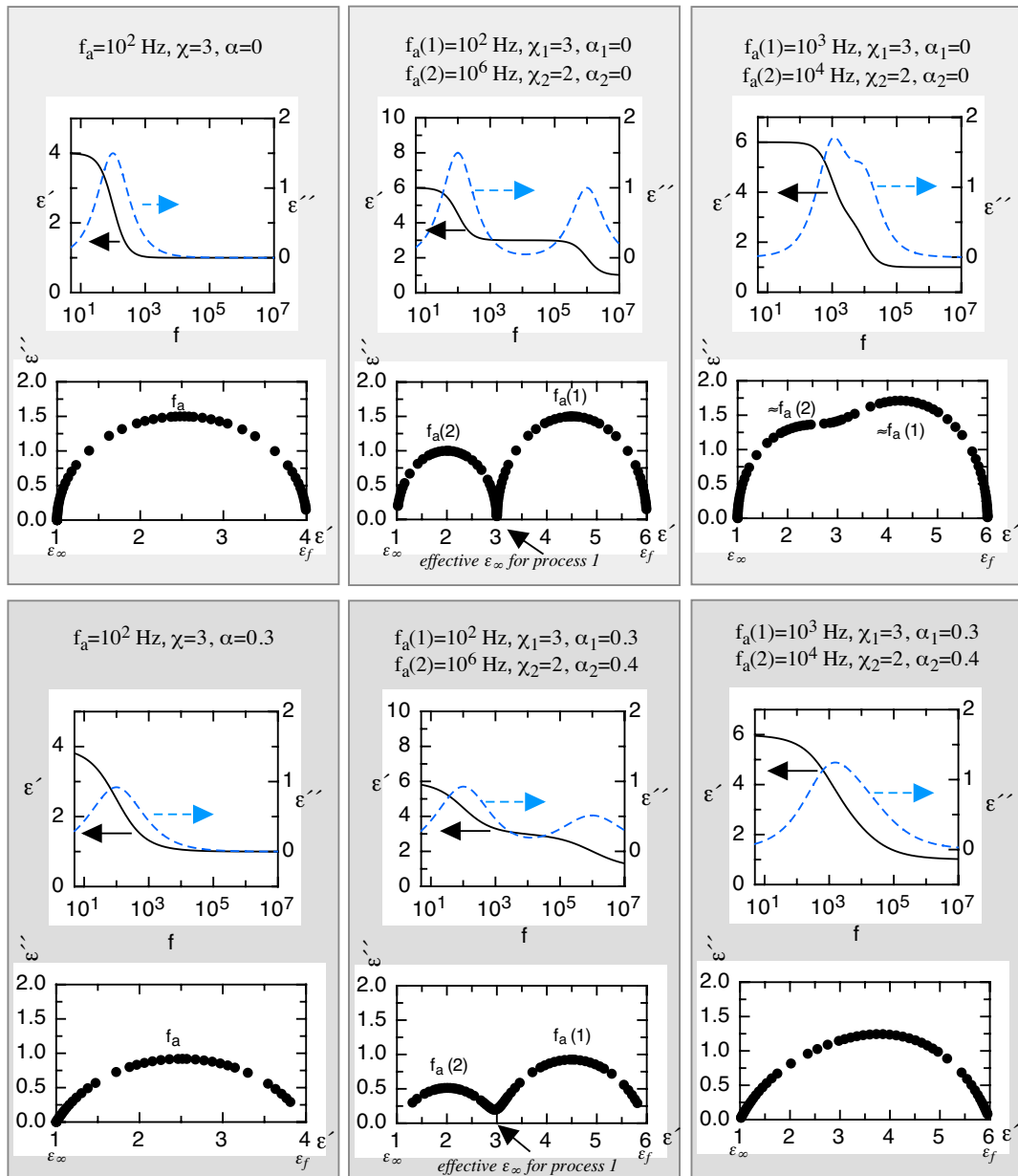


Figure 15. Dispersion/absorption curves and corresponding Cole-Cole plots for simulated data. From left to right: one mode, two separate modes, two overlapping modes. Upper row: all modes pure Debye. Lower row: all modes with distribution of relaxation times ( $\alpha \neq 0$ ).

### 2.3.5. Plotting Cole-Cole equation parameters obtained from fitting

Since liquid crystal polarization mechanisms most often obey the Cole-Cole equation (equation (29)) one of the most informative ways of treating the experimental data is to fit this equation to the data. In practice this usually means fitting equation (31) to the measured  $\epsilon''$  values<sup>7</sup>. At the end of the fitting procedure one has hopefully obtained exact values for the susceptibilities, absorption frequencies and distribution parameters

7. It has been suggested that a better fit can be obtained by fitting the complex Cole-Cole equation to the complete set of data, but so far I have not pursued this method, which is quite involved.

of the modes, as well as the number of modes present at each temperature (if one tries to fit an equation containing the wrong number of modes, one will usually fail to get a good fit). The result may be presented in an easy-to-understand way in diagrams like those in figure 16.

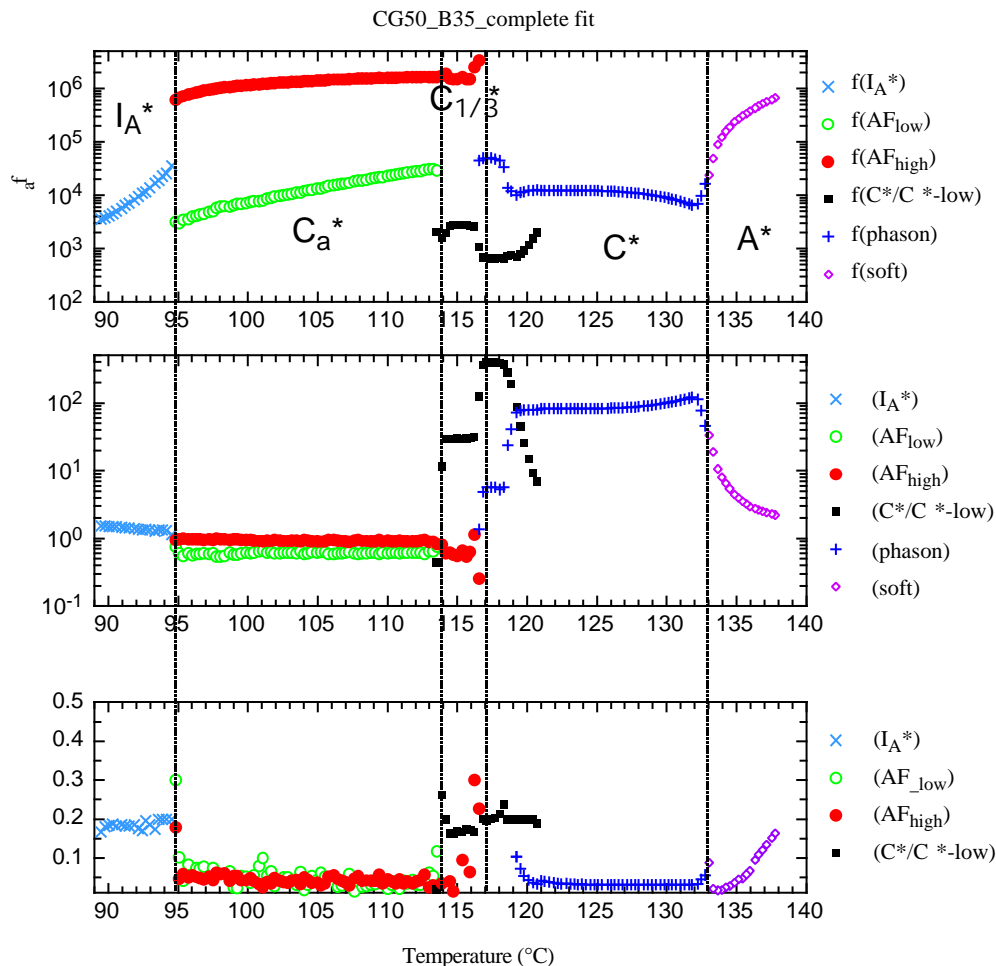


Figure 16. Data obtained on fitting equation (31) to the CG50 example data.

The problem with presenting fitted data is that the data have been processed. It is the result of a fitting procedure, and depending on how good the fit was, or on how carefully it was performed, the result can look very different. In other words, it is easy to “lie” with this kind of presentation - certainly not consciously, but the person doing the fit has to make decisions concerning how many modes are present, if they may be distributed, etc., in order to obtain starting values for the fitting procedure (a Cole-Cole plot may be of much help here). He or she must also decide on what to call the different modes, since they show up separated in the fit. Due to the slightly chaotic terminologic situation in liquid crystal dielectric spectroscopy this may further increase the confusion. Bearing these problems and risks in mind, an honest diagram illustrating fitting results should *always* be complemented with a 3D-overview of the real experimental data.

Finally, it should be pointed out that obtaining a good fit can often be quite difficult and very time-consuming. Fitting the equation to data from one single phase is usually quite easy and can be automated to a high degree, but on passing phase transitions, one

usually has to fit each set of data more or less manually. It is thus quite an effort to produce good fits to a large number of measurement series. In some cases, especially where distorted modes, induced by surface or field effects, show up, it may be impossible to get a realistic fit. Better than presenting the poor fitting results, which in such cases are directly misleading, is then to present the raw data in form of a 3D overview.

## **2.4. Summary**

In dielectric spectroscopy we measure how the behavior of the polarization mechanisms present in the material under study depends on the frequency of the polarizing electric field. Parameters varied in an experiment are typically temperature, applied DC-bias, measuring amplitude, etc., and they may all influence the result. In the case of liquid crystals, the dielectric spectrum may be a good fingerprint of the phase present at a certain temperature, since certain mechanisms are only active in certain phases.

Normally the dielectric response in the material can be modelled by the Cole-Cole equation. By fitting this to experimental data one may obtain much quantitative information about the active modes.

There are several ways of presenting dielectric spectroscopy results, and usually the best is to combine some of them. A good rule of thumb is to always present both the raw experimental data, for instance in a 3D-plot, together with analysis results (obtained through fitting or by analyzing Cole-Cole plots).

## 3. DIELECTRICALLY ACTIVE FLUCTUATIONS IN LIQUID CRYSTALS

---

---

*Twinkle, twinkle, little bat ! How I wonder what you're at !*  
– Lewis Carroll

### OVERVIEW

*This chapter deals with the different polarization mechanisms possible in liquid crystals, and how they influence the dielectric spectrum. After a brief review of the non-collective molecular reorientation mechanisms which are common to all liquid crystals, I will come to the main interest of this thesis, namely the collective polarization mechanisms present in chiral smectics. These are intimately connected to the presence of a spontaneous polarization, but as this is a local property the macroscopic structure of the phase has a large impact on the dielectric response. There will in this context be a substantial part devoted to the discussion of what a Goldstone mode is, since this is a term frequently used in reports on the dielectric properties of the smectic C\* phase family.*

*I will not discuss experimental details such as the spurious contributions from the cell relaxation and ionic impurities. These problems are instead covered in appendix section 2.*

*As the focus of my work is on calamitic (rod-like) liquid crystals, I will not discuss other kinds of liquid crystals (discotics, etc.). Hence, when I refer to liquid crystals in the following, I mean calamitic liquid crystals.*

### ***3.1. The importance of dielectric spectroscopy in liquid crystal research***

With the discovery of polar liquid crystals in the 1970's dielectric spectroscopy became an even more important characterization technique in the field of liquid crystal research. The presence of a spontaneous polarization leads to a very interesting dielectric response, far from the rather dull spectra of achiral liquid crystals. Later on, when antiferroelectric liquid crystals and the plethora of subphases in the smectic C\* family were discovered, dielectric spectroscopy became a necessity. Each polar phase has a specific dielectric response, and a dielectric spectrum may therefore provide very good help in identifying the phases of a new material. However, the new phases are by no means completely understood, and neither is their dielectric behavior.

Another very appealing characteristic of dielectric spectroscopy is that it works equally well for thin and thick cells, and actually even for free-standing films [40].

This makes it an ideal technique to study how the influence of surfaces affects the phase sequence of a material. Also, the alignment of the sample is, with some exceptions, not so crucial for the results. Therefore dielectric spectroscopy is a very good complement to techniques which are more sensitive to the alignment problem.

Quantitatively, we can also use dielectric spectroscopy data to calculate the dielectric anisotropy and biaxiality [21], the director orientation relative to the measuring field [59] and, in the case of polymer systems, we can measure segmental chain mobility.

As liquid crystals are anisotropic media with  $\epsilon_{\parallel} \neq \epsilon_{\perp}$ , we will get very different results depending on the geometry of our sample. Since the measuring field is directed perpendicular to the plane of the cell, we should in principle measure  $\epsilon_{\parallel}$  in homeotropic alignment, and  $\epsilon_{\perp}$  in a planar cell. However, one should keep in mind that no cell is perfectly aligned, and a non-zero tilt or the presence of a helix will of course also lead to an effective mixture of director orientations throughout the cell, so in many cases we may observe a combination of  $\epsilon_{\parallel}$  and  $\epsilon_{\perp}$  in the same measurement. Even though the effect normally is small, it may sometimes play an important role, for instance in the case of antiferroelectric liquid crystals (see section 3.4).

### 3.2. *Non-collective (molecular) polarization mechanisms in liquid crystals*

As motivated in chapter 2, any fluid with polar molecules will show orientational polarization, *i.e.* an applied electric field will bias the fluctuations of the individual molecules such that a non-zero average dipole moment appears parallel to the field. Liquid crystal molecules are dipoles and hence we expect to see orientational polarization from all liquid crystals (with the possible exception of the highly ordered “soft crystal” phases like SmG, etc. – if one regards them as liquid crystal phases – where the molecules are much more hindered to reorient).

We differentiate between *collective* and *non-collective* polarization processes, where the first kind (also referred to as *elementary excitations*) involve the coherent motion of a large number of molecules, while the second kind is related to non-correlated motion. The existence of collective dynamics is a consequence of ordering, and hence collective fluctuations are unique to crystalline and liquid crystalline phases. In spite of the long-range nematic order, no collective excitation of this phase can, however, be excited in dielectric spectroscopy due to the *quadrupolar* character of nematic order. The same is also valid for non-chiral smectic phases. An easily observable difference between the two fluctuation types is that collective processes, being related to a macroscopic configurational change, will lead to a change in the optical properties of the sample, while the non-collective will not [26]. The latter are illustrated in figure 17. In the case of liquid crystals, the non-collective processes are reorientations around the short and long molecular axes, respectively, which will now be discussed in some more detail.

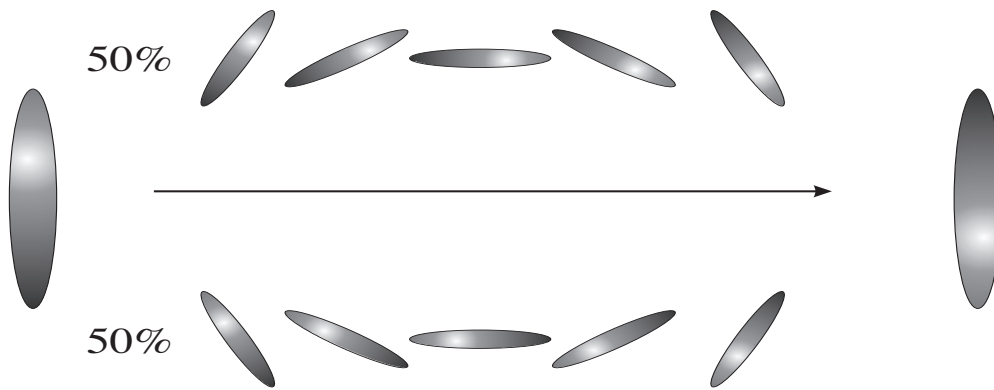


Figure 17. An example of non-collective reorientation processes. The rotation around the short axis (in a fixed plane) may take place in two different ways (clockwise and anti-clockwise), which are equally probable and uncorrelated. Each choice corresponds to opposite changes of the optic axis, and the net result is therefore no change in the optical properties, but since the coupling to the electric field in the case of molecular dipoles is quadratic,  $\epsilon \sim \mu^2$ , the dielectric effect of the two motions will be the same.

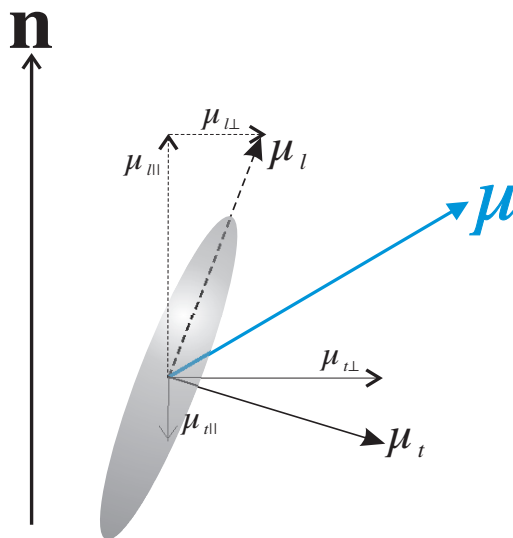


Figure 18. The molecular dipole moment of calamitic liquid crystals may have an arbitrary direction in relation to the molecule, and thus it may have non-zero components both parallel and perpendicular to the molecular long axis.

The direction of the molecular dipole moment depends on the chemical structure of the compound, and in general it may have components both parallel and perpendicular to the long axis of the molecule, as depicted in figure 18. In a dielectric spectroscopy experiment we apply a measuring field perpendicular to the plane of the sample cell, *i.e.* along or perpendicular to the director depending on if the cell is homeotropically or planar aligned, so only the dipole moment in this direction will interact with the field and give a contribution to the measured dielectric permittivity. Since the orientational order is never perfect, both the longitudinal and the transverse dipole moments will in principle have a projection both along and perpendicular to the director (see figure 18), but one component usually dominates heavily [27]. In homeotropic measurement geometry, the field thus couples mainly to the longitudinal dipole moment, and the field-induced fluctuation bias is therefore equivalent to *reorientations around the molecular short axis* – if in the relaxed state half of the molecules are oriented dipole

up, and half down, an orientation polarization must effectively mean that the field "flips" some of the molecules. Such flips will clearly be much hindered by the nematic potential, having cylindrical symmetry around  $\mathbf{n}$ , and thus we may expect the absorption frequency for this process to be substantially lower than in the isotropic phase. This is indeed observed. At the isotropic to nematic transition, the absorption frequency for this mode typically decreases by one order of magnitude.

In planar alignment, on the other hand, an analogous reasoning leads us to the conclusion that the relevant non-collective polarization mechanism will be the *reorientation around the long axis*. This rotation does not interact with the nematic potential, and therefore its absorption frequency is not lowered at the isotropic to liquid crystal phase transition. It may in fact even *increase* [25], reflecting the increased ease of this process when the medium is orientationally ordered along  $\mathbf{n}$ .

A characteristic of the non-collective polarization processes in liquid crystals is that the absorption frequencies of both follow an Arrhenius dependence on temperature [26], *i.e.*:

$$f_a = e^{-\frac{E_a}{kT}} \quad (38)$$

where  $E_a$  is the activation energy of the process. The Arrhenius dependence is clearly seen in figure 19, where the data again originates from our sample compound CG50, but this time in quasi-homeotropic alignment. The absorption process observed is thus the reorientation around the short axis. As the susceptibility of this process is connected to the projection of the longitudinal dipole moment along the direction of the measuring field, it is strongest in the SmA\* phase. The decrease in susceptibility at the transition to the inclined phases is easily seen in the 3D absorption spectrum.

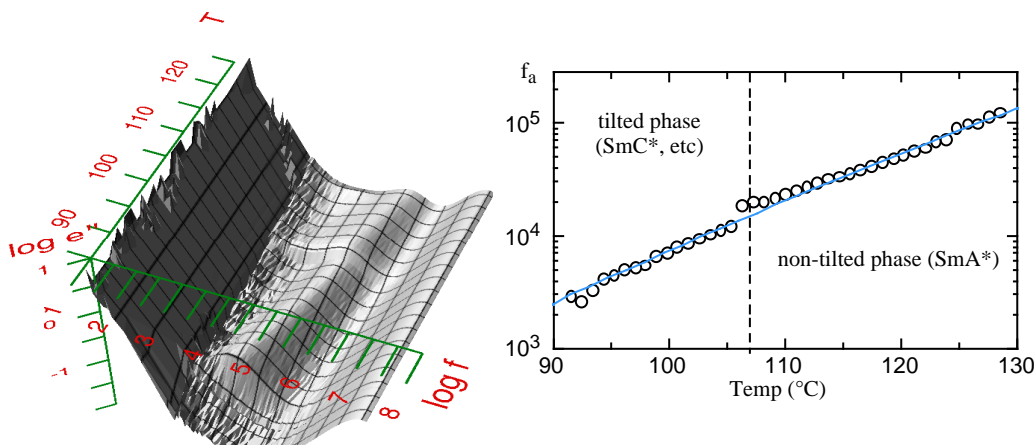


Figure 19. 3D absorption spectrum (left) and temperature dependence of absorption frequency as obtained by fitting (right), for the mode corresponding to molecular reorientation around the short axis. The line in the right graph shows the best fit of an Arrhenius function of temperature, to the experimental data. The data is obtained on a  $2\mu\text{m}$  quasi-homeotropic sample of CG50. Two phase transitions are clearly seen, the first of which is from SmA\* to one of the tilted phases, at about  $106^\circ\text{C}$  (considering the low cell thickness it is not certain which subphases are still present). The appearance of a tilt results in a weakening of the dipole moment component parallel to the measuring field, which is clearly reflected in the decrease in the susceptibility, as seen in the absorption spectrum. Next, the transition to SmI<sub>A</sub>\* is easy to see, since in this phase the viscosity is too high for the reorientation around the short axis to occur, and so the mode disappears below the transition temperature.

The absorption frequency of the short axis rotation is typically in the range kHz to MHz, while that of the reorientation around the long axis is usually found in the GHz regime. While the former normally is very close to a Debye-type mechanism, the latter normally is distinguished by a distribution of relaxation times ( $\alpha \neq 0$ ). This is an effect of the fact that different segments of the molecule may rotate around the long axis quite independent of each other. The typical characteristics of the non-collective liquid crystal modes are summarized in table 3.

Table 3: Characteristics of the non-collective polarization mechanisms in liquid crystals.

<i>Mechanism</i>	<i>Observation geometry</i>	$f_a$	$\chi$	$\alpha$	<i>Temperature dependence of <math>f_a</math></i>
Reorientation around the short axis	Homeotropic	kHz-MHz	$\approx 1$	0	Arrhenius
Reorientation around the long axis	Planar	GHz	$\approx 1$	$> 0$	Arrhenius

### 3.3. The collective polarization mechanisms of the $SmA^*$ and $SmC^*$ phases

Shortly after Meyer's *et. al.* epoch-making paper on the ferroelectricity of  $SmC^*$  [1], Blinc and Zeks studied the  $SmA^*$  and  $SmC^*$  phases theoretically, with the focus on the fluctuations to be expected in these systems [31]. Instead of taking Meyer's result, that the spontaneous polarization is directed along the  $C_2$  symmetry axis of the molecules, as a starting point, they let both  $\mathbf{P}$  and  $\mathbf{n}$  be independent variables in a Landau free energy expansion. In reality they study a two-dimensional XY-model, with  $\mathbf{n}$  represented by the vector  $\xi$ , proportional to the  $\mathbf{c}$ -director, and  $\mathbf{P}$  as another two-dimensional vector in the layer plane, and without a fixed relation to  $\xi$ . Minimizing the energy, they come to the same conclusion regarding the equilibrium configuration (*i.e.*  $\mathbf{P} \perp \xi$ ), but their approach allows independent fluctuations in both quantities. Thus they end up with the result that there exist four dielectrically active types of fluctuation in the  $SmA^*/SmC^*$  system: one amplitude (*amplitudon mode*) and one orientational (*phason mode*) fluctuation of each order parameter,  $\xi$  and  $\mathbf{P}$ . In the  $SmA^*$  phase, however, the phasons are degenerate with the amplitudons (instead of amplitude fluctuations along  $\hat{\mathbf{x}} = \sqrt{\hat{x}^2 + \hat{y}^2}$  and orientational fluctuations along  $\hat{\phi}$ , we have amplitude fluctuations along the x-axis and along the y-axis), so here we should only be able to observe two modes. As all modes are related to the spontaneous polarization, they should be observed with the measuring field along the smectic layers, *i.e.* in planar sample geometry. The polarization modes have considerably higher absorption frequencies than the director fluctuations, which are the ones usually observed in dielectric spectroscopy (for observing the polarization fluctuations one must perform high-frequency, *i.e.* MHz-GHz, measurements, which cannot be done with the most common equipment).

Blinc and Zeks introduced the names *soft mode* and *Goldstone mode* for the director excitations, where the former corresponds to tilt-angle (amplitudon) and the latter to phase-angle (phason) fluctuations. The discussion of these concepts, and their relevance in the field of dielectric spectroscopy, is the main topic of subsections 3.3.1 and 3.3.2.

In the eighties the theoretical analysis of the Ljubljana group was extended and in 1990, based on a generalized Landau model, Carlsson, Zeks, Filipic and Levstik presented a complete description of the temperature and frequency dependence of the complex dielectric permittivity [33], which agreed well with the experimental knowledge available at the time<sup>1</sup>. With this approach it turned out that the soft and Goldstone modes are actually coupled through the amplitude fluctuation which enters both modes, but as a good approximation (except very close to  $T_c$ ) this mixing can be disregarded since the phason susceptibility is much higher than that of the amplitudon. As the polarization fluctuations are much faster than the director fluctuations, another simplification is introduced by regarding the director as being fix when studying the fluctuations of the polarization, and the polarization as being stable at its average (equilibrium) position when studying the director fluctuations.

I must point out that the physical nature of the polarization modes is a rather puzzling matter which nobody has been able to clarify. In the first paper of Blinc and Zeks [31] the discussion of this is in principle completely avoided, while Carlsson *et al.* [33] discuss it in some more detail. It turns out that both modes are connected to the molecular reorientation around the long axis, which is reasonable as the dipole moment of interest is the transverse ( $\mathbf{P}$  cannot have a component along the director). In the paper they state that the total dielectric permittivity is equal to the sum of the susceptibilities<sup>2</sup> of the director fluctuations, of the polarization fluctuations and the electronic susceptibility (induced polarization). In other words, they leave no explicit room for non-collective excitations. This, together with the high absorption frequencies predicted for the polarization modes, gives the impression that these are actually equivalent to the non-collective molecular rotations described in section 3.2. The problem that the theoretical study predicts two long axis rotation modes, while the non-collective modes are divided into one short axis rotation and one long axis rotation, could possibly be resolved by taking into account the deviation from a perfectly planar measurement geometry – a “flip” around the short axis, which may be induced by the electric field also in a planar sample if the molecules are tilted or if a helix is present (see section 3.2), may have the same effect as a 180° rotation around the long axis, as illustrated in figure 20.

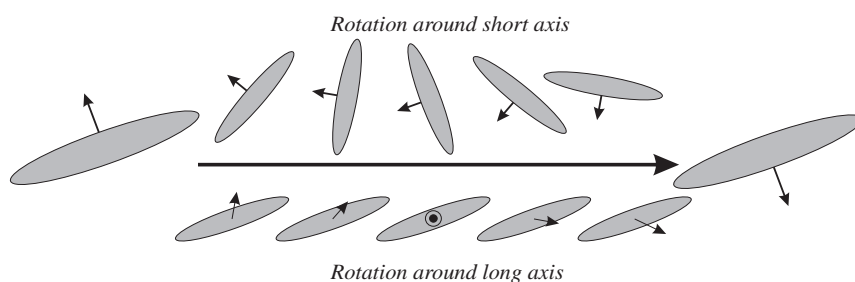


Figure 20. A “flip” around the short axis and a half-turn rotation around the long axis will have the same effect on the direction of the transverse molecular dipole, if this is perpendicular to the short axis around which the molecule flips.

1. The theoretical predictions were compared only to the case of DOBAMBC, which today would probably not be considered as a very typical SmC\* compound, since this has a rather unusual pitch dependence on temperature close to the SmC\*/SmA\* transition.

2. If you do not feel comfortable with the mixing of permittivity and susceptibility, please remember that  $\epsilon = \chi + 1$  which means that summing of permittivity contributions amounts to summing susceptibilities. See page 19.

However, such an interpretation soon runs into problems in several respects. First of all, the predicted temperature dependence of  $f_a$  for the polarization modes is very far from the Arrhenius dependence observed for the non-collective molecular reorientations [59] – both polarization modes actually are predicted to have *increasing* absorption frequency with decreasing temperature. Second, the absorption frequency of the short axis rotation is experimentally found in the kHz-MHz regime, thus several orders of magnitude lower than what is predicted for the polarization modes. While at the time of the work of Carlsson *et al.* the experimental high-frequency dielectric studies needed to verify the polarization mode predictions were scarce, this is no longer the case. To the best of my knowledge, no experimental study up to this day has been able to confirm the predictions. In a paper from 1982, Benguigui reports results (which he describes as qualitative and preliminary) [34] indicating high-frequency modes with the expected temperature behavior in DOBAMBC – and he also finds two different high-frequency modes in the isotropic phase – but he never returns to these observations in later dielectric work on chiral smectics. Finally, and perhaps most severely, the polarization modes show up as a result of an energy minimization of an *ordered* system, and are intimately related to one of its *order parameters*. How can they then be the same as the modes existing in *unordered systems* (isotropic) ? The place of the non-collective dynamics in the theoretical approach is unfortunately very obscure. They are either completely forgotten, or they must be, in some strange way, related to the polarization modes.

### 3.3.1. Tilt-angle fluctuations

It is a general property of second order phase transitions that the magnitude of the order parameter fluctuations will diverge, the temperature dependence being characterized by a critical exponent, on approaching the transition temperature from either side [35]. In case the order parameter couples, direct or indirect, with an external field, the susceptibility describing this interaction will thus also diverge. In the achiral SmA/C system the order parameter is the tilt-angle  $\theta$  which cannot on its own be influenced by an external field. Hence, we will not be able to observe the diverging behavior of  $\theta$  by means of dielectric measurements. On the other hand, in the chiral version of this system there is also a secondary<sup>3</sup> order parameter; the polarization. This certainly interacts with our electric measuring field, and we thus have a dielectric susceptibility which shows a diverging-like behavior at the transition temperature.

As the tilt and polarization are related through the relationship [17]

$$P = s^* \theta \tag{39}$$

where  $s^*$  is called the structure coefficient, any fluctuation in the polarization is linked to a fluctuation in the tilt-angle (and vice-versa), and hence also in the macroscopic optic axis (if we consider a well-aligned sample). The field-induced collective behavior is therefore of great importance, especially in the field of electrooptics where it is referred to as the *electroclinic effect*. At the SmA/C transition, as well as at the SmA\*-C\* transition, the elastic constant which constitutes the restoring force against tilt fluctuations, weakens or softens, and therefore these tilt fluctuations constitute a soft mode which grows in strength as the transition is approached. In the chiral system, where

---

3. The primary order parameter is still the tilt, but as  $P$  and  $\theta$  are intimately linked, we may also use the polarization as an order parameter.

this mode can be observed via the connected polarization fluctuation, the dielectric mode is therefore commonly referred to as the *soft mode*. As the polarization in question is perpendicular to the director, the soft mode is experimentally observed in *planar* aligned samples.

Not only does the softening of the equilibrium-restoring elastic constant result in a large and increasing susceptibility of the mode, but also in a rapidly diminishing value of the absorption frequency. This may be intuitively clear, but it may also be easily motivated by considering the behavior of the free energy close to the transition temperature (figure 21). If the system is disturbed from its equilibrium state, the restoring force will be proportional to the increase in potential due to the disturbance. Well above  $T_c$  the potential curve is a steep function of the polarization and we may thus expect a quick relaxation back to the equilibrium value. Close to  $T_c$ , on the other hand, the curve is quite flat which results in a large value of the relaxation time since the potential increase is small even for a large deviation from equilibrium. Conversely, the susceptibility will be large close to the transition where the curve is flat, and it costs only a small amount of energy to induce a large polarization, and it will be small far away from the transition, reflecting the steeper slope of the energy-polarization curve. Below  $T_c$ , the equilibrium polarization is non-zero, but the same reasoning holds also here, as the steepness of the free energy curve in the vicinity of the new minimum value, again increases when departing from the transition temperature.

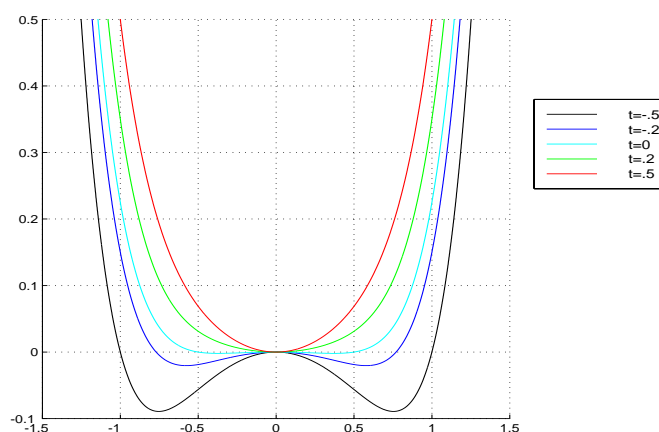


Figure 21. Close to a second order phase transition, the free energy (as obtained by a Landau expansion up to sixth order) as a function of the order parameter, is a quite flat curve in the vicinity of the minimum value. The elastic constant constituting the restoring force against fluctuations from equilibrium gets soft, hence both the magnitude of the susceptibility and the relaxation time for fluctuations in the order parameter diverge. This is called a *soft mode* behavior.

The soft mode is an *amplitudon* mode since it is connected to fluctuations in the tilt-angle. The simplest possible Landau expansion gives the same dynamics [3] of Debye type as given by equation (7), illustrating that the soft mode is a new relaxation mechanism and therefore a new dielectric mode. It further gives the result that the relaxation time tends to infinity at the transition temperature:

$$\tau = \frac{\gamma_{\theta}}{\alpha(T - T_c)} \quad (40)$$

where  $\gamma_\theta$  is the soft mode viscosity. Experimentally, however, such a complete divergence is not observed. A more careful analysis ([31] - [33]) shows that several terms must be added to the simple equation (40), the most important of which is a quadratic term in the helicoidal wave vector  $q_c = 2\pi/p$  (this wave vector is often called the *critical* wave vector, hence the index  $c$ ), where  $p$  is the pitch directly below the SmA\* $\rightarrow$ SmC\* transition. This explains why the absorption frequency of the soft mode in short-pitch materials typically does not decrease below 1 kHz. Furthermore, the presence of the helicoidal modulation also means that no critical divergence of the soft mode as observed in dielectric spectroscopy can be expected [32]. This is due to the fact that at  $T_c$  the SmA\* phase becomes unstable with respect to *helicoidal* fluctuations, with wave vector  $q_c$ , in both the director and the polarization. While in dielectric measurements a spatially homogeneous external field will couple to the  $q = 0$  fluctuations (and  $q = 2\pi/p$  below  $T_c$ , see [32]), only the response of the system with respect to a modulated external field ( $q_E = 2\pi/p$ ) could be infinite.

A result of the mean field character of any Landau expansion, is that the absorption frequency and the inverse susceptibility,  $1/\chi$ , follow straight lines when plotted against temperature (the Curie-Weiss law) [27]. The slopes of these lines in the low temperature phase should according to the theory be twice as high as the corresponding slopes in the phase above  $T_c$  [28]. This prediction is fairly close to what is usually observed in solid ferroelectrics, but in liquid crystals the ratio of the slopes varies much more. Experimentally, it is generally observed (most clearly in the case of a direct SmA\*-SmC<sub>a</sub>\* transition, where there is no phase-angle fluctuation mode covering the soft mode beneath the transition), that the susceptibility decreases much faster on departing from  $T_c$  below the transition.

Concerning experimental details, the soft mode can normally be well described with a single relaxation time (Debye-type) expression, *i.e.* the distribution parameter  $\alpha \approx 0$ , except very close to the transition temperature [28]. This is certainly the case above the phase transition, while below  $T_c$  it depends on how well other polarization mechanisms can be quenched (see below). Its behavior, as such, does not depend on whether the measurement is performed on heating or on cooling. However, in very thin cells the phase behavior of the compound may be affected, and often a noticeable supercooling of the SmA\* phase appears, with a shift in the soft mode temperature dependence as a result. The magnitude of the maximum susceptibility may also vary in cells of different thickness.

For experimental examples of soft mode behavior at the SmA\*/C\* transition, I direct the reader to references [26] to [29]. Here I would like to end this general description of the soft mode with one of the rare examples of systems where the typical second order characteristics of the SmA\*/C\* phase transition are absent. The compound in question is the AFLC mixture W107, supplied by R. Dabrowski and described in [30], which has a SmA\*/C\*/C<sub>a</sub>\* phase sequence. As is clear from the tilt-angle vs. temperature plot in figure 22, the SmA\*/C\* transition has a clear first order character. This can also be anticipated from the sudden appearance of the SmC\* phase-angle fluctuations at a temperature where the soft mode still has a very low susceptibility, as seen in the dielectric spectrum of the relaxed sample on the upper left. The lower diagrams in this figure show the behavior of the soft mode when a bias-field, strong enough to give us a clear image of the mode also below  $T_c$ , is applied over the cell. The first order character of the phase transition results in an extremely weak soft mode (its maximum susceptibility is approximately 100 times lower than that of the correspond-

ing SmC\* phase-angle fluctuations), which furthermore vanishes almost immediately on entering the SmC\* phase. This example illustrates how dielectric spectroscopy may give important information, in a most illustrative way, on the nature of the phases and phase transitions of a compound.

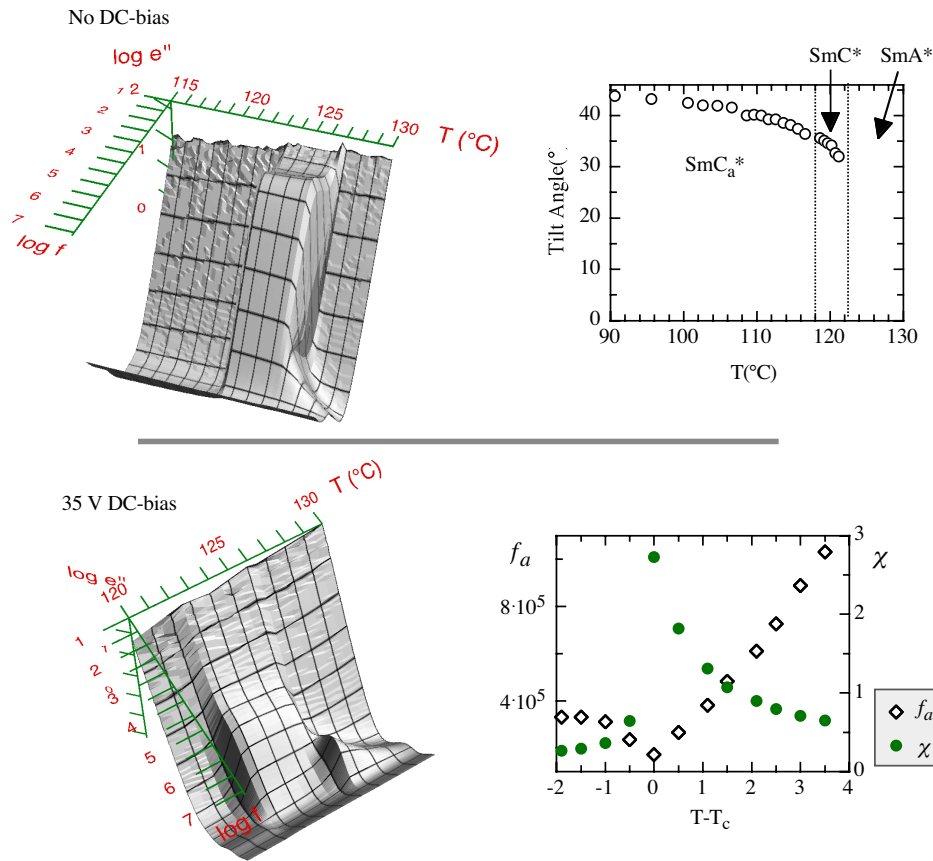


Figure 22. The mixture W107 has a strong 1. order character of the transition between orthogonal and tilted phases (SmA\* $\rightarrow$ SmC\*), as can be seen in the tilt-angle vs. temperature plot and  $\epsilon''$ -spectrum in absence of bias field (upper row). The soft mode behavior as observed with an applied DC-bias, reducing the influence of the SmC\* phase-angle fluctuation mode, is given in the lower diagrams. Note the very abrupt decrease of the soft mode after the phase transition, and the extremely low values of its susceptibility (as a comparison, the susceptibility of the fully developed SmC\* phason mode of the same compound reaches  $\chi$ -values well above 200), both signs of the 1. order character of the transition. The cell thickness is  $36 \mu\text{m}$ .

### 3.3.1.1. The influence of a DC-bias electric field on the soft mode

The field-induced tilt and polarization first grow linearly with the amplitude of the electric field but then saturate. Dielectrically this means that the soft mode susceptibility decreases if a DC-bias field of high enough amplitude is applied over the sample. The fluctuations in the electric field corresponding to the measurement signal have only a small effect if the bias-voltage already induces a saturated polarized state.

F. Gouda and co-workers have performed thorough studies of the bias-field dependence of the soft mode in the vicinity of the SmA\*/C\* transition (references [29] and [27]). Since in such systems the fluctuations in the phase-angle give a very large contribution to the dielectric permittivity in the SmC\* phase (see below), the study was performed on the SmA\* side of the phase transition. The decrease of the soft mode

susceptibility with increasing bias voltage was confirmed in these studies, in particular very close to the phase transition temperature. The effect decreases very quickly when leaving the phase transition temperature, and  $2^\circ\text{C}$  above  $T_c$  the effect is almost not to be seen.

An interesting example of soft mode behavior may be seen in the chiral-dopant mixtures which are the topic of chapter 4. By adding a chiral dopant to a racemic SmC or SmC<sub>a</sub> mixture, the new mixture becomes chiral and thus polar effects appear. The magnitude of the spontaneous polarization is, however, often not very high, and the typical dielectric response connected to the chiral phases is weak and usually easily affected by a DC-bias field. In the case of the soft mode, this is not only weakened by the field, but the temperature of maximum susceptibility and minimum absorption frequency, *i.e.* the actual phase transition temperature may be shifted, as can be seen in figure 23. The higher the field strength, the higher the transition temperature. This is an example of a compound in which the transition to the SmC\* phase from SmA\* may be field-induced above the zero-field transition temperature.

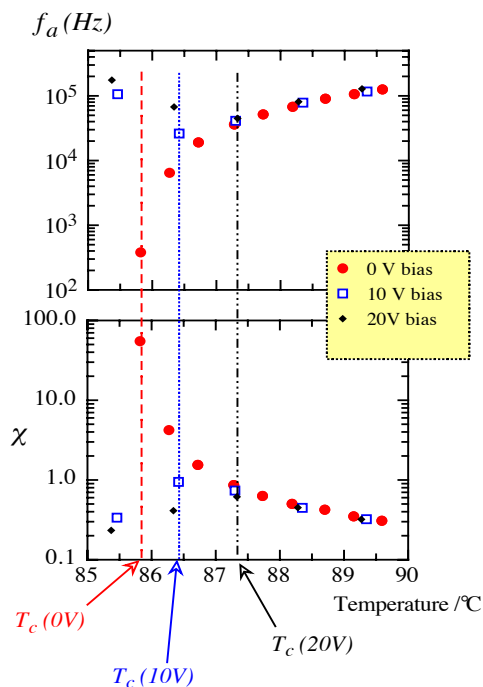


Figure 23. The soft mode behavior of a chiral-doped racemic mixture ((R/S)-10F1M7 + (S)-MHPOBC) in a  $4\ \mu\text{m}$  thick planar aligning cell, as obtained on cooling with a DC-bias field of varying strength. The compound has a direct SmA\*-SmC\* transition. It is clear from the susceptibility maxima and absorption frequency minima, that the temperature of the phase transition is raised by the application of the DC-bias, thus indicating that the transition to the SmC\* phase can be field-induced.

### 3.3.1.2. Does the soft mode behavior depend on the underlying phase ?

The above description has mainly dealt with the soft mode at the SmA\*/C\* transition. However, in the field of antiferroelectric liquid crystals, one may often encounter compounds with direct SmA\*-C<sub>α</sub>\* or SmA\*-C<sub>a</sub>\* transitions (transitions from SmA\* directly to SmC<sub>1/3</sub>\* or SmC<sub>1/4</sub>\* have, to my knowledge, not been observed). In contrast to the case of a SmA\*/C\* transition, where the dielectric spectrum of the SmC\* phase will generally be dominated by a strong phase-angle mode, such transitions have the attractive feature that the soft mode can be easily studied also on the cold side of the phase transition. The new modes observed in the SmC<sub>a</sub>\* phase (they will be discussed in section 3.5.2) have a very low susceptibility ( $\chi \approx 1$ ), and its soft mode will thus by far be the most important mode one or two degrees below  $T_c$ . The SmC<sub>α</sub>\* phase may,

on the other hand, have a distinct mode connected to phase-angle fluctuations (the  $\text{SmC}_\alpha^*$  “Goldstone” mode), but its susceptibility is often quite low directly below the transition and it is never as intense as the soft mode.

An important question is whether the soft mode behavior is independent of which phase follows below  $\text{SmA}^*$ , or not. For instance, if the lower-lying phase has a spontaneous polarization, a dielectric soft mode has to be expected in the  $\text{SmA}^*$  phase. However, the primary order parameter is the tilt, and this can become non-zero in the lower phase without any macroscopic polarization arising. Hence, this soft mode would not be dielectrically observable and it has been suggested that the soft mode at the  $\text{SmA}^*-\text{C}_a^*$  transition cannot be found, or at least not develop to the same extent as at the  $\text{SmA}^*/\text{C}^*$  transition [36]. Therefore, the answer to the general question is by no means evident, but based on experimental observations I can find no general difference between the systems. I will come back to each transition in turn in sections 3.4 to 3.5.

Let me finish the discussion on tilt-angle fluctuations by pointing out that in early papers on AFLCs ( $\approx$  earlier than 1995) one often encounters a “soft mode” which extends throughout the whole  $\text{SmC}_a^*$  phase with in principle constant susceptibility. Such a behavior is not characteristic of a soft mode, which is distinguished by its diverging behavior at the phase transition, and this description was therefore criticized. The mode soon received a better explanation (to be reviewed in section 3.5.2) and today nobody describes it as a soft mode. This example shows the danger of overinterpreting dielectric spectroscopy data; if one finds absorptions at similar absorption frequencies and with similar susceptibilities on both sides of a phase transition, it must not mean that they correspond to the same process ! Such a reasoning might lead to the absurd belief that the soft mode extends throughout the whole  $\text{SmC}^*$  phase, just because the tilt- and phase-angle fluctuations are degenerate at the  $\text{SmA}^*/\text{C}^*$  phase transition, and that the characteristics of the two modes are therefore similar close to  $T_c$ . While it is well known that this is not the case, the situation in new polar liquid crystal systems may lead to results which are difficult to interpret, and incorrect conclusions are easily drawn. Cautiousness in interpreting dielectric spectroscopy results is thus always a necessity.

### 3.3.2. Phase-angle fluctuations

When scanning through the last fifteen years or so of the literature on dielectric spectroscopy in liquid crystals, the reader is likely to be bewildered by the frequent use of the expression “Goldstone mode”, normally without any indication what it actually stands for. It might therefore be worthwhile to devote some discussion to this notion and its meaning in this area of physics.

#### 3.3.2.1. What is a Goldstone mode ?

In condensed matter physics Goldstone modes refer to certain excitations above the lowest energy state of a system. “Broken symmetry”, “Goldstone mode” and “Higgs mechanism” are examples of concepts which have been taken over from condensed matter to particle physics and field theory (where they got the names frequently used) [37]. They are all related to the description of phase transitions in many-body theory and were further developed by field theorists like Nambu, Goldstone, Salam and Weinberg ([38], [39]) when the phase transition formalism began to be adopted in cosmological and particle physics.

Broken symmetry means that the lowest stable state does not contain the full sym-

metry of the free energy (Lagrangian, Hamiltonian). By a spontaneous symmetry breaking we mean a reduction in symmetry appearing on changing a scalar control variable, such as the temperature, which in itself can have no influence on the symmetry. It may, however, take the system to a new phase, and if this is less symmetric than the initial phase, the system has spontaneously lowered its symmetry. The lower symmetry means higher order and the description of the new ground state thus requires a new order parameter. For instance, below the paramagnetic-to-ferromagnetic transition a non-zero magnetization  $M$  appears. If we consider a two-dimensional magnet, we could describe the direction of the magnetization by adding an azimuthal angle, a phase variable  $\varphi$ . However, this variable does not enter the Hamiltonian (free energy) which is only a quadratic function of  $M$ . In the same way, below the SmA-C transition, a non-zero tilt  $\theta$  of the director appears. The full order parameter is  $\psi = \theta e^{i\varphi}$ , where  $\theta$  describes the magnitude,  $\varphi$  the azimuthal direction of the tilt. However, the Hamiltonian is only a function of  $|\psi|^2$  and can be written

$$H = H_0 + a\theta^2 + b\theta^4 + \dots \quad (41)$$

However, below the transition the system must choose a particular value of  $\varphi$  – rendering the ground state asymmetric – but the energy is not influenced by the choice. The energy function can be described by the “Mexican hat” potential of figure 24, which is degenerate with respect to the azimuthal variable  $\varphi$ . In a magnetic system the spin direction is such a variable – on cooling below  $T_c$ , the system must magnetize in one particular direction, but all possible directions are energetically equivalent. As all directions are energetically equivalent, no energy is lost or gained by just changing the spin direction. Therefore, an excitation where the spin direction is slowly and continuously changed – a movement around the center of the hat – will not cost any energy. Such an excitation is referred to as a *Goldstone excitation* or a *Goldstone mode*.

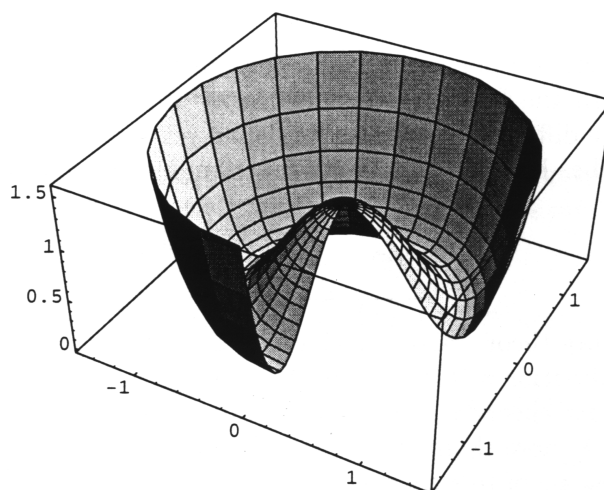


Figure 24. A system exhibiting a Goldstone mode has a ground state, the energy of which is degenerate with respect to one parameter. This can be illustrated with a “Mexican hat” energy function, where the degenerate parameter is the azimuthal angle around the center of the hat. From reference [35].

The Goldstone theorem (or conjecture) in field theory states that if a continuous global symmetry in the Lagrangian is spontaneously broken, spinless particles of zero mass appear. These are called the Goldstone bosons. In condensed matter, zero mass corresponds to zero energy or frequency. A condensed matter version of the theorem could, for instance, be formulated: if a continuous symmetry is spontaneously broken, gapless excitations of frequency  $\omega$  and wave vector  $k$  appear such that  $\omega \rightarrow 0$  when  $k \rightarrow 0$ . The word “gapless” means that they cost no energy in the limit  $\omega = 0$ ,  $k = 0$ . Strictly the theorem only applies in this limit, but if there are only short-range forces it is effectively fulfilled in the limit  $k \rightarrow 0$ , which is the case for so-called hydrodynamic modes. Examples of such Goldstone excitations in condensed matter systems are the magnetic spin waves. In the case of a magnetic spin system we can actively excite a Goldstone mode. When an external magnetic field is applied, the spin direction enters the Hamiltonian – the spins will want to align with the field – lifting the degeneracy, and a minimum, the depth of which depends on the strength of the field, appears. As the directional change virtually costs no energy, even an extremely weak field can excite the system into a spin-directional movement. Note that the Goldstone theorem requires that a *continuous* symmetry be broken. An example of such a symmetry is the spherical rotational symmetry in the paramagnetic state, or the cylindrical symmetry of the SmA state. Thus we can expect a Goldstone mode to appear at the SmA-C transition.

### 3.3.2.2. Goldstone modes in liquid crystals

In liquid crystals we have a great number of cases of broken continuous symmetries. The most obvious is maybe the isotropic to nematic phase transition where the continuous spherical symmetry of the isotropic phase is broken and replaced by the cylindrical symmetry of the nematic phase. We have no intrinsic long-range forces in liquid crystals and without external constraints, such as resulting from interactions with very close boundaries, the orientation of the nematic cylinder axis, *i.e.* the director, is arbitrary and there is thus a degeneracy in this parameter. Hence, in a bulk sample of a nematic we will have thermally excited Goldstone modes giving a continuously changing director and a strong light-scattering effect, which is a most conspicuous phenomenon to anybody looking at a nematic sample.

A compound with a SmA to SmC transition will have another kind of Goldstone mode, this time related to the appearance of a tilt. In the SmA phase the director is parallel to the layer normal, the tilt is zero, and the azimuthal angle describing rotations around the director is degenerate both in the energy function and in the physical ground state. The symmetry of the phase is  $D_{\infty h}$ . At the phase transition to the SmC phase this symmetry is spontaneously broken through the appearance of a non-zero tilt, and in order to describe the system completely we have to introduce the phase-angle  $\varphi$ , specifying the azimuthal position of the director with respect to the smectic layer normal. The new system, now with  $C_{2h}$  symmetry, has to choose one particular value of phase-angle, but the choice does not affect the energy of the system. As a result, Goldstone modes, corresponding to a very slow and continuous variation of the phase-angle, will appear when crossing the SmA  $\rightarrow$  C transition.

The Goldstone mode is often described as a symmetry-restoring fluctuation; on a global scale it tends to restore the original continuous rotational symmetry which is lost at the onset of tilt. Thus, due to the Goldstone fluctuations, all possible values of the phase-angle will appear, with equal probabilities, if we just wait long enough. Therefore, a nematic is macroscopically isotropic. This also means that in the bulk of

the SmC phase, in the absence of boundary constraints, the  $D_{\infty h}$  symmetry of the SmA phase is restored by the collective phase fluctuations in SmC, insofar as space and time averages are concerned. These Goldstone modes exist, but they are not dielectrically active because they are not connected to any local polarization.

### 3.3.2.3. Is the SmC\* phase Goldstone mode dielectrically active ?

At the tilt transition  $\text{SmA}^* \rightarrow \text{SmC}^*$  in a corresponding chiral system a local non-zero polarization  $\mathbf{P}$  appears which is everywhere perpendicular, thus sterically bound to the director  $\mathbf{n}$ . Therefore phase fluctuations also means polarization fluctuations. In the chiral SmC\* phase, which in contrast to the achiral one thus is of large interest for study by means of dielectric spectroscopy, the c-director rotates in a helical fashion when moving along the layer normal, *i.e.* the phase-angle changes with a constant amount from layer to layer. This spatial modulation has important implications on the dynamics of the chiral SmC\* phase. The Goldstone mode fluctuation described above for the achiral SmC, *i.e.* a slow and continuous change of the phase-angle, must in the chiral SmC\* phase correspond to a *rotation of the whole helix* [22], as illustrated in figure 25. Note that this is a rotation *without distortion*, otherwise the mode would not correspond to fluctuations between energetically equivalent ground states, which is a necessity for the mode to be called a Goldstone mode. As can easily be seen in the figure, an arbitrary rotation of the helix is actually equivalent to a translation along the helix axis. Thus the Goldstone mode may also be regarded as a translational fluctuation of the helical structure, mediated through the phase-angle fluctuations (the molecules do not move along the helix axis).

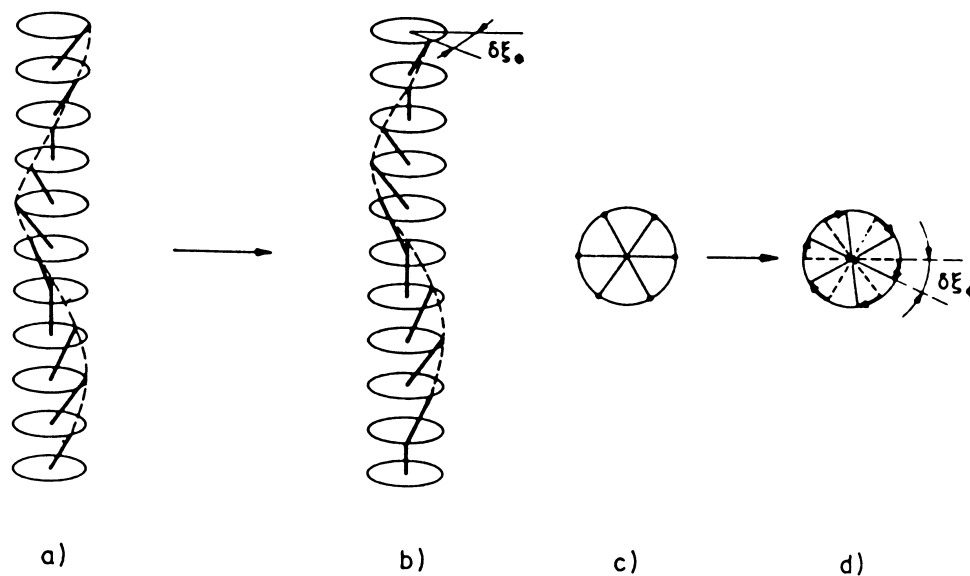


Figure 25. The Goldstone mode in the helical SmC\* system corresponds to a rotation an angle  $\delta\varphi$  (denoted  $\delta\xi_\varphi$  in the figure) of the whole helix around its axis. However, as rotation and translation of a helix are equivalent, it can equally well be regarded as a translational fluctuation along the helix axis. If an external electric field is applied over the sample, distorting the helix but not unwinding it, the equivalence between rotation and translation is absent, and only the translational Goldstone mode persists. From reference [22].

At the  $\text{SmA}^* \rightarrow \text{SmC}^*$  transition the continuous rotational symmetry is only broken locally – globally the symmetry of the  $\text{SmA}^*$  phase and the helical  $\text{SmC}^*$  phase is the same,  $D_\infty$ . However, a continuous translational symmetry (not related to the smectic layers but to the phase angle) is broken. Therefore the translational fluctuations in the non-distorted helix can be looked upon as symmetry restoring.

Does the appearance of spontaneous polarization mean that we can excite the Goldstone mode with an electric field, just like we could excite it in a spin system with a magnetic field? As this question is related to the polar order of the system, it again brings up the important concepts ferro- and antiferroelectricity. The point is that, while the spin system considered above undergoes a transition from a paramagnetic to a ferromagnetic phase, the equivalent polar phase transition does not occur for the liquid crystalline system because the bulk  $\text{SmC}^*$  phase is helical antiferroelectric (see section 1.3.2). The degenerate ground state is no longer designated by a particular value of  $\varphi$  but with a particular value of  $\varphi$  for one specific layer – all other values of  $\varphi$  will simultaneously be present in other layers. As all values of  $\varphi$  are present with equal probability, so are all directions of  $P$  and the macroscopic electric polarization is therefore zero. We still have a degenerate ground state – we can rotate the complete helix without changing the energy of the system – but, considering a rigid helix, there can be no interaction with an electric field. In the presence of a field, the total amount of “happy” layers in the undistorted system will always be exactly the same as the amount of “unhappy” layers.

As we all know the FLC helix is not completely rigid but it is easily deformed by applying an electric or magnetic field. In this way we can induce a slight macroscopic polarization in the system even if the field is very weak. The deformation of the helix is equivalent to a small change in phase-angle in all layers where the polarization is not exactly parallel to the applied field, but as the motion is connected to a deformation of the helical ground state, the energy of such a fluctuation will not be equal to zero and it cannot be considered a real Goldstone mode. In contrast to the ferromagnetic spin system (or to a truly ferroelectric system), the ground state with the field is *not* equivalent to any ground state in the absence of a field. As the applied field is homogeneous in the plane of the cell, its interaction with the helicoidal polarization structure can be described as a superposition of a “constant phase-angle wave”, *i.e.* a wave with infinite periodicity and wave vector  $q_E = 0$ , and the helicoidal modulation of the phase-angle with wave vector  $q_c = 2\pi/p$  where  $p$  is the pitch of the material. Therefore one sometimes says that dielectric spectroscopy probes the phason behavior in the  $q = 0$  limit. In this terminology the true Goldstone mode is a phason mode with wave vector  $q_c$ , but it is a mode which cannot be excited in a dielectric experiment.

Let us now, following reference [23], study what happens if we apply a small constant field, just enough to distort the helical  $\text{SmC}^*$  structure somewhat, over our sample in the  $\text{SmA}^*$  phase, and then cool it down to the  $\text{SmC}^*$  phase. Is the phase transition still connected to a spontaneous symmetry breaking, or in other words, would we still expect the appearance of Goldstone modes? As far as continuous rotational symmetry is concerned, the answer is obviously no. By applying the field, we have removed this symmetry already in the  $\text{SmA}^*$  phase, manifested through the appearance of a non-zero polarization parallel to the field, and the system now has symmetry  $C_2$ . However, while the  $\text{SmA}^*$  phase even with the field applied has continuous (degenerate) *translational* phase-angle symmetry, the  $\text{SmC}^*$  phase does not (provided that the applied field is not strong enough to unwind the helix). The structure of the distorted system is illustrated in figure 28 for some different values of the field

strength. There will now be a discrete translational symmetry (incommensurate with the layer ordering) along the axis of the distorted helix. Thus, also the distorted SmC\* system will have Goldstone modes, only this time related to translational motion, not rotational<sup>4</sup> (but again mediated through phase-angle fluctuations). However, these fluctuations still do not correspond to a macroscopic change in polarization, and so also this type of Goldstone mode will not be dielectrically active.

In summary, we realize that the phase-angle mode observed with dielectric spectroscopy in a helical sample of SmC\* liquid crystal, is related to, but not equivalent, to the Goldstone mode of the system. The non-equivalence can be illustrated in several ways:

- while the Goldstone mode fluctuation takes the system continuously through a number of infinitely degenerate ground states, the field-induced fluctuations constantly change the energy of the system
- due to the chiral coupling forces between layers, the field-induced change of the phase-angle will be in different directions in different parts of the same helix, resulting in a distortion of the macroscopic ground state and thus an increase in elastic energy. The ground state with an applied field is thus not equivalent to *any* of the degenerate ground states in the absence of a field.
- while a Goldstone mode takes the system from one degenerate ground state to another, the ground state after relaxation from the field-induced distortion is the same as before – the helix has not even been rotated (or translated).

A better name for the dielectrically active mode, a name which also has the good property of describing what is actually happening, is *helix distortion mode*, and I would therefore like to promote the use of this name for the fluctuation. It is a phason-mode, as has been noticed by several researchers, but since other phase-angle fluctuations may be simultaneously present (as will be discussed in the last two subsections of section 3.3) the name phason-mode on its own would not be sufficiently specific. However, in many practical cases it may be very difficult to say exactly which phase-angle fluctuation gives rise to the observed response, and then the term phason mode is very useful as a general name. The true Goldstone modes of all liquid crystal phases may be successfully studied by means of quasi-elastic light scattering, and there are several examples of such studies in the literature (see for instance [23] and [24]).

#### 3.3.2.4. The Goldstone mode as the limiting case of the helix distortion mode

The helix distortion mode is experimentally observed in planar alignment, *i.e.* with the measuring field parallel to the smectic layers so that it can interact with the spontaneous polarization of the material. In order to get a feeling for what susceptibility we can expect from the mode, we pursue the following reasoning, following reference [32]. While it is clear that the coupling to the field is related to the magnitude of the spontaneous polarization, it cannot depend on the sign of it, so the dependence should be quadratic,  $\chi \sim P^2$ . Furthermore, the decrease in energy obtained by adopting the

---

4. While translational and rotational motion are perfectly equivalent for an undistorted helix, this is not the case when a distorting field is applied.

helicoidally modulated structure is given by

$$\Delta E = \frac{K_\varphi \theta^2}{2} \left( \frac{2\pi}{p} \right)^2 \quad (42)$$

where  $K_\varphi$  is the elastic constant counteracting phase-angle fluctuations,  $\theta$  the equilibrium value of the tilt angle, and  $p$  the helical pitch. The susceptibility connected to a helix distortion should then be inversely proportional to the energy decrease given by equation (42). By finally calculating the numerical prefactor [32], we end up with the expression:

$$\chi_{hd} = \frac{1}{8\pi^2 K_\varphi} \left( \frac{Pp}{\theta} \right)^2 \quad (43)$$

The helix distortion mode susceptibility can thus be very high, especially in a long-pitch material, which renders the mode quite spectacular in a dielectric spectrum (see for example the upper left-hand diagram of figure 22). The value is typically in the range 100 - 1000.

Regarding the absorption frequency, a similar reasoning based on elasticity theory leads us to the expression [27]:

$$f_{hd} = \frac{K_\varphi 2\pi}{\gamma_\varphi p^2} \quad (44)$$

where the parameter  $\gamma_\varphi$  is the viscosity counteracting changes in the phase-angle. If one inserts typical parameter values for a SmC\* compound, for instance  $p = 1 \mu\text{m}$ ,  $K_\varphi = 5 \text{ pN}$ ,  $\gamma_\varphi = 0.01\text{-}0.1 \text{ Ns/m}^2$ , one ends up with an absorption frequency in the range  $f_{hd} \approx 300 \text{ Hz}\text{-}3000 \text{ Hz}$ . This fits well with experimentally observed absorption frequencies for the mode.

We note that the frequency  $f$  in equation (44) goes to zero and the susceptibility  $\chi$  in (43) to infinity when  $p \rightarrow \infty$ . This behavior does indeed remind us of the true Goldstone mode, which should be observed at zero frequency. It turns out that there is actually a continuous transformation from the helix distortion mode at finite pitch to the true Goldstone mode, which constitutes the limiting case at infinite pitch. In fact, it would in this limit be strange to speak of a helix distortion mode, since we have no helix which can be distorted. The Goldstone mode can then only be observed when the helix is absent, *i.e.* in an infinite-pitch SmC\* material, since only in that case will it correspond to a homogeneous zero-wave vector  $\varphi$ -wave which can be excited by a weak applied electric field.

A material with an infinite pitch, but with non-zero polarization, would not be too difficult to make. However, a normal experiment would still give values of  $f_a$  and  $\chi$  corresponding to a finite pitch or, rather length – as we will see in the following subsection, the characteristic length would now be the thickness of the sample. Therefore, an infinite-pitch material is not enough: one has to get rid of the influence from the bounding surfaces, *i.e.* perform an experiment on a free-standing smectic film. To my knowledge only one such experiment has been performed, and even quite recently, by

D. Pocięcha *et al.* [40], and it is very illustrative, *cf* figure 26. It was not performed on an infinite-pitch material, but on a material which shows an inversion of the helix handedness at a certain temperature  $T_c$ . Thus the pitch will be infinite at this temperature.

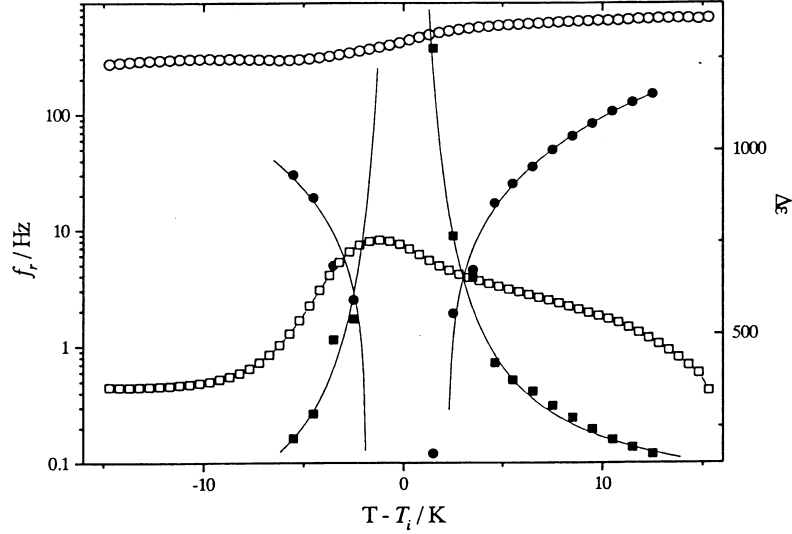


Figure 26. Observation of true Goldstone mode behavior by D. Pocięcha *et al.*[40]. Absorption frequency (circles) and susceptibility (squares) of the modes connected to phase-angle fluctuations as observed in the vicinity of a helix inversion of a SmC\* material. The unfilled data points are obtained in a standard liquid crystal measurement cell (25  $\mu\text{m}$  thick) while the filled symbols show the results from an experiment on a free-standing film. As the pitch gets infinite, the helix distortion mode is expected to diverge in susceptibility and its absorption frequency should slow down critically. This is then a true Goldstone mode which can be observed in the free-standing film experiment, but in the cell, the surfaces suppress the helix with the result that instead of the helix distortion mode, we see a mode connected to phase-angle fluctuations in a surface-related structure.

The dielectric experiment was performed on cooling past the inversion temperature, with the electric field directed along the smectic layers in order to probe the modes connected to phase-angle fluctuations. In addition to using a free-standing film (filled symbols), the experiment was performed also on a 25  $\mu\text{m}$  thick standard glass substrate liquid crystal cell (unfilled symbols). It is evident from the two measurement series that the behavior corresponding to a Goldstone mode is actually seen in the free-standing film as  $T_c$  is approached, but in the other experiment the behavior is radically different. A strong deviation from the predictions of equations (43) and (44) is seen, which is reasonable in this case, because in this case of a strongly temperature-dependent pitch the surface effects will dominate. Neither do we see the absorption frequency approach zero, nor does the susceptibility diverge, when approaching the inversion temperature. The explanation lies in the fact that, as the influence of the cell surfaces gets higher the longer the pitch [2], even quite thick measurement cells will be able to suppress the helix. When the pitch diverges in the cell, the helical structure thus disappears long before the inversion temperature  $T_c$  is reached, and instead of the helix distortion mode, we will get a new kind of phase-angle fluctuations connected to a surface-induced twist-bend structure. Once the helix-free state is obtained the helix does not reform, as verified by optical texture studies [40], neither on continued cooling nor on reheating up to the SmA\* phase. This means that the influence from the surfaces

may also have the effect that the results obtained on heating are very different from those seen on cooling. As the study of helix inversions may supply us with important information also in other areas (see for instance paper 1) this observation is of importance. However, dielectric spectroscopy experiments performed on free-standing films are rare, mainly due to the large spacing between the electrodes in film holders. This means that the voltage supplied by a standard dielectric bridge results in a very weak measuring field, and it may be difficult to obtain good results.

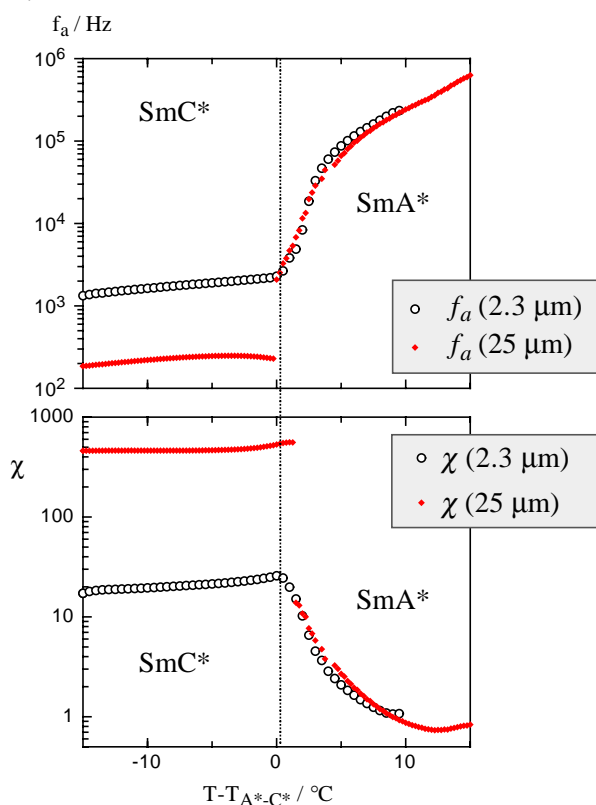


Figure 27. The absorption frequency of the amplitudon and phason modes in the SmA\* and SmC\* phases of a mixture with a SmA\*/C\*/C<sub>a</sub>\* phase sequence [61]. In the thin cell the two modes of the SmC\* phase could not be resolved. This was possible in the 25 μm cell, but for comparative reasons only the helix distortion mode (phason) has been plotted in the SmC\* phase, while the soft mode (amplitudon) is plotted in the SmA\* phase. Note the large cell thickness dependence of the phason mode behavior.

If one cannot perform measurements on free-standing films, one should thus use very thick cells in order to study the helix distortion mode in its “purest” possible form. The longer the pitch, the closer will the behavior be to that of a real Goldstone mode, but the requirements on the cell thickness get accordingly more and more severe. In a cell of intermediate thickness, the helix is constantly in a distorted state, and this will of course influence the behavior; the susceptibility will decrease and the absorption frequency increase (the situation is analogous to the DC bias-induced distortion discussed below). An example illustrating this, which may also serve as a good summary of the SmA\*/C\* collective dielectric behavior, is given in figure 27, partly from reference [61]. The empty symbols show the response as observed in a thin cell (2.3 μm). At decreasing temperature in the SmA\* phase, the divergence-like rise of the susceptibility on approaching the lower-temperature phase, combined with the slowing-down in frequency, is the expected characteristic for a soft mode which is a precursor to a phase with strongly collective polar order. The onset of this polar order at the SmA\*/C\* transition is confirmed by the cusp after which the susceptibility falls down more slowly. In the SmC\* temperature region, the measured  $\chi$ -value is about 20 to 25 and the absorption frequency about 1 kHz. In a 25 μm cell (filled symbols), on the other hand, the corresponding  $\chi$ -value is about 500 and the frequency about ten times lower

( $\approx 100$  Hz). In both cases the response is due to phase-angle fluctuations, but while the response in the thick cell is comparable to the predictions of equations (43) and (44), the thin-cell response is a result of fluctuations in a permanently distorted structure of which the characteristics are difficult to predict in a precise way. In contrast to the phason modes, the amplitudon (soft) mode behaves very similarly in the two cells.

### 3.3.2.5. The influence of a DC-bias electric field on the helix distortion mode

As the director structure is easily influenced by a field, it is not only possible to distort the helix but also to completely freeze all phase-angle fluctuations. Such a state, where the helix is totally unwound, may be of large interest and we therefore sometimes perform dielectric spectroscopy experiments where a constant DC-bias is applied. If one for instance wants to study the soft mode behavior within the SmC\* phase, this is a necessity as the soft mode otherwise is completely covered by the dominating phase-angle mode. At intermediate DC-field strength, *i.e.* below the threshold for complete helix unwinding, we have a contribution due to the helix distortion mode, but the susceptibility quickly decreases and the absorption frequency increases. This may be understood [41] by considering that a partially unwound structure consists of a number of layers with uniform director orientation, separated by “walls” in which the phase-angle rotates  $360^\circ$ , *cf* figure 28. When the field-strength is raised, the walls turn thinner and thinner, resulting in a tighter and tighter twist with a corresponding increase in the effective elastic constant of equation (44). Thus the absorption frequency increases. At the same time the regions of field-locked phase-angle grow, while the regions where fluctuations are possible diminish, resulting in a decreasing susceptibility.

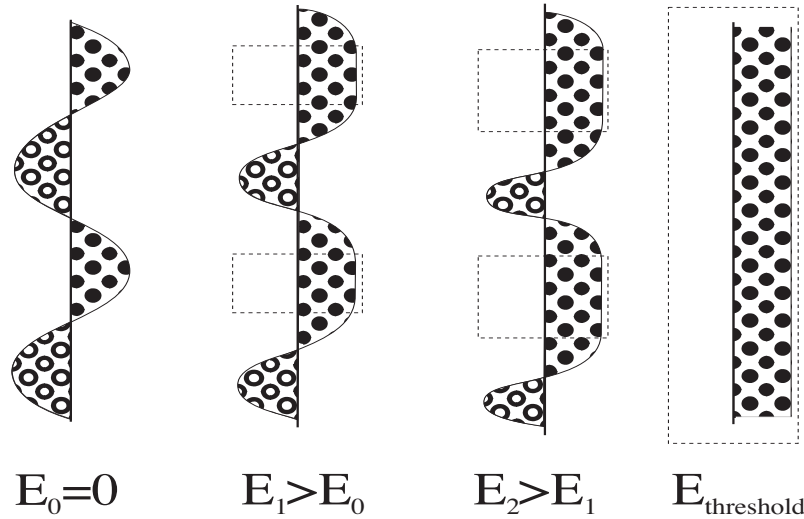


Figure 28. On applying an electric field perpendicular to the SmC\* helix (*i.e.* along the smectic layers) the helix will distort into a periodic structure with discrete translational symmetry. This is a spatial soliton structure where, at regular intervals the director will twist  $360^\circ$  in a confined region. In between these periodic “twist dislocations” the director will be homogeneously directed along the field. These uniform regions are enclosed in a dashed box in the figure. When the field-strength increases, the uniform regions will grow and the twisted ones will diminish in size, and at the threshold field the helix will be completely unwound. The different cases are illustrated through the projection of the director on the paper plane, with the filled circles corresponding to a net polarization along the field, and the empty circles to a net polarization against the field.

The unwinding of the helix by means of an application of an electric field is sometimes mistakenly pictured as the same process that appears for instance when mixing the two different enantiomers of a SmC\* liquid crystal. Such an unwinding, where the pitch continuously increases to infinity, would be accompanied by a divergence in the helix distortion mode susceptibility and a critical slowing down of its absorption frequency, just as in the example of a helix inversion discussed above. This is a behavior which is quite opposite of what is observed in a field unwinding process. While the first kind of helix unwinding is an *untwisting* operation, where the structure is always helical, the unwinding induced by the bias field is a *distorting* operation, and the helical structure is lost as soon as the field strength is raised from zero.

### 3.3.2.6. Phase-angle fluctuations in thin cells

The above analysis mainly deals with the bulk SmC\* liquid crystal, where the helix forms more or less unhindered. In experimental conditions the compound is, however, usually filled into a measurement cell and the structure will thus inevitably be influenced by the cell surfaces. If the cell thickness is reduced down to the same order of magnitude as the pitch, the helix is completely suppressed and the helix distortion mode will be absent. However, often in chiral smectics we have a strong polar surface anchoring, and this forces the director at the two surfaces to tilt in opposite directions, since the surface polarization is normally directed out of the surface. The system will thus develop a *twist-splay-bend* in the 3D director configuration, corresponding to a splay-bend in  $\mathbf{P}$ , which is a 2D deformation in the layer plane. For planar boundary conditions and neglecting chevrons, this would correspond to a director twist of  $2\theta$  along the cell substrate normal when we go across the cell in the field direction, as depicted in figure 29. Such an idealized cell will have no net macroscopic UP or DOWN polarization, but the local  $\mathbf{P}$  vector in the middle will couple to the applied field. If we have a chevron, we would in addition have a net UP or DOWN polarization [3]. The actual case may be more complex but in any case we will in general at least have a net polarization in the plane of the cell which will couple to our measuring field. Since no helix is present, the induced phase fluctuations will be observed as a new, different, dielectric mode. In fact, this mode is actually present also in thick cells, where the helix can develop more or less unobstructed, but since the fluctuations related to the polarization splay will also result in a distortion of the helix, there is no way of distinguishing this mode from the normal helix distortion mode.

The experimental observation of this “splay mode” in different SmC\* compounds is well described in reference [43]. As could be expected, it turns out that the characteristics are strongly dependent on the cell thickness  $d$ ; the susceptibility is approximately proportional to the square of the cell thickness,  $\chi_{splay} \sim d^2$ , while the absorption frequency decreases with increasing cell thickness according to  $f_{splay} \sim 1/d^2$ . One may note that the dependence on the cell thickness thus is the same as the dependence on the pitch of the helix distortion mode. In other words, the cell thickness replaces the pitch as characteristic length in unwound samples. This is of course what we would expect from dimensional arguments.

In case the cell is very thin ( $\approx 1 \mu\text{m}$ ) or if the polar surface anchoring is not very strong, the director configuration at one of the two substrates may be reversed, and the surface-stabilized state will then not be twisted. There will be in-layer phase-angle fluctuations related also to this structure ([42], [43]), in the case that  $\mathbf{P}$  makes an angle to the layer normal at the surfaces, and thus is prevented from being homogeneous across the cell. The small susceptibility that now prevails, due to the inhomogeneity,

empirically falls off as  $\chi_{unsplayed} \sim d$ . The cell thickness dependence of the absorption frequency is found to be the same as for the polarization splay state.

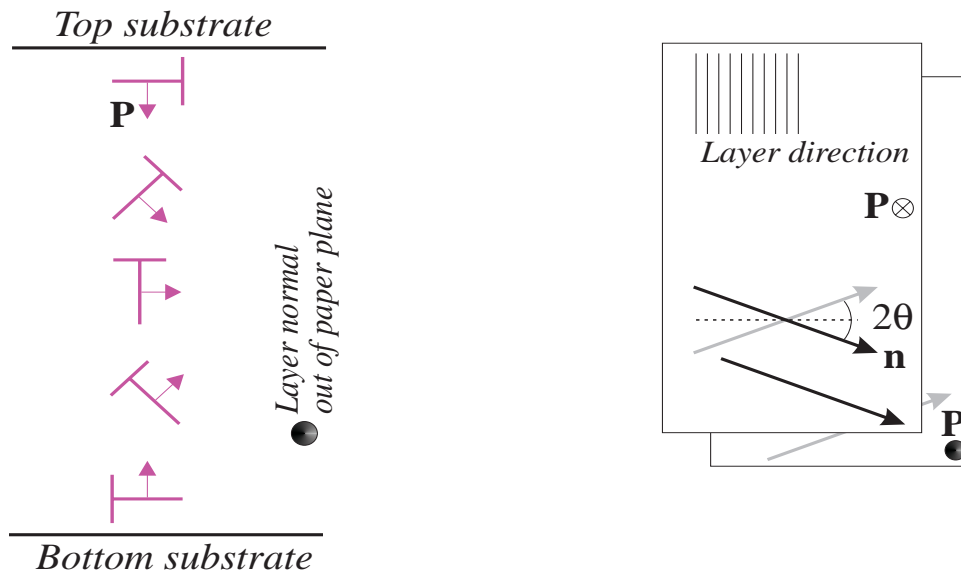


Figure 29. The sterically coupled  $\mathbf{n}$  and  $\mathbf{P}$  vector fields in a “splayed cell” in the idealized chevron-free planar configuration, left in a cut along one layer (the layer normal pointing out of the paper plane), right in the cell as seen from above. The heads of the director “nails” to the left are supposed to point out of the paper.

In the discussion on how to study the soft mode in the  $\text{SmC}^*$  phase, one might believe that in a thin cell, where the helix is intrinsically absent due to the surface interactions, the phase-angle fluctuations would be absent and one would thus not need to apply a DC-bias. The two fluctuations now discussed constitute the reason that this is not a solution to the problem. Even when the helix formation is suppressed, the soft mode may be covered by a mode connected to in-layer phase-angle fluctuations.

The thickness-dependent phason modes observed in thin cells have sometimes been called *thickness modes*, where the name refers to the fact that the cell thickness is the characteristic length parameter in the equations governing the behavior of the modes. This name is not particularly attractive, since it does not convey anything about the physical process involved. Basing the name on a parameter is in my opinion not a very good naming strategy. I think a better choice is to give the modes names after the structures in which they occur, and as a first tentative name, I would therefore propose to call the mode of the splayed polarization configuration the *splay mode*, and that of the unsplayed structure the *unsplayed mode*. As a general term, one could use surface-induced phason modes, rather than thickness modes.

### 3.3.2.7. The “domain” mode

As a final example of the phase-angle fluctuations possible in  $\text{SmC}^*$ , I would like to briefly discuss the so-called domain mode [44]. This mode, introduced by the Darmstadt group, corresponds to cross-layer phase-angle fluctuations in the absence of a helix, which may be observed in  $\text{SmC}^*$  mixtures with a high value of spontaneous polarization ( $>100 \text{ nC/cm}^2$ ). The circumstances under which it may appear are not very clear, but it seems to be most easily seen in the presence of an intermediate bias field

where the helix is unwound, but where the phase-angle is not completely uniform throughout the sample, as illustrated in figure 30. The reasoning is that the system may decrease its electrostatic energy by modulating the direction of the in-layer polarization vectors slightly, in a way similar to when ferroelectrics form UP and DOWN domains. In the SmC\* case this means that the phase-angle is periodically modulated around the equilibrium value  $\varphi_0$  given by the applied field (*i.e.* at which the polarization is exactly parallel to the field), when travelling in the plane of the cell along the layer normal. The structure may therefore be described as an in-plane, cross-layer, periodic twisted structure. A deviation from  $\varphi_0$  results in a raised energy due to the electrostatic interaction with the field, so for such a structure to be stable this energy increase must be smaller than the decrease produced by avoiding the uniform polarization structure. If the field strength is modulated, as during a dielectric spectroscopy experiment, the system would therefore have to adapt its structure, resulting in a fluctuation of the deviation from  $\varphi_0$ . This is illustrated in figure 30 where the fluctuation corresponds to changing back and forth between the A and B structures. Hence, this kind of twisted structure should be connected to a dielectrically active phase-angle mode.

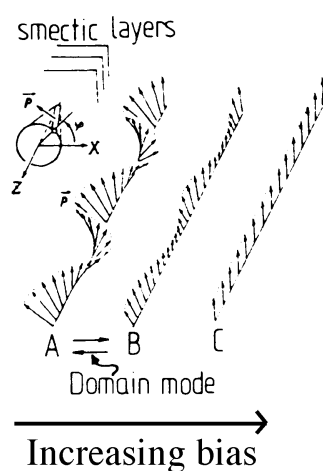


Figure 30. The phase-angle fluctuations corresponding to the so-called “domain mode”, introduced by Haase and co-workers. It may occur in high polarization SmC\* mixtures, under the influence of a bias field, sufficiently strong to unwind the helix, but low enough to permit slight phase-angle fluctuations. There may thus be a spatially periodic modulation of the phase-angle along the layer normal, which results in a slight variation in polarization direction such that the electrostatic energy of the system is somewhat lowered. From [44].

The occurrence of the in-plane, cross-layer, twisted structure has in [44] been verified through optical texture studies, where the modulation is seen as periodic lines perpendicular to the rubbing direction of the cell. Judging from the photos provided in the paper, this could be mistaken for pitch bands, but the pattern has also been observed in a mixture with infinite pitch (they are studying chiral-dopant mixtures, where one can obtain an infinite pitch without losing the spontaneous polarization), which shows that the periodicity is not pitch-related. The characteristics of the dielectric mode connected to the structure are summarized in [44] and [45]. As it is connected to the unwound structure it is only observed under the application of a bias field, except in the case of the mixtures with infinite pitch, and the susceptibility is typically much lower than other phase-angle fluctuation modes; in the range 0-10. On increasing the bias field the susceptibility decreases towards zero. The absorption frequency has in [45] been found to follow an Arrhenius dependence on temperature.

It is furthermore stated that the bias field actually results in the formation of two domain modes; one related to fluctuations close to the surfaces and one in the bulk. The reason for the splitting up would be that the DC-field pushes the ionic charge car-

riers in the liquid crystal towards the surfaces, and thus the spontaneous polarization is effectively “screened” close to the surfaces, but not in the bulk. Hence the periodicity of the twisted structures in the bulk and at the surfaces would not be the same, and the dielectric response would then contain contributions from two domain modes.

One should point out two problems with the reports on the domain mode. First of all, the authors do not at all discuss the occurrence of the surface-induced modes discussed in the previous section. As the mixtures under consideration all have a high value of spontaneous polarization, especially the splay mode ought to appear in these experiments. While the DC-bias normally applied may suppress it, some experiments are performed on mixtures of infinite pitch without a DC-bias, and there the splay mode cannot be expected to be absent. Instead, the authors argue that in these measurements the Goldstone mode is absent since there is no helix. As pointed out previously, this is actually the opposite of what is true, at least considering the bulk SmC\* liquid crystal: the case of an infinite helix is the *only* case where we could expect to observe the Goldstone mode dielectrically. However, the cell surfaces play an important role, so the dielectric behavior should rather be some combination of a surface-influenced Goldstone mode and the splay mode. All experiments on which the results in [44] and [45] are based, are performed in 16.5  $\mu\text{m}$  cells, so the dependence on the cell thickness has not been investigated. Secondly, many results are obtained on chiral-dopant mixtures rather than pure materials, and as will be discussed in the next chapter, the behavior of such mixtures may not be completely comparable to that of pure compounds.

The name proposed by the Darmstadt group is based on the similarity with ferroelectric domains. However, I find this name rather misleading as one might think that it involves spontaneous domains which appear in an SSFLC cell, or in a solid ferroelectric, which is not at all the case. A more descriptive name would be welcome.

### 3.4. The collective (or non-collective ?) modes of SmC<sub>a</sub>\*

If the situation is fairly clear for the SmC\* phase, it is considerably less clear for the SmC<sub>a</sub>\* phase, and still very confused concerning the sub-phases. The structure of the antiferroelectric SmC<sub>a</sub>\* phase is well understood, but the dielectric response is still a matter of considerable discussion, even if there are models proposed which seem to gain some acceptance. In planar-aligned samples the SmC<sub>a</sub>\* dielectric spectrum is characterized by two modes of very low susceptibility which may be distinguished by their respective absorption frequencies  $f_a$ . The low susceptibility is to be expected considering the antipolar order of the phase; in fact, it is only due to fluctuations from this equilibrium state that we may have a coupling to the measuring field. Therefore, a straight-forward Goldstone mode, in which all the layer directors turn around the cones in phase, keeping their anticlinic order from layer to layer, cannot be dielectrically detected. The high-frequency<sup>5</sup> mode has only a weak temperature dependence of  $f_a$ , usually with a maximum somewhere within the SmC<sub>a</sub>\* phase. This mode has in several papers been proven to be collective and is now generally regarded as being due to an anti-phase motion of molecules in adjacent layers [46]. If the molecules in neighboring layers fluctuate with a different sign of  $\Delta\varphi$ , this will result in a temporary non-

---

5. When in this context I speak of high and low frequency modes, it is only to differentiate the two SmC<sub>a</sub>\* modes from each other. Both frequencies are observed well within the intermediate frequency range of the standard dielectric bridge HP4192A, *i.e.* in the range 5 Hz - 13 MHz.

cancellation of neighboring dipoles, as illustrated in figure 31, and thus we may expect this fluctuation to couple to our measuring field.

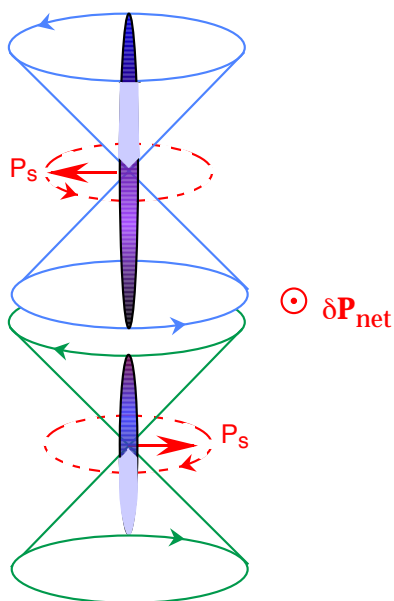


Figure 31. The most commonly adapted model for the origin of the high-frequency  $\text{SmC}_a^*$  dielectric mode. If the molecules in neighboring layers fluctuate in an anti-phase fashion, *i.e.* they experience a change in phase-angle  $\Delta\varphi$  with different signs, there will be a net polarization in the plane perpendicular to the  $C_2$  axis of the phase.

In my work, I have concentrated more on the origin of the low-frequency antiferroelectric mode, in this text referred to as the  $C_a^*_{\text{low}}$  mode. It is still subject to much discussion, and a general consensus regarding the nature of the mode has not yet been reached. There is some evidence, like the clear Arrhenius behavior of  $f_a$ , for interpreting this as a *non-collective* molecular mode, and in many papers it is therefore concluded that the mode is due to rotation of the molecules around their short axes [47]. If the molecules would lie parallel to the plane of the substrate (*i.e.* zig-zagging in this plane from layer to layer), such rotations could not be detected with dielectric spectroscopy (see section 3.2). Some other groups have reported observations contradicting the short axis rotation explanation. The susceptibility of the mode has for instance been found to be initially increased by applying a DC-bias field, and a decrease in temperature (accompanied by an increase in tilt angle) has in some cases led to a decrease in  $\chi$  [46]. The absorption frequency of the short axis rotation mode seen in quasi-homeotropic orientation, at a specific temperature, has furthermore often failed to coincide perfectly with the corresponding frequency of the  $C_a^*_{\text{low}}$  mode measured in a planar cell ( $f_a$  of  $C_a^*_{\text{low}}$  is typically a factor of 5 higher than that of  $f_{\text{hom}}$ ). These observations are difficult to explain in the frame of a non-collective mode, and therefore it seems reasonable that the mode could be collective in character.

### 3.4.1. The “low-frequency” $\text{SmC}_a^*$ mode as affected by a helix inversion

In the model proposed by Buivydas *et al.* [46] the  $C_a^*_{\text{low}}$  mode corresponds to a collective reorientation of the molecules in the same direction around the cone (in-phase motion), where the coupling to the electric field is made possible by the helical superstructure and a corresponding small shift in the local polarization directions. Because of the helix there is a small deviation from the  $180^\circ$  angle between the directors in adjacent layers (*cf* figure 32). Hence, the dipoles do not cancel completely and a small net polarization appears. This mesoscopic polarization itself describes a helical struc-

ture which is isomorphic with the helical  $\text{SmC}^*$  case. We would therefore expect a helix distortion mode which could be detected by dielectric spectroscopy.

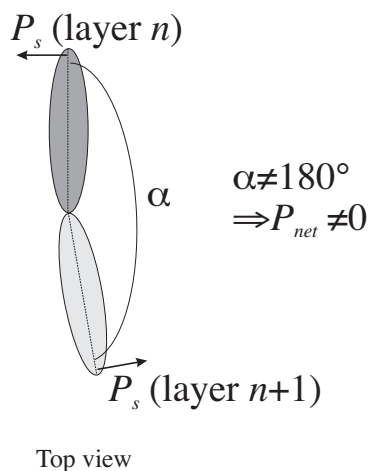


Figure 32. Due to the helical superstructure the molecules in adjacent layers are not at exactly  $180^\circ$  angle to each other. Therefore the polarizations in adjacent layers do not cancel totally and a small net mesoscopic polarization appears.

In a material featuring a helix inversion this deviation from a perfect anti-tilt structure should diminish continuously when we approach the point of inversion, since at this point the pitch diverges and the helical superstructure disappears. The dipoles of neighboring layers should then really cancel, and the susceptibility of the mode should tend to a minimum.

Together with colleagues from the Berlin group, I studied the  $C_{a^* \text{low}}$  mode in two antiferroelectric liquid crystalline systems featuring helix inversions, a work described in paper 1. We investigated a pure liquid crystal compound with a temperature-induced helix inversion in the  $\text{SmC}_{a^*}$ -phase (EHPOCBC), and we also prepared and studied a mixture system where the two pure components ((S)-EHPnCBC-12 & (S)-TFMHP-nBC-11) have different helical handedness but the same sign of the spontaneous polarization  $P_s$ . At a certain mixing ratio a helix inversion is thus induced and, as the spontaneous polarizations of the two mixture components do not cancel, one might hope to see mainly the effect of the pitch change on the antiferroelectric mode in such a sequence of mixtures. It turned out, however, that for different mixing ratios not only the pitch varied, but also the  $P_s$  value and tilt angle, as well as the phase transition temperatures and even phase sequences. Furthermore, from an experimental point of view a different cell has to be prepared for each chosen ratio, which results in non-identical alignment for different measurements. Thus, the data taken on the mixture were very difficult to interpret, and in the following I will describe only the results obtained with EHPOCBC.

Considering the large influence from the surfaces which can be expected on a material where the pitch diverges, we made experiments only on very thick cells (we had no possibility to perform measurements on free-standing films). The results for a  $50 \mu\text{m}$  cell are shown in figure 33. In the vicinity of the inversion temperature a dip in  $\chi$  of  $C_{a^* \text{low}}$  is apparent, even though the magnitude of the change is not very high. A surprising result is that this seems to be accompanied by an *increase* in absorption frequency compared to the normally observed Arrhenius behavior. The expected effect, if any, would be a lowering in  $f_a$  at diverging pitch  $p$ . However, it seems that for  $p \rightarrow \infty$  even a  $50 \mu\text{m}$  thick cell starts to behave as thin, scaled as  $d/p$ , such that the surfaces contribute to a small increase in the helical elasticity. The high-frequency mode (not shown) also exhibited a clear decrease in  $\chi$  as well as in  $f_a$  at the inversion point.

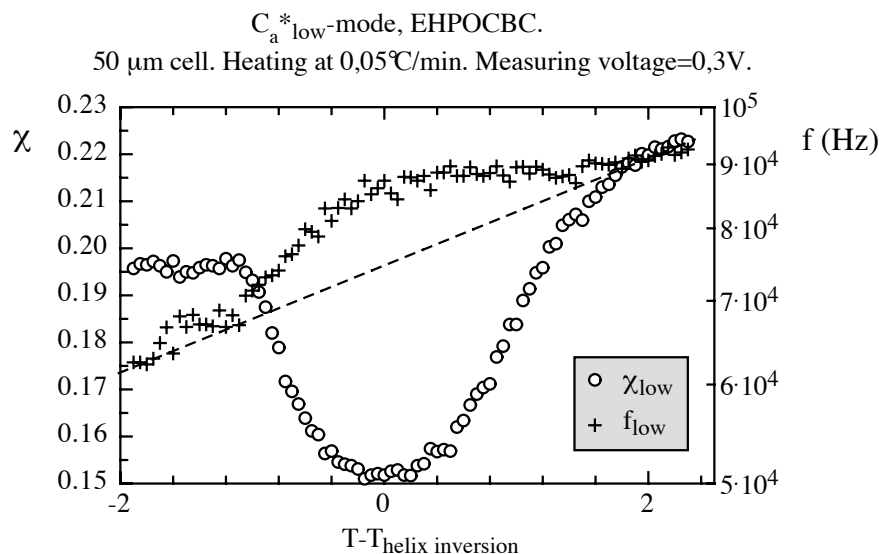


Figure 33. The absorption frequency  $f_a$  and susceptibility  $\chi$  of the low-frequency  $\text{Sm}C_a^*$  mode ( $C_a^*_{\text{low}}$ ) in the vicinity of the helix inversion. The effect on  $\chi$  from the pitch divergence is clearly seen. An unexpected result is that  $f_a$  seems to increase as an effect of the pitch divergence. The dashed line is drawn to indicate the expected Arrhenius-like temperature dependence of the absorption frequency.

In order to compare the activation energy of  $C_a^*_{\text{low}}$  with that of the molecular reorientation around the short axis, we prepared a quasi-homeotropic cell with EHPOCBC. It turned out that the activation energies measured in the two alignments are more or less identical; the difference is within experimental error. This supports the short axis reorientation model for  $C_a^*_{\text{low}}$ .

In summary, therefore, the question can still not be considered permanently settled. The strong resemblance in absorption frequency between  $C_a^*_{\text{low}}$  and the short axis reorientation, seen in the comparison between quasi-homeotropic and planar measurements, lends support to the idea that the low-frequency  $\text{Sm}C_a^*$  mode is indeed identical to the *non-collective* molecular reorientation process. On the other hand, the observations in the planar cell close to the helix inversion supports the *collective* model for the mode, even though it must be pointed out that the susceptibility decrease is not very dramatic. The present work is, however, based on measurements in cells, where the diverging helix may be strongly affected by surfaces, and a natural extension would therefore be to perform similar measurements on a free-standing film of the material.

### 3.4.2. The $\text{SmA}^* - C_a^*$ transition

We are now in a position to continue the discussion on the soft mode for the case of the  $\text{Sm}C_a^*$  phase. An interesting example is given in figure 34 where the soft mode behavior of the mixture W101 (same origin as W107, mentioned previously), described in paper 5, is illustrated. The compound is studied in both a thin (2  $\mu\text{m}$ ) and a thick (36  $\mu\text{m}$ ) planar aligned cell, on cooling and on heating. In bulk, as approximated by the 36  $\mu\text{m}$  sample, the compound exhibits a direct  $\text{SmA}^* - C_a^*$  transition, and it is clear both from the experimental data (3D-plots) and fitting results that the soft mode susceptibility decreases much quicker in the  $\text{Sm}C_a^*$  phase than in the  $\text{SmA}^*$  phase, on departing from  $T_c$ .

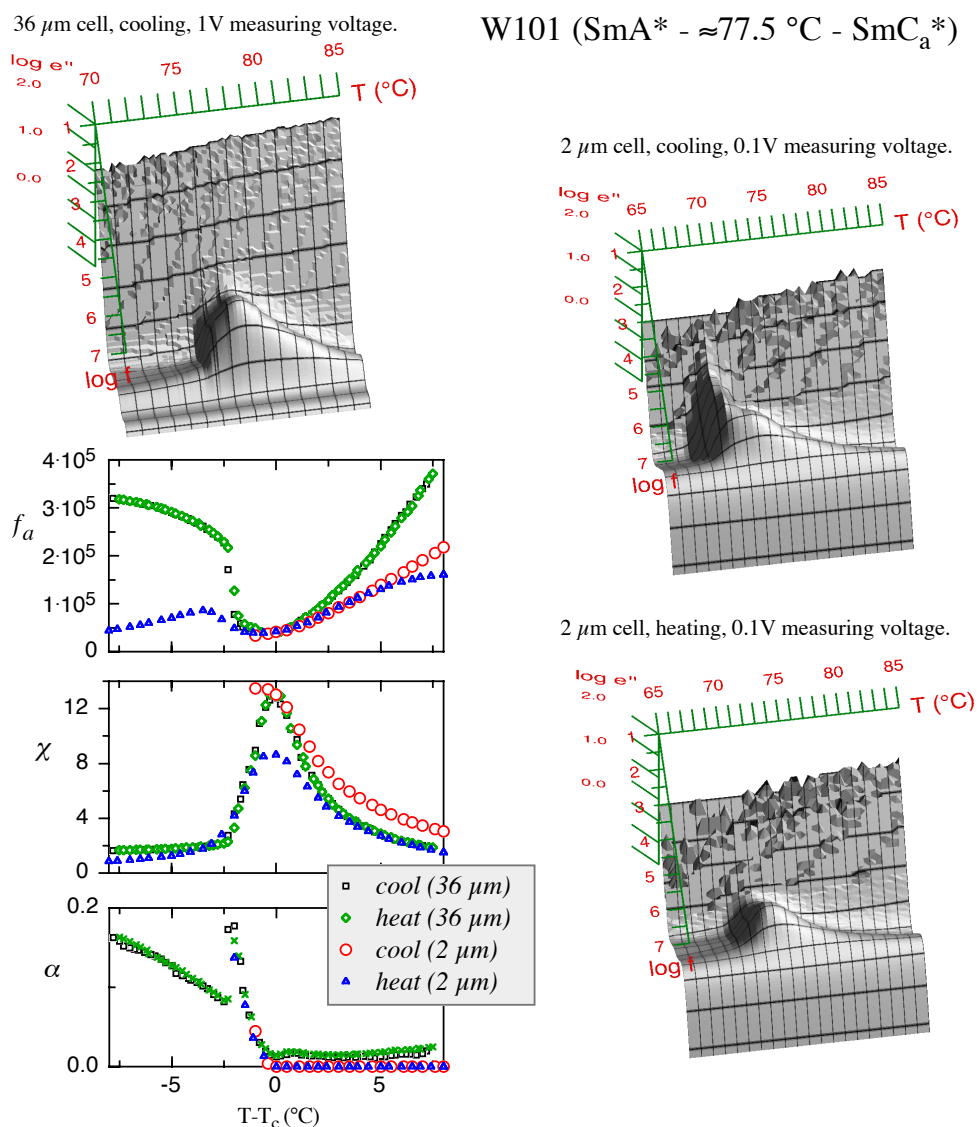


Figure 34. An example of the soft mode behavior in a compound (W101) having a direct SmA\* $\rightarrow$ C<sub>a</sub>\* transition. The bulk behavior, approximated in the 36  $\mu\text{m}$  cell, is virtually identical on cooling and heating. In the thin cell, the general phase behavior of the compound is clearly affected, and apart from the transition temperature being shifted downwards by several degrees (the SmA\* phase is thus stabilized by the surfaces), we also see that supercooling effects appear. Not only is  $T_c$  on cooling lower than on heating, but there also appears a low-frequency absorption, indicating a short temperature interval of surface-induced order, which is not present on heating. Fitting of the Cole-Cole equation to the experimental data was considerably more difficult in the thin cell, partly due to this new absorption (on cooling), but also due to the increased importance of the cell relaxation. From the distribution parameter values it is clear that the soft mode in the SmC<sub>a</sub>\* phase is accompanied by relaxations typical of this phase.

In thin cells we see an example of a phenomenon which will be more extensively covered in chapter 5, namely that surfaces have an ordering effect. First of all, the SmA\* phase is stabilized several degrees below the transition temperature in bulk, which may be seen as a sign of the incompatibility between the surface anchoring and

the antiferroelectric structure of the  $\text{SmC}_a^*$  phase [3]. On heating, the mixture in other respects behaves as previously, but on cooling the transition from the  $\text{SmA}^*$  phase is first of all supercooled, and furthermore we see a new low-frequency absorption just below the phase transition. A possible explanation for this absorption is that the compound, when entering the tilted phase, in a short temperature interval partly forms a *synclitic* structure due to the ordering effect of the surfaces.

### 3.5. The collective modes of the $\text{SmC}^*$ subphases

#### 3.5.1. The dielectric response of $\text{SmC}_{1/3}^*$ and $\text{SmC}_{1/4}^*$

For the sub-phases between  $\text{SmC}^*$  and  $\text{SmC}_a^*$  the situation is still very unclear. While the  $\text{SmC}_{1/4}^*$  is generally reported to be virtually “dead” concerning dielectric response, several different behaviors of the  $\text{SmC}_{1/3}^*$  phase have been reported. The absence of dielectric response of the  $\text{SmC}_{1/4}^*$  phase fits well with the polarization canceling (antiferroelectric) structure proposed for the phase, as described in section 1.2.3. The in many respects (texture, etc.) similar  $\text{SmC}_{1/3}^*$  phase has, on the other hand, often been reported to exhibit a phason mode of extremely high susceptibility and low absorption frequency, which is explained in terms of the very long helical pitch of this phase. This would indicate that there is no local antiferroelectric ordering in this phase, and that we may thus excite a helix distortion mode, or a splay mode in case the helix is suppressed by surfaces, with the measuring field. In some cases, *e.g.* paper 2 or [48], the response of the phase seems instead to be very weak, at least without applying a bias field. However, this does not have to rule out the above description as the general  $\text{SmC}_{1/3}^*$  dielectric behavior, since a very low-frequency absorption may actually be “hidden” by the ionic contributions, at least if the phase appears at high temperatures which is the case of paper 2. In [48] all measurements are performed using 10  $\mu\text{m}$  cells, so here the weak response may be a result of the surface influence.

One should point out, remembering our previous discussion on the influence of cell surfaces, that the very long-pitch of the  $\text{SmC}_{1/3}^*$  and  $\text{SmC}_{1/4}^*$  phases makes the study of them in standard cells difficult. It has several times been observed that the whole phases can actually be quenched out in thin cells (see for instance paper 2), but also in thicker cells, where the phase transitions are still visible, one must take into account that the response is most probably related to a surface-induced distorted structure, not to a helical one. To my knowledge, no dielectric experiments on free-standing films of  $\text{SmC}_{1/3}^*$  and  $\text{SmC}_{1/4}^*$  materials have been done. This is definitely a future task of importance for all researchers active in the field.

#### 3.5.2. The $\text{SmC}_\alpha^*$ phase

The  $\text{SmC}_\alpha^*$  phase is also a helical phase, but with an extremely short pitch. As discussed in section 1.2.3, the pitch may furthermore change substantially within the narrow temperature range of the phase. Since it is a tilted phase with no inherent local antipolar ordering, we may expect some kind of phason mode. Considering the very short pitch, it is reasonable to assume that this would be of the helix distortion type even in fairly thin cells. As the elastic constant of a tightly twisted structure furthermore should be quite high, we may according to equations (43) and (44) expect a low

susceptibility and fairly high absorption frequency. Experimental observations show that the behavior of the phase may vary considerably; from a very weak response where the  $\text{SmA}^*/\text{C}_\alpha^*$  transition is only noticed by a change of slope in the soft mode temperature dependence [49], to a clear phason contribution, weaker than the soft mode but still of substantial susceptibility, throughout the phase [48]. It is thus difficult to formulate a typical  $\text{SmC}_\alpha^*$  behavior.

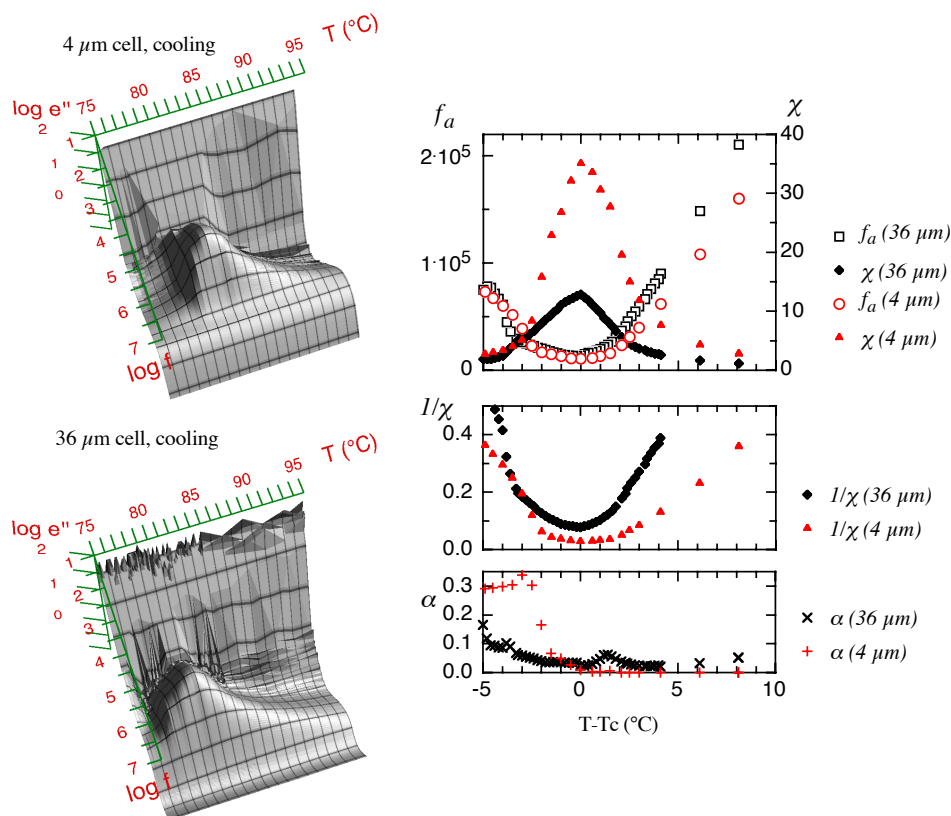


Figure 35. The soft mode of 10F1M7, which has a  $\text{SmA}^*/\text{C}_\alpha^*$  transition around  $81^\circ\text{C}$ , as observed on cooling. The increase of the soft mode susceptibility on approaching the phase transition seems to be slower in the  $\text{SmC}_\alpha^*$  phase than in  $\text{SmA}^*$ . However, the  $\text{SmC}_\alpha^*$  phase normally shows a contribution to  $\epsilon$  due to phase-angle fluctuations, and it might be the influence of this mode that affects the fitting results shown on the right. A sign of warning, strengthening this hypothesis, is the large increase in the distribution parameter  $\alpha$  below the phase transition. The sudden increase in distribution of the mode is also the explanation to what in the 3D-plots looks like a sudden step decrease in susceptibility of the soft mode; as illustrated in figure 9, an increase in  $\alpha$  leads to a lower maximum value in the absorption spectrum. The slight shift in transition temperature between the cells may be an experimental artifact related to the difficulties of maintaining correct temperature control of the two different cell types.

The transition  $\text{SmA}^*-\text{C}_\alpha^*$  constitutes the final example of a soft mode as observed in dielectric spectroscopy. In figure 35 I show this transition in the pure compound (S)-10F1M7, supplied by D. Parghi (Berlin). In this case the soft mode behaves quite differently from the cases described previously. First of all the rate of susceptibility increase on approaching the phase transition actually seems to be lower in the  $\text{SmC}_\alpha^*$

phase than in SmA\*. However, below the phase transition the distribution parameter  $\alpha$  increases in magnitude, and in the case of the thin cell, the increase is quite large. This indicates that we no longer see a pure soft mode, but a mixture of this and the SmC $_{\alpha}$ \* phason mode. Had we seen only the soft mode, it is possible that we would have seen a much steeper decrease in susceptibility when lowering the temperature from  $T_c$ . This may be a general problem when studying the SmC $_{\alpha}$ \* phase, and fitting results from within this phase can therefore be in the position of being doubted.

### 3.6. Summary

In all calamitic liquid crystals we may expect contributions to the dielectric permittivity from the non-collective (molecular) processes which correspond to rotations around the long and short axes, respectively, of the molecules. The short-axis rotation is observed in quasi-homeotropically aligned cells, at absorption frequencies typically in the kHz or MHz regime, and the long-axis rotation is seen in planar alignment, with absorption frequencies in the GHz regime. As chiral tilted smectics have a symmetry permitting a local mesoscopic dipole moment, we may in these phases also expect collective processes to contribute to the permittivity. In the SmA\*/C\* system, including possible subphases of SmC\*, these may be divided into phason and amplitudon modes, where the former correspond to phase-angle fluctuations and the latter to tilt-angle fluctuations.

While there is only one type of amplitudon mode – the soft mode present at the onset of tilt – we may experience several types of phason modes, depending on the thermodynamic phase and on the measurement geometry. The most common of these is a fluctuation in the helical SmC\* structure, here called the helix distortion mode, which in the limiting case of an infinite pitch material, studied without the influence of boundaries, becomes the Goldstone mode of the phase. While the Goldstone mode exists also in other cases, it cannot be detected by dielectric measurements. In thin cells we may also see modes related to the surface-influenced structure of the system. This should be taken into account, especially if one studies long-pitch materials. In such cases, a very attractive possibility is to instead study free-standing films of the compound.

In practice, it is often impossible to say which phase-angle fluctuation gives rise to the measured permittivity contribution. In such cases the best choice is to simply call the mode a phason mode, which is the general term applicable to all phase-angle fluctuations possible. On the other hand, the term Goldstone mode, which in literature often is used without criticism, should be avoided as a general term for fluctuations in the phase-angle.

## 4. DOPING OF ANTICLINIC RACEMIC HOSTS WITH CHIRAL DOPANTS

---

---

*Kaffe utan cognac är en djäfla blandning<sup>1</sup>*  
– Albert Engström

### OVERVIEW

*This chapter deals with a possible new way of achieving antiferroelectric liquid crystal compounds for commercial applications: the so-called chiral-dopant technique. I will briefly present the basic ideas, and the reasons for why this technique might be useful for AFLCs, as it is indeed used for FLCs today – or why it is not. The main part of the chapter is devoted to a summary of my experimental results, obtained together with Deven Parghi from the anisotropic fluids group at TU-Berlin, on six different prototype chiral-dopant mixtures.*

### **4.1. Why chiral-dopant mixtures ?**

The liquid crystals used for prototype and commercial SSFLC devices are not pure compounds, but mixtures of an achiral or racemic host material, together with a chiral dopant providing the ferroelectric properties. The main reason for this is that chiral smectics often have a high viscosity making them inconvenient to use in a device. The chiral-dopant mixture concept gives compounds with much more attractive characteristics. The same technique has up to now not been used for AFLC devices, because the recognition of achiral anticlinic materials is quite recent and the corresponding chiral/achiral relationship much more sophisticated. Together with Deven Parghi, I have studied such systems in order to get a picture of how antiferroelectric chiral-dopant mixtures may behave. The work is still in progress, but by now we have a fairly good understanding of how the combinations of host and dopant influence the resulting chiral phases. The details may be found in papers 3 and 4, but here I will give a summary as well as some more recent observations.

#### **4.1.1. The choice of a host**

When choosing a host, there are in principle two routes to follow. Either one mixes the two enantiomers of a chiral compound in equal quantities, in order to get a racemic mixture, or one uses a pure achiral compound. In both cases, the existence of an anticlinic phase is of course essential for our purpose, and this very much limits the possi-

---

1. “Coffee without brandy is a Devil’s mixture”

bilities in following the second route. There are simply not very many achiral compounds forming anticlinic phases (the question why, is fundamental, but unanswered), making the supply of host materials in this category very small. In following the first route, on the other hand, there is today a fairly large number of chiral compounds exhibiting the  $\text{SmC}_a^*$  phase, and one only has to make sure that the anticlinic phase persists also in the racemic mixture. For commercial purposes one would of course also pay a lot of attention to the viscosity, birefringence, etc., of the host, but in our study these parameters are not of primary importance. Instead the existence of syn- and anticlinic tilted phases in the racemic mixture is what interests us the most, and hence we have chosen the three host mixtures listed in figure 36. With these three racemic mixtures we can study the cases of a purely synclinic host, (R/S)-8F1M6, a purely anticlinic host, (R/S)-10F2E7, and a host exhibiting both syn- and anticlinicity, (R/S)-10F1M7. We do not expect to obtain an antiferroelectric chiral-dopant mixture using the purely synclinic host, but it is of interest for comparative reasons.

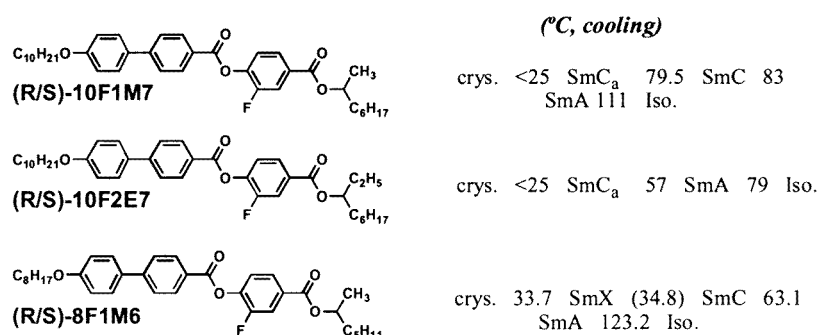


Figure 36. The three racemic host mixtures and their phase sequences. The  $\text{SmX}$  phase of (R/S)-8F1M6 is an as-yet unclassified hexatic phase, probably  $\text{SmI}$  or  $\text{SmF}$ .

One should point out that some of the hosts, in their optically pure versions, actually feature also other smectic  $\text{C}^*$  subphases than  $\text{SmC}^*$  and  $\text{SmC}_a^*$ , and in fact they do not necessarily exhibit the chiral versions of the phases appearing in the racemic mixture. For instance, (S)-10F1M7 has a  $\text{SmC}_\alpha^*$  phase and probably no  $\text{SmC}^*$  phase (this is currently under examination), but the racemic mixture has a  $\text{SmA-C-C}_a$  phase sequence.

We actually studied also a system based on an achiral anticlinic host, but it turned out to be difficult to get unambiguous results in this case. With too much dopant, the liquid crystalline phases were lost completely, which limited us to quite small dopant quantities. Hence the resulting chiral system had a very weak dielectric response. Furthermore, even for dopant quantities which did produce an antiferroelectric liquid crystalline system, we experienced large problems with crystallization within the  $\text{SmC}_a^*$  phase. In the following, this system will therefore not be discussed.

#### 4.1.2. The relevance of the dopant

In the first stage of the project our intention was to prepare binary mixtures where the three different hosts were doped with additives which are strongly  $\text{SmC}^*$ - or  $\text{SmC}_a^*$ -promoting. For the first type of mixtures we used the dopant (S)-IGS97 [50], which is a standard non-liquid-crystalline dopant used in chiral-dopant FLC mixtures. Its structure is very similar to the typical structure of  $\text{SmC}^*$  materials [51], and it is known to strongly promote the  $\text{SmC}^*$  phase when used as a dopant. As a dopant of the second

category we chose (S)-MHPOBC which is well known to have a broad antiferroelectric  $\text{SmC}_a^*$  phase and only a narrow  $\text{SmC}^*$  phase. Later on we have also complemented the study using other dopants. As a very strongly  $\text{SmC}_a^*$ -promoting dopant we have used (S)-TFMHPOBC and as an intermediate-type dopant, which can be expected to promote both clinicities, we have chosen (S)-11F1M7. However, the study of these mixtures is far from finished and the results will not be discussed here.

In principle one should study the behavior with a varying amount of dopant as well, but the number of mixtures then quickly increases to an unmanageable amount. Hence, we settled with one chiral-dopant concentration for each mixture, chosen low enough that the liquid crystal phases were not destabilized by the dopant (which is a risk especially when using (S)-IGS97 as dopant) but high enough to produce a dielectric and electrooptic response in the mixture. For the two dopant materials used in the present study, we chose 10% (by weight) of (S)-IGS97 and 15% of (S)-MHPOBC. The components were mixed in the isotropic phase in standard DSC pans.

## **4.2. The induced chiral phases**

The mixtures were first studied in quasi-homeotropically aligning slides in a polarizing microscope. Based on the observed textures, we could write down a preliminary phase sequence for each mixture. The  $\text{SmC}_a^*$  phase was identified by the existence of the two-brush defects characteristic of anticlinic phases [52]. As could be expected in mixtures of this type, there was no sign of smectic  $\text{C}^*$  subphases ( $\text{SmC}_{1/3}^*$ ,  $\text{SmC}_{1/4}^*$  or  $\text{SmC}_\alpha^*$ ). The transition temperatures for the chiral phases induced by (S)-MHPOBC turned out to be raised in comparison with the non-chiral phases of the pure host material. This is no doubt due to the miscibility of the phases of the host material with the analogous chiral phases observed at higher temperatures in the dopant compound. On the other hand, although the other dopant is miscible with the host material in the quantity used, its non-liquid-crystalline nature clearly has a destabilizing effect on all of the observed phases, and the transition temperatures in mixtures where this is used are consequently lowered. We did not perform any quantitative measurements of the pitch in the different phases, but from the quasi-homeotropic textures it was obvious that the values were rather large for all mixtures; clearly much longer than visible wavelengths.

After this initial investigation the mixtures were studied with respect to their electrooptic switching behavior at room temperature, *i.e.* nominally in the  $\text{SmC}_a^*$  phase, except for the strictly synclinic mixtures which were studied in the  $\text{SmC}^*$  phase at 40°C. The results, which are summarized in figure 37 indicated that the phase sequences were more complicated than what was concluded from the optical texture studies. In particular there were strong signs of phase coexistence with  $\text{SmC}^*$  within the nominal  $\text{SmC}_a^*$  temperature range in some cases. Especially the combination (R/S)-10F1M7 with (S)-IGS97 would not show the tristate switching typical of a  $\text{SmC}_a^*$  phase in any thickness of cell, not even at frequencies as low as 1 mHz. In a 10  $\mu\text{m}$  cell at 5 mHz the compound showed a mixed switching behavior, and in all other cases the switching reminded more of a  $\text{SmC}^*$  phase. Furthermore, a general trend was that the mixtures doped with (S)-IGS97 had a much lower switching threshold than those doped with (S)-MHPOBC.

For dielectric spectroscopy studies we prepared planar-aligned samples of varying thickness with the six mixtures. The alignment layer was, except when stated otherwise, spin-coated polyimide with anti-parallel buffing. The systems were in general rather

sensitive to external influence, in particular those doped with (S)-IGS97. This made their study slightly problematic as even the measuring field itself, also at low amplitude, was often enough to distort the response. I will here summarize the results grouping the mixtures according to their host compounds.

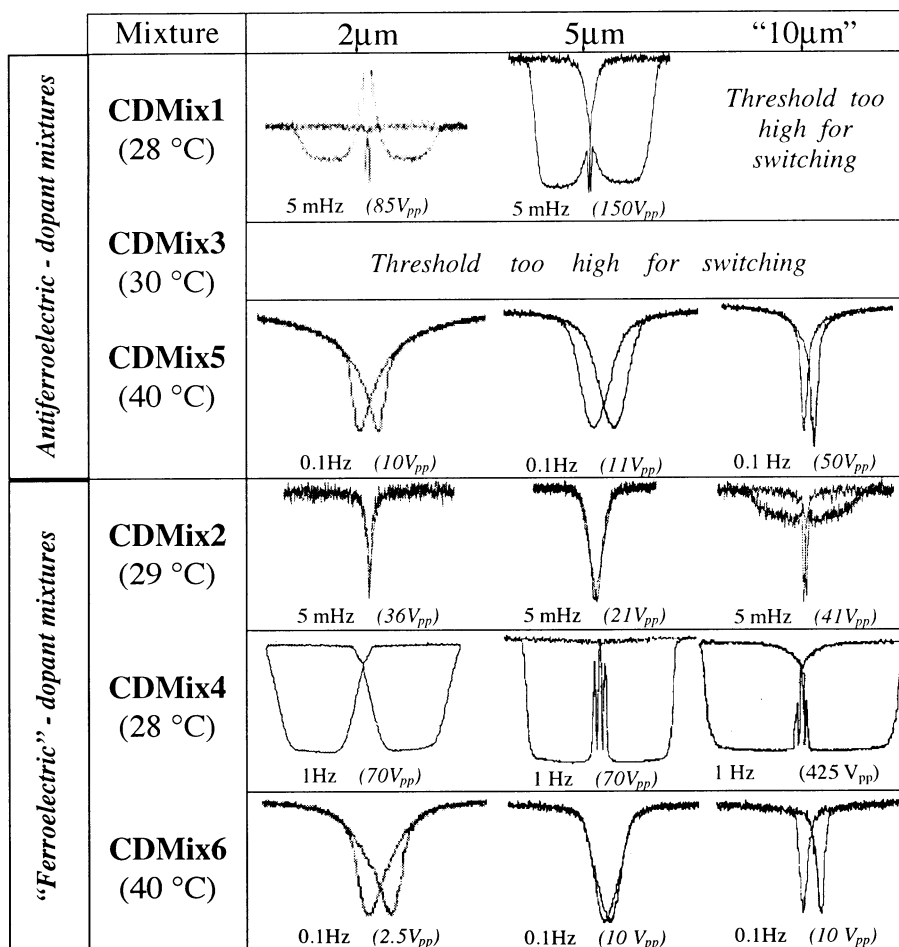


Figure 37. Transmission vs. applied voltage curves obtained for the binary chiral-dopant mixtures. All compounds were studied at room temperature, and should, according to texture observations, be in the  $SmC_a^*$  phase, except CDMix5 and 6 which were studied at 40°C, in the  $SmC^*$  phase. For each type of dopant, the mixtures are listed following the host; (R/S)-10F1M7 (syn- and anticlinic) first, followed by (R/S)-10F2E7 (strictly anticlinic), and finally (R/S)-8F1M6 (strictly synclinic).

#### 4.2.1. Syn- and anticlinic host

The two mixtures based on (R/S)-10F1M7 exhibited both  $SmC^*$  and  $SmC_a^*$  phases, but in both cases with some degree of phase coexistence within the temperature range of the latter phase. In the (S)-MHPOBC-doped mixture the transitions were perfectly sharp in thick cells, but in a 4  $\mu$ m cell the range of  $SmC^*$  was not only extended by approximately 2°C, but the transition to the  $SmC_a^*$  phase was no longer distinct, especially on cooling. (S)-IGS97 destabilized the anticlinic character of the  $SmC_a^*$  phase to a very high degree. First of all the mixture had a very low threshold for switching to the ferroelectric state, and as the mixture had a tendency to be surface-stabilized even in thick cells (see figure 38), the relaxation back to a helical structure was very slow. This clearly influenced also the dielectric measurements, which turned out quite differ-

ent depending on for instance the measuring field amplitude. In figure 39 are shown some representative 3D-diagrams obtained on the mixture in a  $25 \mu\text{m}$  cell. By just raising the measuring voltage from 0.15 V to 0.5 V we increase the  $\text{SmC}^*$  phason mode susceptibility by a factor of 2.5 and halve its absorption frequency.



Figure 38. The texture of (S)-IGS97-doped (R/S)-10F1M7 in a  $25 \mu\text{m}$  thick planar-aligned sample at the transition from  $\text{SmC}_a^*$  to  $\text{SmC}^*$ . The  $\text{SmC}^*$  regions are distinguished by the clear domain texture. About 20 seconds later, the domains have disappeared, indicating that the ferroelectric state is not really surface-stabilized, but transforms to a helical structure.

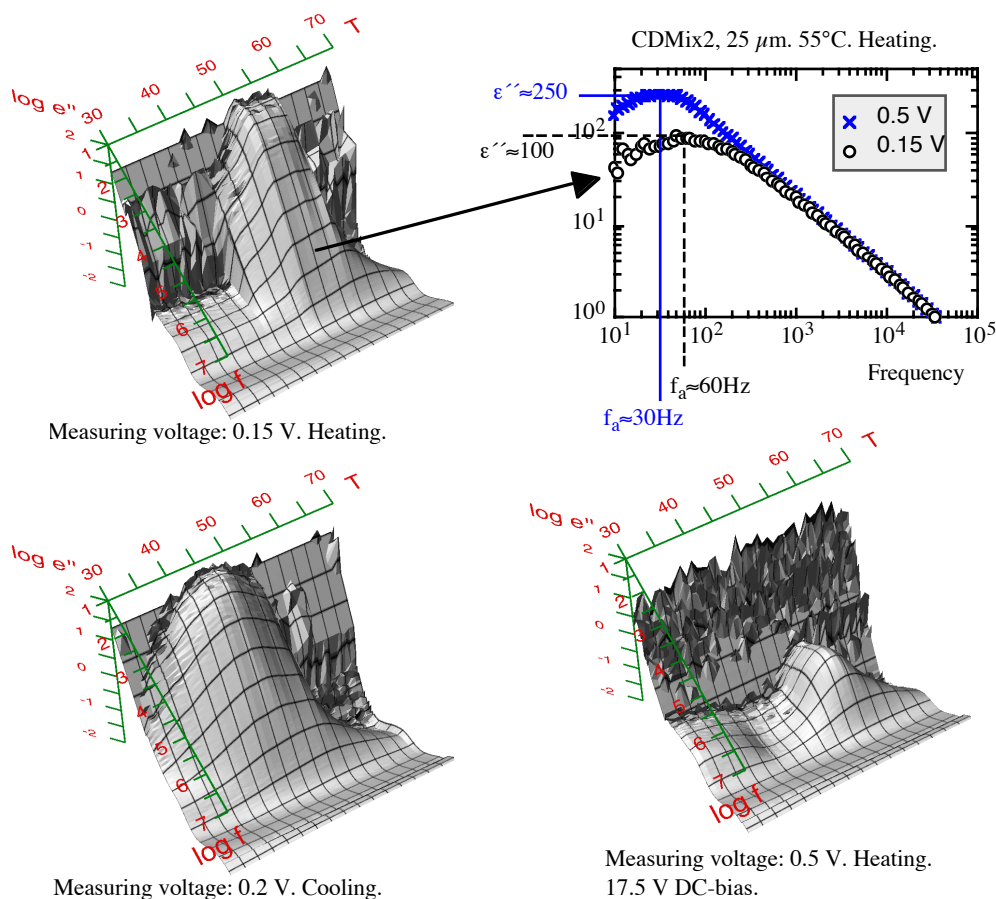


Figure 39. The mixture of (R/S)-10F1M7 with (S)-IGS97 exhibited a high degree of phase coexistence between  $\text{SmC}^*$  and  $\text{SmC}_a^*$ , as seen especially in the cooling spectrum (lower left). By applying a DC-bias the  $\text{SmC}^*$  phason mode is quenched and one can then fairly well see the nominal temperature range of the  $\text{SmC}_a^*$  phase (lower right). All spectra are obtained with a  $25 \mu\text{m}$  commercial EHC cell.

Furthermore, the  $\text{SmC}^*-\text{SmC}_a^*$  transition is very blurred out in all measurements, and on cooling, the  $\text{SmC}^*$  phason mode extends all the way down to room temperature even in the  $25\ \mu\text{m}$  cell. To observe the characteristic  $\text{SmC}_a^*$  absorptions, one therefore has to perform the experiment on heating (after having stabilized the room temperature structure for a long time) or apply a weak DC-bias while measuring on cooling. In a  $4\ \mu\text{m}$  cell the phason mode was present with undiminished susceptibility down to room temperature also in heating runs. However, while the mode in the thick cell was observed at very low frequencies, the absorption frequency in the thin cell was about 100 Hz for all values of measuring field, indicating that the mode in this case corresponded to the surface-induced in-layer phase-angle fluctuations. At higher voltages also the thin sample responded with additional low-frequency contributions, probably corresponding to the ferroelectric switching.

#### 4.2.2. Anticlinic host

The dielectric experiments on the mixtures based on (R/S)-10F2E7 confirmed the preliminary  $\text{SmA}^*-\text{C}_a^*$  phase sequence, even though these compounds gave a very small dielectric response (*cf.* figure 40). In particular the compound doped with (S)-MHPOBC, gave an almost featureless spectrum when placed in a  $2\ \mu\text{m}$  cell, and even in the  $23\ \mu\text{m}$  cell the absorptions were very weak. The soft mode at the  $\text{SmA}^*-\text{C}_a^*$  transition had a remarkably low susceptibility, and if a DC-bias field was applied over the sample, the small maximum at  $T_c$  was pushed down to such an extent that one could mistakenly take it for a continuation of the  $\text{C}_a^*_{\text{low}}$  mode. This can be interpreted either as a sign that the resulting mixture is very “weakly chiral”, or it could be quite the opposite; if the  $\text{SmC}_a^*$  phase is “strongly antipolar” one could expect a behavior similar to that of solid antiferroelectrics, *i.e.* that there should be no, or very little, soft mode behavior at the transition between paraelectric and antiferroelectric order (see the discussion on the soft mode in section 3.4.2).

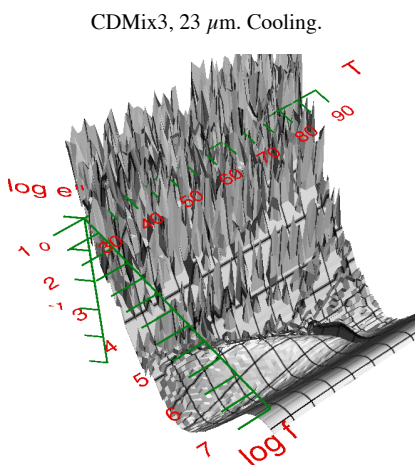


Figure 40. The remarkably featureless absorption spectrum of (S)-MHPOBC-doped (R/S)-10F2E7 in a  $23\ \mu\text{m}$  cell. No sign of the “high”-frequency  $\text{SmC}_a^*$  absorption can be seen, which is the case also when this host is doped with the  $\text{SmC}^*$ -promoting dopant (S)-IGS97, as well as in the combination of (S)-MHPOBC and (R/S)-10F1M7. On the other hand, the  $\text{C}_a^*_{\text{low}}$  mode susceptibility is of the same order of magnitude as that of the soft mode at the phase transition.

An interesting observation is that none of the chiral-dopant mixtures exhibiting a normal  $\text{SmC}_a^*$  phase showed any sign of the “high”-frequency  $\text{C}_a^*$  mode. This does not mean that it is completely absent, but its susceptibility must at least be so low that it cannot be distinguished from the cell relaxation absorption. The  $\text{C}_a^*_{\text{low}}$  mode, on the other hand, has a quite normal susceptibility in all mixtures, and in view of the discussion on the  $\text{SmC}_a^*$  dielectric response in section 3.4, this has interesting consequences. These observations support the idea that only the higher  $\text{C}_a^*$  mode is in fact collective,

and thus related to the antipolar order, which either is very weak or very strong in these mixtures. A weak order will naturally diminish any collective response while a strong antipolar order could be expected to counteract the anti-phase fluctuations proposed as an explanation for the higher  $C_a^*$  mode. The persistence of the  $C_a^*_{low}$  mode in the chiral-dopant mixtures is then a strong argument for the non-collective short-axis rotation model, since this fluctuation should have little to do with the order of the phase.

### 4.2.3. Synclinic host

The synclinic nature of (R/S)-8F1M6 apparently had a strong influence on the resulting chiral mixtures. Neither of its chiral-dopant mixtures showed any sign of  $SmC_a^*$  phases. The high-ordered  $SmX^*$  phase, distinguished by a virtually featureless spectrum, was seen in the (S)-MHPOBC-doped mixture but not in the mixture with (S)-IGS97. Also when it was present, it seemed that the  $SmC^*$  structure was much favored. First of all the  $SmC^*$  phase was easily supercooled into the  $SmX^*$  temperature range; in both thin ( $2\ \mu m$ ) and thick ( $23\ \mu m$ ) cells the  $SmC^* \rightarrow SmX^*$  transition appeared approximately  $13^\circ C$  below the corresponding transition temperature obtained on heating. Furthermore, if a measurement without DC-bias was performed immediately after a 35V bias scan, the  $SmX^*$  phase exhibited a fairly strong absorption in the low kHz range, reminding of a phason mode. This must be related to a bias-induced  $SmX^*$  distortion with long relaxation time.

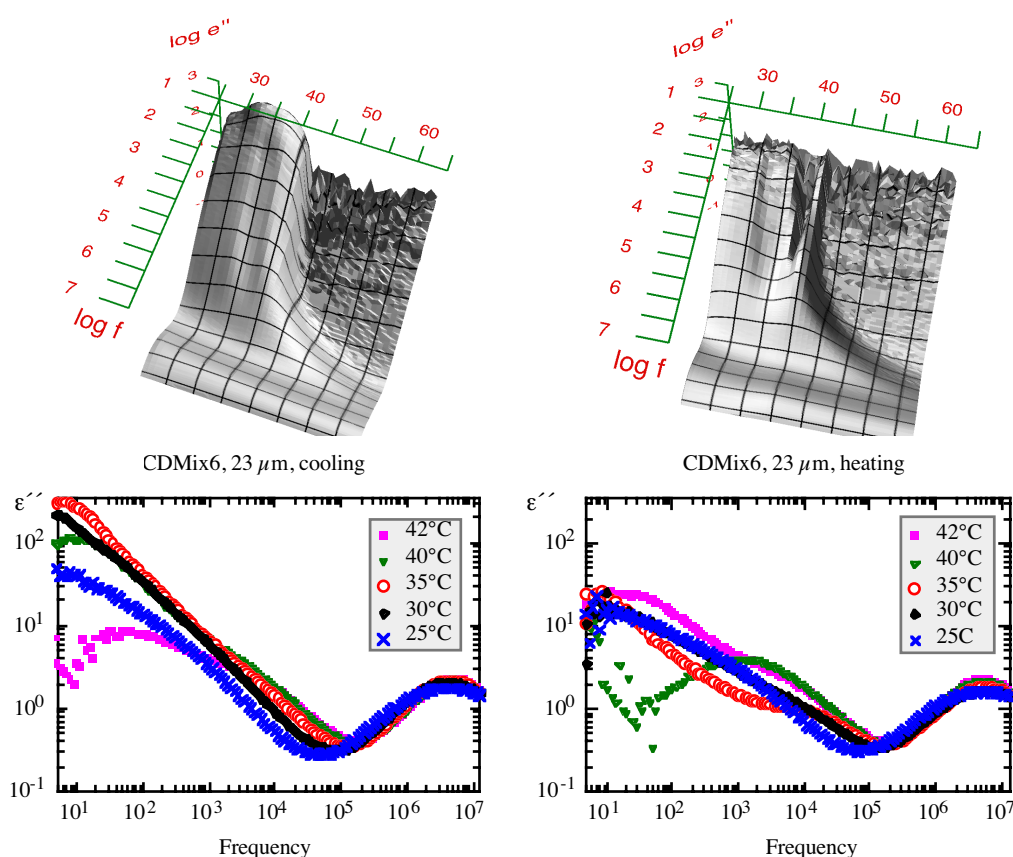


Figure 41. The imaginary part of the dielectric permittivity of CDMix6, *i.e.* synclinic host and  $SmC^*$ -promoting dopant, in a  $23\ \mu m$  cell. The phason mode behaves quite differently on cooling and on heating, in particular in the temperature region  $30-40^\circ C$ . The cooling and heating diagrams are drawn on the same scale.

The (S)-IGS97-doped compound showed a quite unusual  $\text{SmC}^*$  phase behavior, which perhaps could be connected to the presence of the hexatic phase in the host. In all experiments, the phason mode had a much higher susceptibility on cooling than on heating, especially in the temperature range 30–40°C where the  $\text{SmC}^*$  phase appears to be more sensitive to external influence. In this range the mode was easily quenched by applying a DC-bias, while it was still present even at maximum bias field (35V over 23 $\mu\text{m}$ ) below 30°C. Furthermore, if a zero-bias scan was performed immediately after the 35V bias scan, the mode did not reappear at all on heating. On cooling it did reappear but quite distorted. A distinct kink was then visible at 30°C in the spectrum. Finally, the phason mode completely disappeared in a narrow temperature interval below the  $\text{SmC}^*\text{-A}^*$  transition (39–41°C) on heating (see right 3D-spectrum in figure 41). On the other hand, it *was* present at the transition ( $\approx 42^\circ\text{C}$ ) and about half a degree below. One possible explanation is that the  $\text{SmC}^*$  phason mode is not a helix distortion mode, but a surface-induced splay mode. As the doped mixtures generally have quite low  $P_s$ -values, it is possible that the polarization close to the  $\text{SmA}^*$  phase is so low that the splayed polarization structure is not stable. The low-frequency response at the very transition temperature could in this view be attributed to a combination of soft mode, which should have a very low absorption frequency in long-pitch compounds, and a helix distortion mode, which may be present just before the transition if the  $\text{SmC}^*$  pitch decreases on heating. In any case, the collective contribution at the transition is clearly due to two modes, so it cannot be the soft mode on its own.

By performing a bias sweep we noticed that the maximum susceptibility temperature of the soft mode was shifted to slightly higher temperatures at higher bias voltage, indicating that the  $\text{SmA}^*\rightarrow\text{SmC}^*$  transition can be field-induced in this material. The difference in transition temperature between zero-field and maximum (35 over a 23  $\mu\text{m}$  cell) field was in the order of 2°C.

### 4.3. Summary

From the present study we may conclude that the induced phase sequence in the chiral-dopant mixtures is mainly influenced by the host. A strictly synclinic host produces only  $\text{SmA}^*$  and  $\text{SmC}^*$  phases, while a strictly anticlinic host leads to  $\text{SmC}_a^*$  in place of the  $\text{SmC}^*$  phase. A host which possesses both clinicities can be doped to a material with both  $\text{SmC}^*$  and  $\text{SmC}_a^*$  phases. Such a mixture may feature coexistence with  $\text{SmC}^*$  within the nominal  $\text{SmC}_a^*$  temperature range, in particular if the dopant is promoting the synclinic  $\text{SmC}^*$  structure.

All mixtures had a long pitch, and those doped with the synclinic-promoting additive (S)-IGS97 were very sensitive to external influence. This made them very easy to switch electro-optically, but it also rendered the interpretation of the dielectric spectra difficult.

The sample thickness also has an important role in the coexistence phenomenon. A high degree of surface interaction, as observed in thin cells, will promote the synclinic  $\text{SmC}^*$  structure, and hence thin samples will exhibit more coexistence than thick ones.

## 5. THE EFFECTS OF SURFACES ON THERMODYNAMIC PHASES

---

---

*Look here, Steward, if this is coffee, I want tea; but if this is tea, then I wish for coffee.*

– Punch

### OVERVIEW

*The topic of this chapter is the important question, from both a fundamental and an applicational point of view, of how liquid crystal phases are influenced by surfaces. I begin by going through some general observations regarding the interactions between cell surfaces and polar liquid crystals. In the rest of the chapter I give some illustrative examples, both from my own research and from literature, on how surfaces may induce phase coexistence and even completely suppress certain phases. The effect of cell surfaces on the helical pitch of a material has already been discussed at length in chapter 3, so this important topic will not be brought up here.*

### **5.1. The meeting of polar surfaces and (anti-) polar smectics**

Experiments on liquid crystals are very often performed on planar-aligned samples in which the compound is confined by glass substrates to a narrow cell gap  $d$ . This is a necessity in order to render a  $\text{SmC}^*$  material ferroelectric, and a standard characterization procedure has therefore often been to prepare test cells of  $d \leq 5 \mu\text{m}$ , and to perform in particular electrooptic and dielectric spectroscopy experiments on these. When AFLCs were introduced, this technique was therefore often used also in the study of other phases of the smectic  $\text{C}^*$  family, giving information about the behavior as influenced by bounding surfaces, while other techniques such as DSC and free-standing film experiments gave information about the bulk behavior. It soon turned out that the results obtained for thin cells did not quite reflect those obtained on bulk samples, and in 1993 the first (to my knowledge) publication [53] appeared, pointing out that there could be a high degree of coexistence between  $\text{SmC}^*$  and  $\text{SmC}_a^*$ , and that the temperature at which  $\text{SmC}_a^*$  appeared was lowered, in thin cells. This is a consequence of the ordering effect of the surface, but when I started my work in 1997 this was still not common knowledge and in some cases, rather far-fetched models appeared to explain the strange behavior of the “ $\text{SmC}_a^*$ ” phase in thin cells [54].

Not only may we see  $\text{SmC}^*$  and  $\text{SmC}_a^*$  coexisting in thin cells, but the smectic  $\text{C}^*$  subphases –  $\text{SmC}_\alpha^*$ ,  $\text{SmC}_{1/3}^*$  and  $\text{SmC}_{1/4}^*$  – can be completely “squeezed out” in thin samples. The phase which replaces these phases, and in fact also  $\text{SmC}_a^*$  in many cases,

is always  $\text{SmC}^*$ . This is not very surprising if one considers the nature of the surface influence. First of all, most samples use a buffed alignment layer, such as polyimide or nylon, where the buffing mechanically introduces an anisotropy in the alignment layer. In other words, there exists one direction at the surface which stands out from all others, and it is then natural to believe that the liquid crystal director aligns in this direction at the surface. There is no practical way of achieving the two-fold degenerate alignment which would correspond to the anticlinic structure of  $\text{SmC}_a^*$ . Secondly, surfaces normally have a certain polar preference, which means it agrees best with a synclinic  $\text{SmC}^*$  state [3]. The anticlinic and antipolar  $\text{SmC}_a^*$  geometry would, considering for simplicity the case where the molecules lie in the substrate plane, always to 50 % be in conflict with the surface polarization and such a structure is thus not very probable for the molecules closest to the surface. A more realistic picture is that the surface regions are always synclinic, and if the bulk is anticlinic, this change of geometry has to be mediated via defects. When the surfaces come closer, it is not very difficult to imagine that the anticlinic bulk structure diminishes in size, and may ultimately be completely absent.

### 5.1.1. Coexisting $\text{SmC}^*$ and $\text{SmC}_a^*$ phases

In [55] an unusually thorough study is presented of the influence of the cell boundaries on the  $\text{SmC}^*$ - $\text{SmC}_a^*$  transition temperature, in which not only the cell thickness but also the type of alignment layer has been varied. The investigated compound, W109a, is a mixture with the following bulk phase sequence, as observed by DSC and polarized microscopy:

Cr 36  $\text{SmC}_a^*$  84  $\text{SmC}^*$  123  $\text{SmA}^*$  142-149 Iso

It is interesting to note that the clearing point was impossible to define for bulk samples of this mixture due to coexistence between the isotropic and  $\text{SmA}^*$  phases. This would normally be regarded as a sign of impurity [56], but I have actually observed the same behavior in another very interesting compound with a behavior which in many respects is similar to that reported for W109a. This is the so-called “Tokyo mixture” exhibiting thresholdless switching [61]. In both this mixture and in W109a, the clearing point was much more well-defined when the compound was studied in a thin cell. This would naturally be interpreted as a surface-stabilization of the  $\text{SmA}^*$  phase which therefore becomes broader, making the coexistence range narrower.

As can be seen in figure 42, the transition point between the syn- and anticlinic phases of W109a could be suppressed by more than 35°C by reducing the sample thickness. Furthermore, the data give some evidence of the fact that not only does the cell thickness play an important role, but also the degree of uniformity in the alignment layers. The sample with both substrates buffed showed the largest extension of the  $\text{SmC}^*$  phase. The polyimide-coated sample had the smallest shift in transition temperature, which may first of all probably be related to the fact that only one substrate was buffed. It would be interesting to see a comparison also with a polyimide cell where both substrates are buffed; its curve would probably end up somewhere between nylon1 and nylon2 in figure 42.

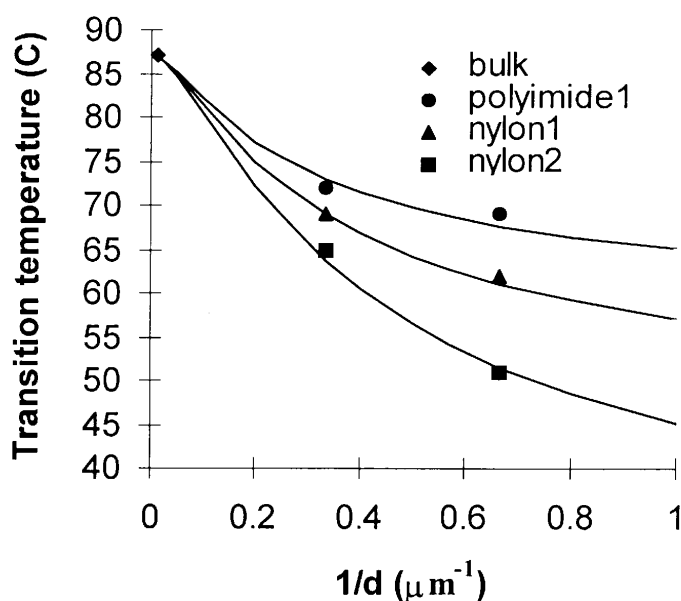


Figure 42. The cell-thickness dependence of the  $\text{SmC}^*-\text{C}_a^*$  transition for the mixture W109a. Three different types of alignment layers have been tested: polyimide with one side rubbed (polyimide 1) and nylon with one and two sides rubbed, respectively (nylon1, nylon2). From reference [55].

The study described in [55] is based on electrooptic measurements and, as the authors point out, this does not permit them to study the effect of untreated alignment layers. For electrooptics the sample has to be well aligned and hence the substrate coating has to be buffed. Dielectric spectroscopy studies would in this respect be a very appealing complement since this is a technique where the alignment of the sample is of less importance, at least for the case of  $\text{SmC}^*$  and  $\text{SmC}_a^*$  phases<sup>1</sup>. In my experimental work I have most often used polyimide-coated cells, where the two substrates are buffed in antiparallel directions, or non-glued cells where an alignment layer of  $\text{SiO}_x$  has been evaporated onto the substrates. The directional anisotropy is in this case introduced by mechanically shearing the cell. In some cases I have also worked with commercial EHC cells in which the alignment layers are parallel-buffed polyimide. The varying alignment techniques thus make it difficult to compare the results from different experiments quantitatively, but qualitatively the conclusions are quite clear.

In [55] coexistence of  $\text{SmC}^*$  and  $\text{SmC}_a^*$  is never mentioned; here the  $\text{SmC}^*$  phase seems to completely replace  $\text{SmC}_a^*$  when decreasing the cell thickness. However, transition shifts of course also occurs in samples where the two phases coexist and, as the following example demonstrates, such a sample may often behave as if it were purely  $\text{SmC}^*$ . I would like to go back shortly to the chiral-dopant mixture CDMix2 ((R/S)-10F1M7 and (S)-IGS97) which showed the strongest coexistence in the series which I investigated (chapter 4). Already in bulk this mixture has a tendency to show coexist-

1. It has been proposed [58] that the study of the  $\text{SmC}_{1/3}^*$  and  $\text{SmC}_{1/4}^*$  subphases requires a uniform planar alignment, as the periodicity of these phases may approach the size of the domains in an un-aligned sample. The response of the  $\text{SmC}^*$  and  $\text{SmC}_a^*$  phases is, on the other hand, quite independent of the quality of the alignment, as long as it is strictly planar (or strictly homeotropic) throughout the electrode area.

ence of  $\text{SmC}^*$  and  $\text{SmC}_a^*$ , and in a thin cell the  $\text{SmC}_a^*$  phase seems to be completely replaced by  $\text{SmC}^*$ , at least judging from the dielectric response (*cf* figure 43). Neither on cooling nor on heating could any sign of  $\text{SmC}_a^*$ , or of a reduction of the amount of  $\text{SmC}^*$ , be observed.

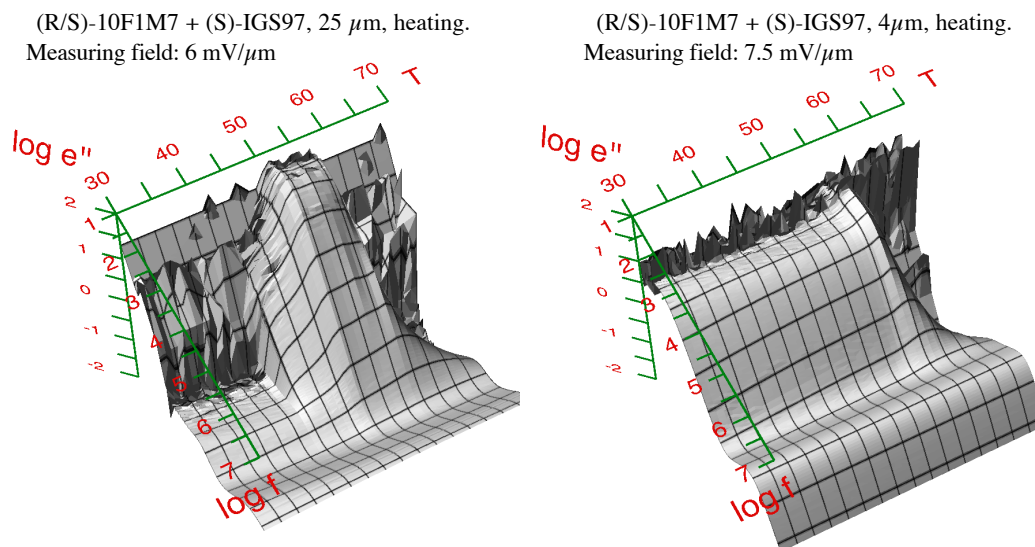


Figure 43. 3D-spectra for CDMix2 (see chapter 4 for details) in a thick and a thin cell, on heating. The  $\text{SmC}^*$  phase mode extends with undiminished strength all the way down to room temperature in the thin cell. There is thus no longer any sign of a  $\text{SmC}^*$ - $\text{SmC}_a^*$  phase transition in the dielectric response, but the compound seems to be in the  $\text{SmC}^*$  phase throughout the investigated temperature range. The 25  $\mu\text{m}$  cell is a commercial EHC cell, while the 4  $\mu\text{m}$  cell is a self-made cell with polyimide alignment layer.

However, while dielectric spectroscopy experiments give the impression that there is no longer any  $\text{SmC}_a^*$  phase in the compound, texture studies show that this is not necessarily the case. The series of photos in figure 44, taken on the relaxed 4  $\mu\text{m}$  sample, clearly show that there are regions of  $\text{SmC}_a^*$  coexisting with regions of  $\text{SmC}^*$ . The latter are easily recognized by the occurrence of domains, and by rotating the sample the two coexisting structures become obvious. However, after switching the sample, this texture is not observed until after a very long time (several hours) of relaxation. This means that the dielectric spectra most certainly do originate from a  $\text{SmC}^*$  liquid crystal, more precisely a surface-stabilized  $\text{SmC}^*$ , as the measuring field probably is enough to switch the cell, and then it stays in  $\text{SmC}^*$  throughout the whole measurement.

This example serves as an illustration to one of the drawbacks of dielectric spectroscopy as a characterization technique; as the measurement is a very lengthy procedure it is totally computerized, and the results are analyzed after the measurements are finished. There is nobody observing the sample while the experiment is actually performed, and thus important information is lost. If a change in alignment or fill factor of the cell occurs during measurements (both are once in a while observed), this will also change the dielectric properties of the sample, and thus be a source of error in the analysis of the experiment. A good complement to the standard dielectric equipment would therefore be a CCD camera taking a picture of the texture before, during and after each measurement.

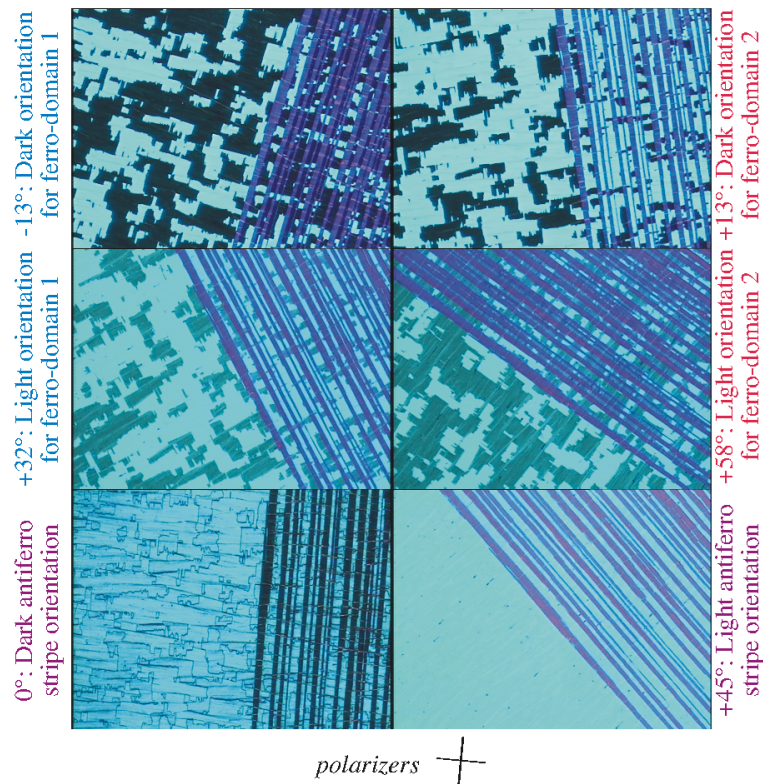


Figure 44. Texture of a 4 μm planar-aligned sample (polyimide alignment layer) with the chiral-dopant mixture (R/S)-10F1M7 + (S)-IGS97 at room temperature (through crossed polarizers). The coexistent ferroelectric and antiferroelectric regions are clearly distinguishable from each other as black and white domains of varying shape on one hand, and the long and thin stripes on the other hand. The tilt-angle is 13°.

Before leaving the matter of  $\text{SmC}^*/\text{C}_a^*$  coexistence, I would like to mention what the effects of such coexistence is on the electrooptic behavior of the sample. In [15] electrooptic curves for this situation were simulated, and it turned out that the resulting curves look just like those which previously had been interpreted as a *ferrielectric* response. Thus many reports of ferrielectric phases, based on electrooptic investigations, may actually be related to  $\text{SmC}^*/\text{C}_a^*$  coexistence. Considering that electrooptic studies are often performed on thin cells, this is quite likely to be the case.

### 5.1.2. The quenching of subphases by surface influence

The typical dielectric response of the  $\text{SmC}_{1/3}^*$  and  $\text{SmC}_{1/4}^*$  phases is still not very well defined, due to the fact that different reports give examples of quite different behavior in these phases. The differences may to a large extent be related to the different thicknesses of cells used to study AFLCs – ranging from 1 μm to 100 μm. It is today quite well established that these phases are very much affected by the cell surfaces and may indeed disappear completely if the cell gap is small enough. As in the case of  $\text{SmC}^*/\text{C}_a^*$  coexistence, this can be related to the ordering effect of the surfaces. The subphases in question are notoriously unstable and very sensitive to external influence in general. As discussed in chapter 1, their bulk structure may be a frustrated one resulting in a deformed unit cell [12]. If such a structure comes in contact with ordering surfaces, it is quite likely that the whole phase gently adopts the order preferred by the

surfaces, and thus we end up with a  $\text{SmC}^*$  phase even in the subphase temperature range.

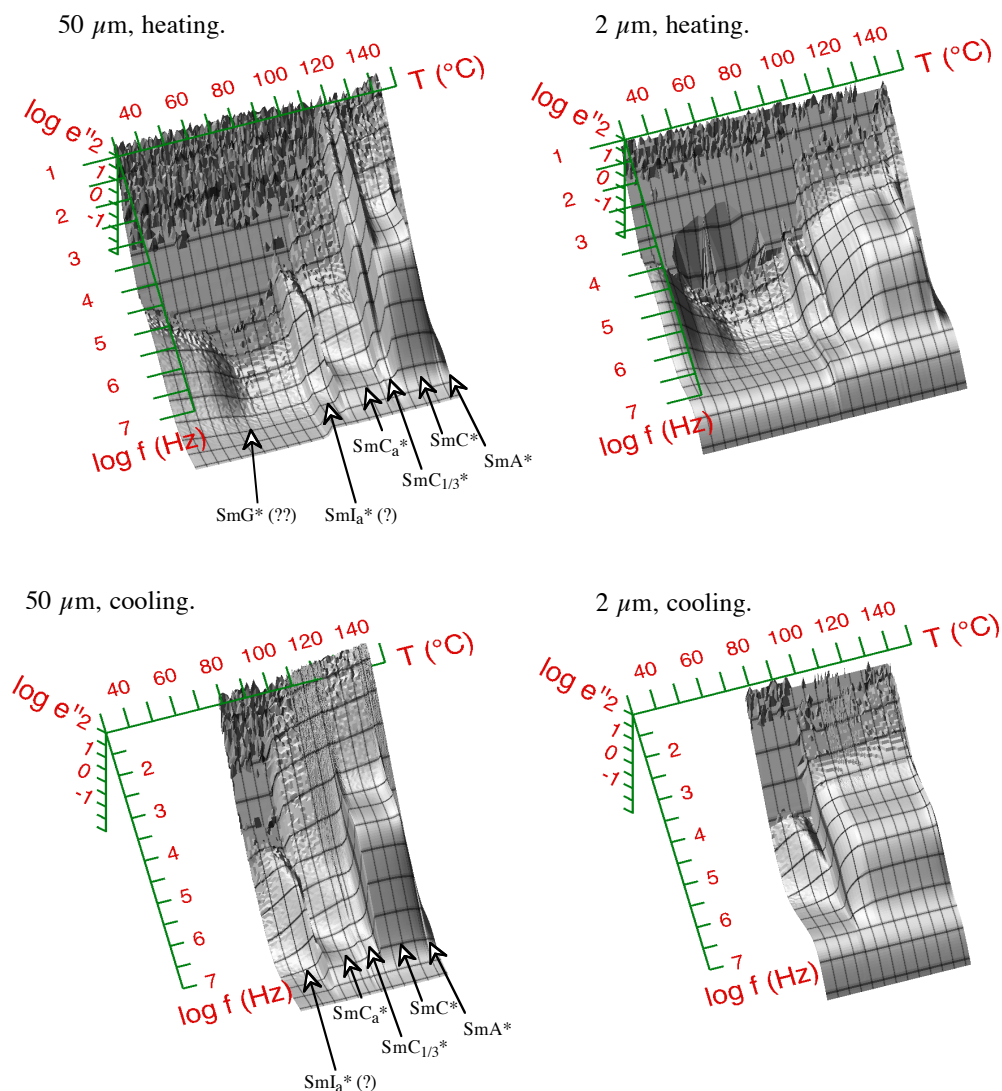


Figure 45. The imaginary component of the dielectric permittivity of A4 in thick and thin planar-aligned samples ( $\text{SiO}_x$  alignment layers), as measured on cooling and on heating. For comparative reasons all graphs have the same scale, even though the cooling spectra did not extend down to room temperature. The temperature range of the  $\text{SmC}^*$  phase, distinguished by a high-susceptibility phason mode, is dramatically extended in the  $2 \mu\text{m}$  cell. Furthermore, both the  $\text{SmC}_a^*$  and the  $\text{SmC}_{1/3}^*$  phases are completely replaced by  $\text{SmC}^*$  on cooling, while the temperature region of these phases on heating is characterized by a gradually increasing fraction of  $\text{SmC}^*$ .

As a good example of the squeezing-out of subphases I give some dielectric spectra obtained on the compound A4 (supplied by Avtar Matharu), related to the previously mentioned CG50 (see chapter 2), in very thin and very thick cells. The compound has a rich smectic mesomorphism in a very broad temperature range, as can be seen in the heating spectrum of the thick cell. Between  $\text{SmC}^*$  and  $\text{SmC}_a^*$  it features at least one subphase, probably the  $\text{SmC}_{1/3}^*$ , and below  $\text{SmC}_a^*$  there are at least two high-order phases. When the compound is filled into a cell of  $2 \mu\text{m}$  cell gap, the  $\text{SmC}^*$  phase tem-

perature range is clearly much extended. On heating, the temperature region corresponding to  $\text{SmC}_a^*$  and  $\text{SmC}_{1/3}^*$  in bulk, is now distinguished by a coexistence between  $\text{SmC}_a^*$  and  $\text{SmC}^*$ . On cooling, the  $\text{SmC}^*$  phason mode persists undiminished in susceptibility down to the onset of the high-ordered phase, indicating that both  $\text{SmC}_a^*$  and  $\text{SmC}_{1/3}^*$  are completely squeezed out.

### 5.1.3. Can surfaces induce phases which do not exist in bulk ?

To finish the discussion on the  $\text{SmC}^*$ -promoting effect of surfaces I would like to bring up an example from paper 5. Here we have studied the compound W101a, which in bulk exhibits a direct  $\text{SmA}^*$ - $\text{SmC}_a^*$  transition, in both thin and thick cells using dielectric spectroscopy. In thin cells also electrooptic experiments have been performed, and the curious switching curve obtained just below the phase transition is presented in figure 46. The behavior is what often is described as “ferrielectric switching” but it is more likely a result of coexisting  $\text{SmC}^*$  and  $\text{SmC}_a^*$  phases. What makes this case very interesting is that the compound does not have a  $\text{SmC}^*$  phase in bulk, nor any other phase between  $\text{SmA}^*$  and  $\text{SmC}_a^*$ . If there are  $\text{SmC}^*$  regions present, these must thus be completely surface-induced.

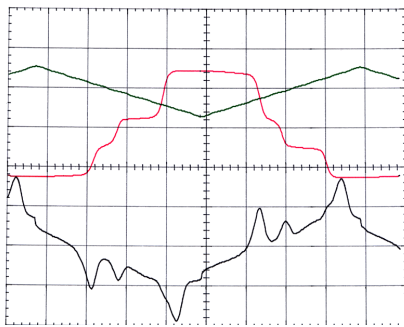


Figure 46. Electrooptic response of W101a in a  $2 \mu\text{m}$  cell ( $\text{SiO}_x$  alignment layer), just below the  $\text{SmA}^*$ - $\text{SmC}_a^*$  phase transition. The behavior indicates a coexistence of  $\text{SmC}^*$  and  $\text{SmC}_a^*$  even though the bulk compound does not have a  $\text{SmC}^*$  phase. Picture courtesy of G. Andersson [57].

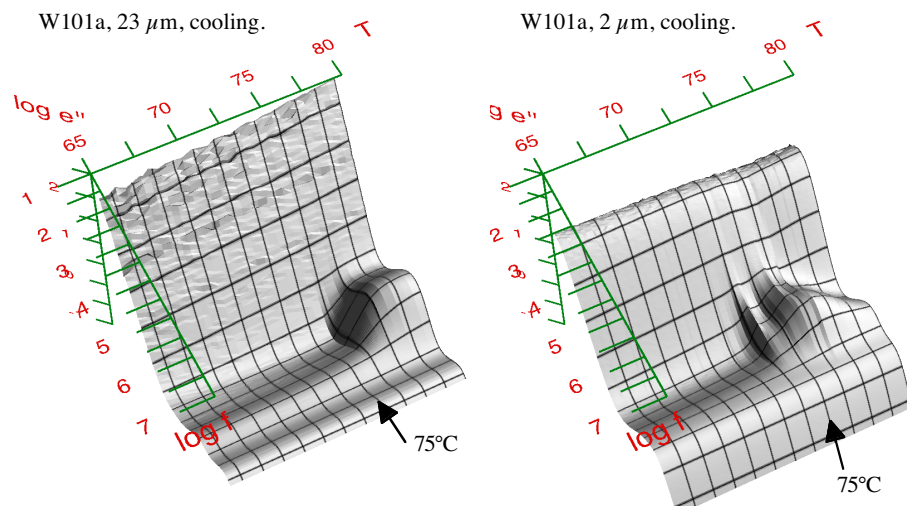


Figure 47. Absorption spectra of W101a in  $23 \mu\text{m}$  (polyimide alignment layer) and  $2 \mu\text{m}$  ( $\text{SiO}_x$  alignment layer) cells. In bulk, as approximated in the thick cell, the compound clearly has a direct  $\text{SmA}^*$ - $\text{SmC}_a^*$  transition with no other phase in between. In the thin cell, the absorption in the vicinity of the transition is clearly distorted, which may be an indication of a surface-induced polar order. The spectra are drawn with the same scale.

The dielectric spectroscopy results (figure 47) support this interpretation. While the spectrum from the thick sample shows a normal soft mode at the transition, followed by the appearance of the  $\text{SmC}_a^*$  modes (in the magnified spectrum of the figure one can see only one clearly) at lower temperatures, the spectrum obtained with the thin cell shows an additional absorption on the cold side of the phase transition which can be attributed neither to a  $\text{SmA}^*$  nor a  $\text{SmC}_a^*$  phase. Instead this could originate from a small amount of the liquid crystal which is in a surface-induced  $\text{SmC}^*$  state. Furthermore, the transition temperature from  $\text{SmA}^*$  is decreased by approximately  $4^\circ\text{C}$ , which most likely is an effect of the incompatibility between the anticlinic  $\text{SmC}_a^*$  structure and the alignment layer.

## 5.2. Summary

As there is no surface exhibiting an alternating polarization direction structure, we can not expect any planar-aligning cell boundary to promote the  $\text{SmC}_a^*$  phase. Instead the synclinic, and hence uni-polar,  $\text{SmC}^*$  phase agrees well with most alignment layers, and thus we may expect this phase to be much favored in thin cells. This is indeed what is experimentally observed. All other subphases of the smectic  $\text{C}^*$  family may be replaced by, or coexisting with,  $\text{SmC}^*$  in thin cells. Especially the long-pitch  $\text{SmC}_{1/3}^*$  and  $\text{SmC}_{1/4}^*$  subphases are easily squeezed out by strong surface interactions, and in planar-aligned samples of cell gap  $d \leq 5 \mu\text{m}$  one cannot expect to see any sign of these phases, no matter what the compound.

## 6. CONCLUSIONS

---

---

*Ah ! Don't say that you agree with me. When people agree with me I always feel that I must be wrong.*

– Oscar Wilde

The collective polarization fluctuations contributing to the dielectric permittivity of the SmA\*-C\* liquid crystal system, including possible subphases of SmC\*, may be divided into amplitudon (tilt-angle fluctuations) and phason modes (phase-angle fluctuations). The latter normally correspond to a field-induced helix distortion fluctuation, but they are often referred to as Goldstone modes. Such a description is generally not strictly true; only in the limiting case of a SmC\* material exhibiting a helix inversion, studied in absence of surfaces, *i.e.* as a free-standing film, the helix distortion mode transforms into the Goldstone mode.

In order to investigate new possibilities of achieving antiferroelectric liquid crystals useful for applications, we have prepared a number of binary chiral-dopant mixtures which exhibit both SmC\* and SmC<sub>a</sub>\* phases. From the present study we may conclude that the induced phase sequence is mainly influenced by the host. A strictly synclitic host produces only SmA\* and SmC\* phases, while a strictly anticlitic host leads to SmC<sub>a</sub>\* in place of the SmC\* phase. A host which possesses both clinicities can be doped to a material with both SmC\* and SmC<sub>a</sub>\* phases. Such a mixture may feature coexistence with SmC\* within the nominal SmC<sub>a</sub>\* temperature range, in particular if the dopant is promoting the synclitic SmC\* structure.

Liquid crystals are normally studied in confined geometries, with the compound contained between glass substrates. As there is no surface exhibiting an alternating polarization direction structure, we can not expect any planar-aligning cell boundary to promote the SmC<sub>a</sub>\* phase. A synclitic arrangement of the molecules is the most likely structure close to the surface, and hence the influence of surfaces on the smectic C\* family of liquid crystals may have a large impact on the observed phase behavior. The SmC<sub>α</sub>\*, SmC<sub>1/3</sub>\*, and SmC<sub>1/4</sub>\* subphases are in thin cells all replaced by SmC\*. The SmC<sub>a</sub>\* phase may survive, but it is normally pushed down towards lower temperatures and often it is found to coexist with SmC\*.



## APPENDIX: EXPERIMENTAL DETAILS

---

---

### ***1. How experiment parameters may influence the results***

A problem faced by all experimentalists is the influence on the results from the experiment itself. In dielectric spectroscopy there are a number of ways to achieve results which do not reflect the truth, or at least not the whole truth (and nothing but the truth). It can easily happen that the experiment is performed under such conditions that the sample is constantly in an unrelaxed state, and therefore behaves different from what other experiments may predict. The most important factor is the cell thickness, but this has already been dealt with at length in the main text, so here I would like to concentrate on some other experiment parameters which may have a large impact on the observations.

#### **1.1. The measuring field strength**

While many liquid crystals will show a response depending very little on the amplitude of the measuring field, this is far from true for all compounds. At least in the SmC\* and SmC<sub>1/3</sub>\* phases, a change in field-strength may drastically change the spectrum from some samples. A good example of such a compound is the previously introduced chiral-dopant mixture CDMix2 (see chapter 4). In figure 1 two series of measurements, where the measuring field-strength is raised from measurement to measurement, on this compound are shown. The left column shows results obtained on a thick (25  $\mu\text{m}$ ) cell and the right one shows the thin-cell (4  $\mu\text{m}$ ) response. It is clear that by changing the measuring field strength, the characteristics of a certain mode may change much, and above a certain level new modes may be induced.

Bearing this in mind, it is a good idea to always start the investigation of a new sample by performing a measuring field-strength sweep in order to find the optimum level. It is not a good solution to simply use the lowest possible level, since with this setting the instrument usually has a very poor resolution, and furthermore the influence of ionic impurities usually gets larger.

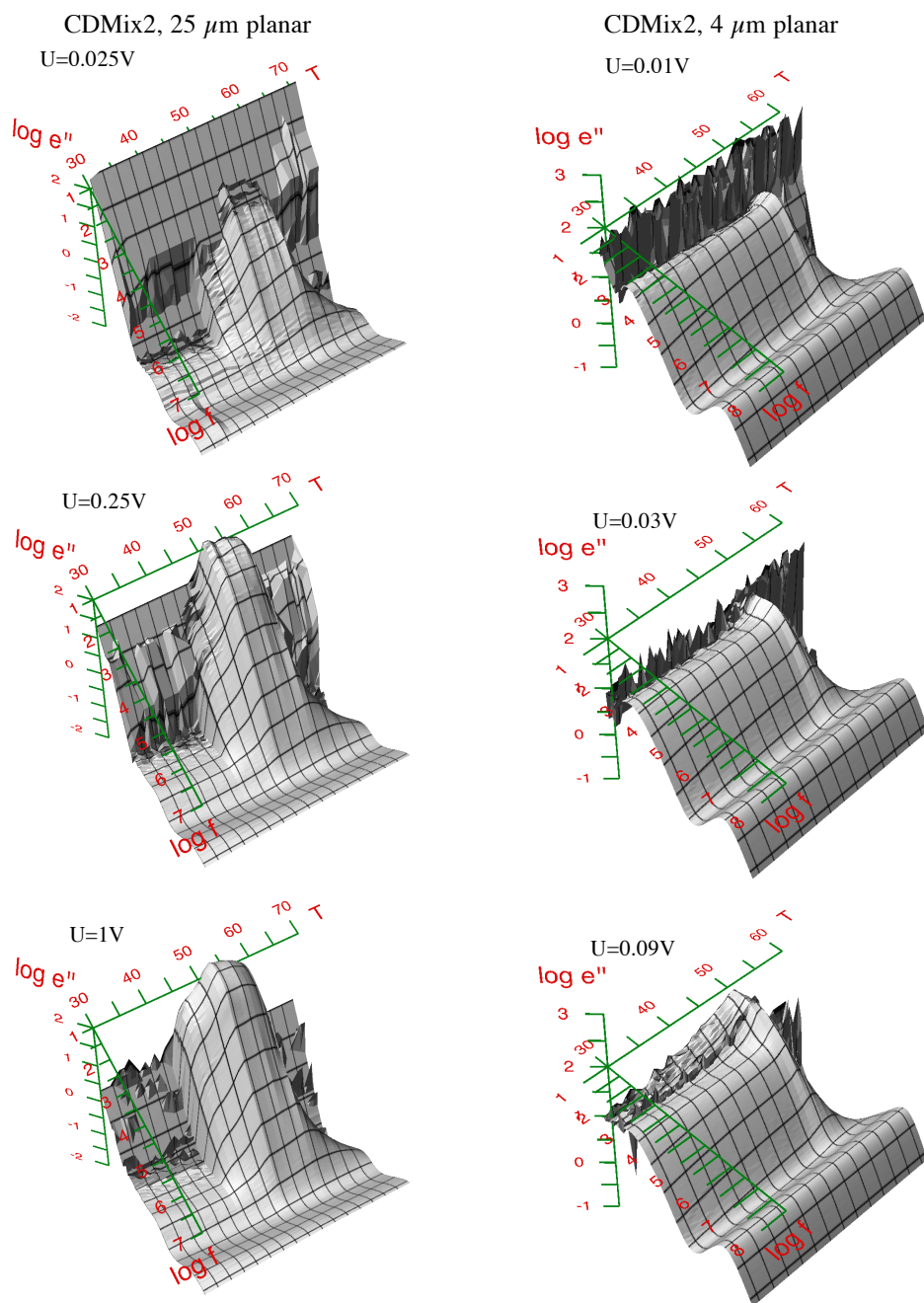


Figure 1. The dielectric permittivity spectrum of CDMix2 is dramatically affected by a change in the measuring field strength. Here the absorption spectra are shown for a 25  $\mu\text{m}$  (left) and a 4  $\mu\text{m}$  (right) cell, for different levels of measuring amplitude.

## 1.2. Heating or cooling ?

Supercooling of phases is a well-known phenomenon in the field of liquid crystals. For 1. order transitions, like  $\text{SmC}^*-\text{SmC}_a^*$ , the transition temperature may differ very much if the compound is studied on heating or on cooling. In spite of this fact, one frequently encounters experimental reports where it is not mentioned if the experiment is performed on heating or on cooling. This may of course make it very difficult to compare the results with ones own.

Not only may the choice of temperature-change direction affect the observed value of  $T_c$ , but there may also be clear memory effects from the preceding phase on the structure of the new phase, as is illustrated in figure 2. Here I show absorption spectra for the compound CG50 obtained on cooling and on heating, respectively. While on cooling, the transition from  $\text{SmC}^*$  to the subphase, which we believe is  $\text{SmC}_{1/3}^*$ , seems quite undramatic, but on heating, the same transition is accompanied by the appearance of a low-frequency mode of high susceptibility. On further heating this decreases in susceptibility but it is not gone until  $\approx 5^\circ\text{C}$  into the  $\text{SmC}^*$  phase.

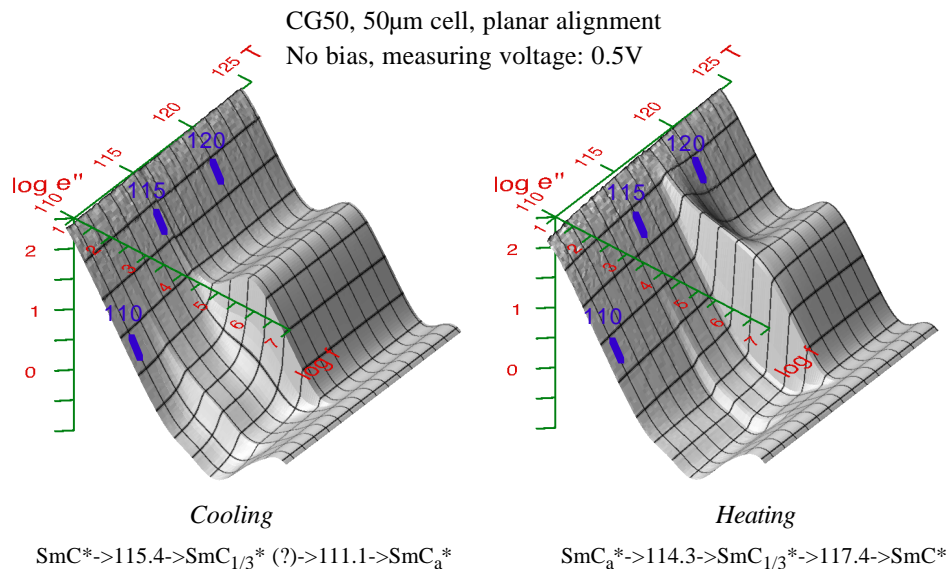


Figure 2. The compound CG50 has a behavior at the  $\text{SmC}^*$ - $\text{SmC}_{1/3}^*$  transition which is very dependent of if one passes the transition on cooling or on heating.

Also the characteristics of a certain mode may differ between cooling and heating runs. For instance, the phason mode observed in a 36  $\mu\text{m}$  cell with CDMix1 (see chapter 4) turned out to change its absorption frequency from 10 Hz to 100 Hz if the experiment was performed on cooling instead of heating.

### 1.3. Memory effects of a DC-bias

If one wants to investigate the influence of a DC-bias field on the behavior of a compound, the quick and easy way to do this is of course to perform several measurements, with varying bias level, at each stable sample temperature. This may give a good hint to what is happening, but it is by no means a good method to investigate the behavior at zero, or at intermediate, bias-level. The reason is that the relaxation from a field-induced state may be very slow, and thus all measurement in such a series will in principle reflect the behavior at maximum bias level. This is illustrated in figure 3 by the compound (S)-12F1M7 which features a  $\text{SmC}^*$ - $\text{SmC}_{1/4}^*$ - $\text{SmC}_{1/3}^*$ - $\text{SmC}_a^*$  phase sequence on cooling. It is quite obvious how all smectic  $\text{C}^*$  subphases ( $\text{SmC}^*$  not included) exhibit a strong memory of the state induced by the recently applied bias field. The same memory effects will of course be present for some time if an aligning electric field has been applied over the sample before the start of the experiment.

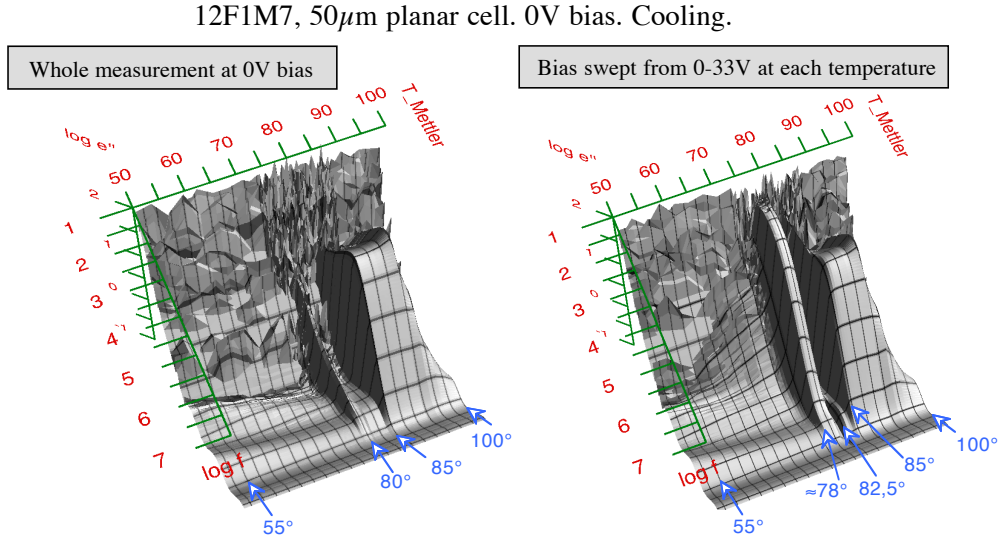


Figure 3. Two cooling scans on the compound (S)-12F1M7 in a 50  $\mu$ m planar cell with no applied bias field. The two measurements are actually performed with identical settings of all parameters, but the right spectrum is obtained within a measurement series where the DC-bias level was swept from 0V to 33V.

## 2. How to cope with unwanted absorptions

### 2.1. The low-frequency ionic contribution

Liquid crystal compounds are unfortunately never free from ionic impurities, and this has severe effects on dielectric spectroscopy measurements. There are two main types of ionic contributions: ionic space-charge polarization, which shows up when the sample contains free ionic charge carriers, and charge build-up at the cell electrodes [62]. Both lead to a non-zero conductivity value for low frequencies (as the ions are heavy they will not be able to follow fields of high frequencies), and this gives a spurious contribution to the measured dielectric permittivity.

In a time-domain spectroscopy experiment one can study processes with relaxation times as long as 100 - 1000 s, and from such measurements it is seen that the ionic contributions lead to Cole-Cole type modes with characteristic frequencies in the mHz-range [62]. In the frequency-domain spectroscopy measurements discussed in this thesis, our frequency window only extends down to 5 Hz, and thus only the right wing of the ionic absorption peak shows up in the spectrum. For our fitting purposes it is therefore sufficient to model the ionic contribution with a simple inverse temperature dependence instead of a separate Cole-Cole process [27]:

$$\epsilon''_{\text{ions}} = \frac{\sigma}{\epsilon_0} \cdot \frac{1}{2\pi f^m} \quad (45)$$

Here  $f$  is the measurement frequency,  $\epsilon_0$  is the vacuum permittivity, and  $\sigma$  and  $m$  are fitting parameters. The parameter  $\sigma$  denotes the conductivity of the sample and  $m$  is needed because often the absorption does not have a perfectly inverse linear dependence on frequency. The value should, however, normally be close to 1.

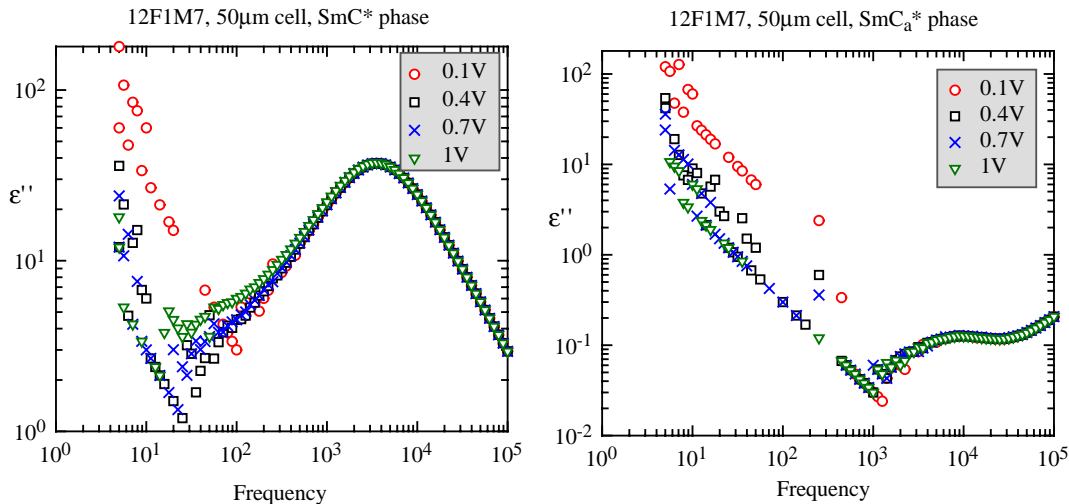


Figure 4. Ionic impurities in liquid crystals give rise to spurious contributions to the measured dielectric permittivity at low frequencies. When the ions are free to move in the bulk, this contribution is reduced by increasing the measuring field, as can be seen in this example. However, a higher measuring voltage may induce new spurious modes at low frequencies, not relevant to the studied compound, as can be seen around  $f = 100$  Hz in the left figure.

According to [63], ionic contributions of the first type (space-charge polarization) decrease if the applied voltage is increased. This is often seen when performing dielectric spectroscopy measurements with varying measuring voltages, thus indicating that this kind of ionic contribution is rather usual (at least in chiral smectic liquid crystals). Figure 4 shows an example of this behavior. However, as can be seen in the left graph, illustrating the response in the  $\text{SmC}^*$  phase, increasing the measurement voltage too much may have a devastating effect on the measurement. In this phase, as well as in  $\text{SmC}_{1/3}^*$  and  $\text{SmC}_{1/4}^*$ , a high measuring field will induce new spurious modes at low frequencies, not relevant to the studied compound. When performing measurements in these phases, one therefore has to find an optimum measuring voltage, where the ionic contributions are suppressed as much as possible, while still no additional field-induced modes appear. This field-strength will vary very much from compound to compound.

The second type of ionic contributions, due to surface charges at the electrodes, is not affected by the measurement voltage [62]. If such a contribution is present, it will thus always give a constant contribution in the low-frequency end of the dielectric spectrum.

## 2.2. The high-frequency “cell relaxation” problem

The measurement cells used for dielectric spectroscopy, as well as for many other standard liquid crystal characterization techniques, are normally coated with ITO (Indium Tin Oxide) electrodes, which are transparent to visible light<sup>1</sup>. This allows us to observe the texture of the sample optically, but the low resistivity of ITO unfortunately leads to a spurious absorption centered around a frequency  $f_{ITO}$  in the dielectric spectrum. The effect is seen as a local increase in  $\epsilon''$  centered around  $f_{ITO}$  and a corresponding decrease in  $\epsilon'$  at frequencies above  $f_{ITO}$ , and it thus mimics a polarization process in the dielectric spectrum. The absorption frequency  $f_{ITO}$  of this spurious mode (often called cell relaxation) decreases with decreasing cell thickness and with increasing electrode

resistance. For this reason one must take care in using cells coated with low-resistive ITO, and for thin-cell measurements it is actually worthwhile considering using really low-resistive, but unfortunately non-transparent, electrodes like gold or copper, in order not to have the interesting part of the spectrum completely obscured.

The cell relaxation peak of ITO-coated cells usually falls well within the frequency window of the measurement equipment, and it is therefore best to account for it with a separate Debye-type absorption process when fitting to experimental data. It normally behaves as a single relaxation time process, so a Cole-Cole term is not needed (*i.e.* the distribution parameter  $\alpha=0$ ).

### 3. The stray capacitance problem

The liquid crystal sample cell constitutes a capacitor which we normally approximate as ideal in the sense that all measuring field lines go straight from one electrode to the other. The value of the capacitance is within this approximation given by

$$C = \frac{A\varepsilon}{d} \quad (1)$$

where  $A$  is the cell area,  $\varepsilon$  is the dielectric permittivity of the compound between the electrodes, and  $d$  is the cell thickness. Unfortunately this simple relation does not quite reflect reality, because some field-lines always “bend out” outside the active cell area, and give a contribution to the capacitance which often is called the stray capacitance. There is therefore a tiny part of the capacitor which is not affected by the introduction of the dielectric material. If we write the empty capacitance as the sum of the ideal empty capacitance and the stray capacitance,

$$C_E = C_0 + C_s \quad (2)$$

we may express the capacitance of a filled cell as:

$$C_M = \varepsilon_r C_0 + C_s \quad (3)$$

where  $\varepsilon_r$  is the (relative) dielectric permittivity of the compound inside. Combining (2) and (3) we obtain an expression for the stray capacitance:

$$C_s = \frac{C_M - \varepsilon_r C_0}{1 - \varepsilon_r} \quad (4)$$

Now we can evaluate the stray capacitance by filling the cell with a compound of

1. The frequency at which a conductor becomes transparent is called the plasma frequency  $\omega_p$ , and its value depends on the charge carrier density of the conductor. Metals have very high plasma frequencies and are therefore opaque for visible light, but a conducting material with a charge carrier density approximately 1% of that of metals would have its plasma frequency in the near infrared, and would thus be transparent for visible light [64]. Such a material is Indium Tin Oxide (ITO) which is therefore used in almost all laboratory liquid crystal measurement cells, and indeed also in commercial liquid crystal displays.

known dielectric permittivity, and henceforth we can compensate for it when using the same kind of cell for liquid crystal experiments.

The stray capacitance problem gets more severe the thicker the cell, and as one often wants to use cells of typically  $d = 25 \mu\text{m}$ , it can have quite a large impact. As an example, dr. J. Schacht has evaluated the stray capacitance of a  $10 \mu\text{m}$  thick EHC cell with  $1 \text{ cm}^2$  active area to be  $C_s = 4.54 \text{ pF}$  [20]. This also means that if one tries to use equation (1) to evaluate the cell thickness, a technique which is not seldom employed, one will get results which are always too low. The thickness of a very thick cell ( $50 \mu\text{m}$ ) may with this technique be evaluated to about half its real value !

#### ***4. Transforming from conductance and capacitance to dielectric permittivity***

All experimental data in this text has been obtained with the medium frequency range (5 Hz-13 MHz) impedance analyzer model 4192A by Hewlett Packard. The output from this instrument is the measured capacitance  $C_M$  and the measured conductance  $G_M$  for the sample. In order to extract the dielectric permittivity for the sample, one can use the following equations [26], where also the contribution of the stray capacitance has been taken into account:

$$= \frac{C_M - C_s}{C_E - C_s} \quad (5)$$

$$= \frac{G_M}{2 \pi f (C_E - C_s)} \quad (6)$$

$C_E$  is the measured capacitance of the empty cell, and  $f$  is the frequency at which the values  $C_M$  and  $G_M$  are measured.



## REFERENCES

---

---

*A classic is something that everybody wants to have  
read and nobody wants to read*  
– Mark Twain

- [1] R. B. Meyer, L. Liebert, L. Strzelecki, P. Keller, *J. Physique Lett.*, **36**, pp. L69-71, (1975)
- [2] N. A. Clark, S. T. Lagerwall, *Appl. Phys. Lett.*, **36**, 11, pp. 899-901 (1980)
- [3] S. T. Lagerwall, “*Ferroelectric and Antiferroelectric Liquid Crystals*”, Wiley-VCH (1999)
- [4] Discussions on nomenclature at the Capri meeting (sept. 1996), the results of which will appear in the forthcoming IUPAC recommendations.
- [5] Y. Galerne, L. Liebert, *Oral presentation at the FLC’89 conference, Göteborg, Sweden* (1989)
- [6] H. Takezoe, A. D. L. Chandani, J. Lee, E. Gorecka, Y. Ouchi, A. Fukuda, Terashima, Furukawa, Kishi *Oral presentation at the FLC’89 conference, Göteborg, Sweden* (1989)
- [7] D. D. Parghi, S. M. Kelly, J. W. Goodby, *poster presentation at FLC’99, Darmstadt, Germany* (1999) and references therein
- [8] K. Hiraoka, A. Taguchi, Y. Ouchi, H. Takezoe, A. Fukuda, *Jpn. J. Appl. Phys.* **29**, 1, pp. L103-106 (1990)
- [9] P. Mach, R. Pindak, A.-M. Levelut, P. Barois, H. T. Nguyen, H. Baltes, M. Hird, K. Toyne, A. Seed, J. W. Goodby, C. C. Huang, L. Furenlid, *Phys. Rev. E*, **60**, 6, pp. 6793-6802 (1999)
- [10] A. Fukuda, Y. Takanishi, T. Isozaki, K. Ishikawa, H. Takezoe, *J. Mater. Chem.* **4**, pp. 997-1016 (1994)
- [11] M. Cepic, B. Rovsek, B. Zeks, *presented at the ECLC 99, Hersonissos, Crete* (1999)
- [12] I. Musevic, *presentation at the Workshop on Dielectric Spectroscopy, Dublin, Ireland* (1999)
- [13] M. Glogarova, H. Sverenyak, A. Fukuda, H. Takezoe, *Liq. Cryst.*, **14**, 2, pp. 463 - 468
- [14] K. Itoh, M. Kabe, K. Miyachi, Y. Takanishi, K. Ishikawa, H. Takezoe, A. Fukuda, *J. Mater. Chem.* **7**, 3, pp. 407-416 (1997)
- [15] P. Rudquist *et al.*, *poster presentation at FLC’99, Darmstadt, Germany* (1999)
- [16] D. K. Cheng, “*Field and Wave Electromagnetics*”, Addison-Wesley (1991)
- [17] S. T. Lagerwall, M. Matuszczyk, P. Rodhe, L. Ödman, “*The Electroclinic Effect*”, Chapter 8 (p. 155-194) in S. Elston, R. Sambles (eds), “*The Optics of Thermotropic Liquid Crystals*”, Taylor & Francis, London (1998)
- [17a] P. Debye, “*Polar Molecules*”, Chemical Catalogue Co., New York (1927)

- [18]K. S. Cole, R. H. Cole, *J. Chem. Phys.* **9**, pp. 341 (1941)
- [19]K. S. Cole, R. H. Cole, *J. Chem. Phys.* **10**, pp. 98 (1942)
- [20]J. Schacht, “*Dielektrische und elektrooptische Untersuchungen zur kollektiven Dynamik in fluiden und hexatischen Flüssigkristallphasen*”, Ph. D. thesis, TU-Clausthal (1997)
- [21]F. Gouda, W. Kuczynski, S. T. Lagerwall, M. Matuszczyk, T. Matuszczyk, K. Skarp, *Phys. Rev. A*, **46**, 2, pp. 951-958
- [22]I. Musevic, “*Elementary excitations and broken symmetries in a ferroelectric liquid crystal*”, Ph.D. thesis, University of Ljubljana (1993)
- [23]I. Musevic, B. Zeks, R. Blinc, Th. Rasing, *Ferroelectrics*, **147**, pp. 77-90 (1993)
- [24]H. Orihara, Y. Igasaki, Y. Ishibashi, *Ferroelectrics*, **147**, pp. 67-75 (1993)
- [25]W. de Jeu, “*Physical Properties of Liquid Crystalline Materials*”, *Gordon and Breach* (1980)
- [26]M. Buivydas, *Ph.D Thesis, Chalmers University of Technology* (1997)
- [27]F. M. Gouda, *Ph.D Thesis, Chalmers University of Technology* (1992)
- [28]F. Gouda, K. Skarp, S. T. Lagerwall, *Ferroelectrics*, **113**, pp. 165-206 (1991)
- [29]F. Gouda, G. Andersson, S. T. Lagerwall, K. Skarp, B. Stebler, T. Carlsson, B. Zeks, *Liq. Cryst.* **6**, 2, pp. 219-230 (1989)
- [30]K. D'havé, A. Dahlgren, P. Rudquist, J. P. F. Lagerwall, G. Andersson, M. Matuszczyk, S. T. Lagerwall, R. Dabrowski, W. Drzewinsky, *Ferroelectrics, to appear* (2000)
- [31]R. Blinc, B. Zeks, *Phys. Rev. A*, **18**, 2, pp. 740-745 (1978)
- [32]A. Levstik, T. Carlsson, C. Filipic, I. Levstik, B. Zeks, *Phys. Rev. A*, **35**, 8, pp. 3527-3534 (1987)
- [33]T. Carlsson, B. Zeks, C. Filipic, A. Levstik, *Phys. Rev. A*, **42**, 2, pp. 877-889 (1990)
- [34]L. Benguigui, *J. Physique*, **43**, pp. 915-920 (1982)
- [35]J. Kinaret, *lecture notes on Statistical Physics, Chalmers*, 1999
- [36]F. Gouda, *personal communication*
- [37]P. W. Anderson, “*Basic Notions of Condensed Matter Physics*”, *Benjamin/Cummings Publishing Co.* (1984)
- [38]Y. Nambu, G. Jona-Lasinio, *Phys. Rev.* **122**, pp. 345 (1961)
- [39]J. Goldstone, A. Salam, S. Weinberg, *Phys. Rev.* **127**, pp. 965 (1962)
- [40]D. Pociecha, J. Szydłowska, M. Glogarova, E. Gorecka, *FLC'99 book of abstracts* (1999)
- [41]M. Pfeiffer, S. Wrobel, L. A. Beresnev, W. Haase, *Mol. Cryst. Liq. Cryst.* **202**, pp. 193-206 (1991)
- [42]Yu. P. Panarin, Yu. P. Kalmykov, S. T. Mac Lughadha, H. Xu, J. K. Vij, *Phys. Rev. E*, **50**, 6, pp. 4763-4772 (1994)
- [43]V. Novotna, M. Glogarova, A. M. Bubnov, H. Sverenyak, *Liq. Cryst.* **4**, 23, pp. 511-518 (1997)
- [44]L. Beresnev, M. Pfeiffer, S. Pikin, W. Haase, L. Blinov, *Ferroelectrics*, **132**, pp. 99-114 (1992)
- [45]W. Haase, S. Hiller, M. Pfeiffer, L. A. Beresnev, *Ferroelectrics*, **140**, pp. 37-44 (1993)
- [46]M. Buivydas, F. Gouda, S. T. Lagerwall, B. Stebler, *Liq. Cryst.* **18**, 6, pp. 879-886 (1995).
- [47]K. Hiraoka, H. Takezoe, A. Fukuda, *Ferroelectrics*, **147**, pp. 13-25 (1993)

- [48]M. Cepic, G. Heppke, J.-M. Hollidt, D. Löttsch, D. Moro, B. Zeks, *Mol. Cryst. Liq. Cryst.* **263**, pp. 207-216 (1995)
- [49]R. Douali, C. Legrand, V. Faye, H. T. Nguyen, *Mol. Cryst. Liq. Cryst.* **328**, pp. 209-219 (1999)
- [50]L. K. M. Chan, G. W. Gray, D. Lacey, R. M. Scrowston, I. G. Shenouda, K. J. Toyne, *Mol. Cryst. Liq. Cryst.* **172**, p. 125 (1989)
- [51]D. D. Parghi, *personal communication*
- [52]Y. Takanishi, H. Takezoe, A. Fukuda, H. Komura, J. Watanabe, *J. Mater. Chem.* **2**, p. 71 (1992)
- [53]H. Moritake, N. Shigeno, M. Ozaki, K. Yoshino, *Liq. Cryst.* **14**, 5, pp. 1283-1293 (1993)
- [54]S. Inui, N. Iimura, T. Suzuki, H. Iwane, K. Miyachi, Y. Takanishi, A. Fukuda, *J. Mater. Chem.* **6**, p. 671 (1996)
- [55]V. A. Lapanik, A. A. Muravski, S. Ye. Yakovenko, W. Drzewinski, K. Czuprynski, R. Dabrowski, *poster presentation at FLC'99, Darmstadt, Germany (1999)*
- [56]N. Gough, *personal communication*
- [57]J. P. F. Lagerwall, G. Andersson, M. Matuszczyk, T. Matuszczyk, R. Dabrowski, W. Drzewinski, P. Perkowski, Z. Raszewski, *poster presentation at FLC'99, Darmstadt, Germany (1999)*
- [58]D. Moro, *personal communication*
- [59]Yu. Panarin, Kalinovskaya, Vij, J. Goodby, *Phys. Rev. E*, **55**, 4 (1997), pp. 4345-4353
- [60]M. Cepic, G. Heppke, J. Hollidt, D. Löttsch, B. Zeks, *Ferroelectrics*, 147 (1993), pp. 159-170
- [61]P. Rudquist, J. P. F. Lagerwall, M. Buivydas, F. Gouda, S. T. Lagerwall, N. A. Clark, J. E. Maclennan, R. F. Shao, D. A. Coleman, S. Bardon, T. Bellini, D. R. Link, G. Natale, M. A. Glaser, D. M. Walba, M. D. Wand, X. H. Chen, *J. Mater. Chem.* **6**, pp. 1257-1261 (1999).
- [62]S. Murakami, H. Iga, H. Naito, *J. Appl. Phys.* **80**, 11, pp. 6396-6400 (1996)
- [63]M. Iwamoto, *J. Appl. Phys.* **77**, pp.5314 (1995)
- [64]J. D. Livingston, "*Electronic Properties of Engineering Materials*", Wiley, MIT Series in Materials Science & Engineering (1999)

